THE MAGNITUDE OF THE PALAEOMAGNETIC FIELD DURING A POLARITY TRANSITION. A NEW TECHNIQUE AND ITS APPLICATIONS.

by

John Shaw

A thesis submitted in accordance with the requirements of the University of Liverpool for the degree of Doctor in Philosophy

November, 1974.

Oliver Lodge Laboratory

CONTAINS
PULLOUTS

ABSTRACT

This thesis describes a new technique for determining the magnitude of the palaeomagnetic field, and the results of applying it to a transition from reversed to normal polarity.

Several successful experiments were carried out on modern lavas and on archaeomagnetic material to test the accuracy of the technique. The results of these experiments demonstrate that this technique gives accurate, consistent results.

The technique was applied to samples from lavas that were extruded during a palaeomagnetic field reversal. The variation of the magnitude of the palaeofield with time was successfully determined with a mean error (standard deviation) of only 0.03T (3000 gamma). The results indicate that the palaeofield was large and stable during a period when the virtual magnetic north pole seems to have lingered at the geographic equator. This and other published results suggest that an intermediate state of the geomagnetic field can exist which is sometimes as strong as the more usual normal and reversed states, and which endures metastably for short periods of time. This means, among other things, that any single transition may appear to be quite complex, although the <u>average</u> transition is known to involve fairly simple geometry. It also constrains future theories of the generation of the geomagnetic field to include the phenomenon of "intermediate metastable states".

ACKNOWLEDGEMENTS

It has been my good fortune to be able to work with the staff (both academic and technical) of the geophysics department and the physics department at Liverpool. I am particularly indebted to my supervisor Professor R.L. Wilson for his patience and understanding and for many hours of interesting and enlightening discussions.

I would like to thank Mr. A.G. McCormack for his advice and assistance in writing the computer programme, Mr. W. Williams and Mr. K. Rawlinson for carefully constructing much of the apparatus used, and Mrs. B. Bridges for her assistance with the magnetic measurements. I would also like to thank Professor B. Collinge, Mr. K. Aitchison and Mr. J. Share for there help and assistance with electronic equipment.

Mrs. D. Jones typed this thesis and I am extremely grateful to her.

My thanks are conveyed to the Natural Environment Research Council for providing a grant throughout the period of this research.

Finally I wish to thank my wife Joan for her patience, help and encouragement without which this thesis would not exist.

ACKNOWLEDGEMENTS

It has been my good fortune to be able to work with the staff (both academic and technical) of the geophysics department and the physics department at Liverpool. I am particularly indebted to my supervisor Professor R.L. Wilson for his patience and understanding and for many hours of interesting and enlightening discussions.

I would like to thank Mr. A.G. McCormack for his advice and assistance in writing the computer programme, Mr. W. Williams and Mr. K. Rawlinson for carefully constructing much of the apparatus used, and Mrs. B. Bridges for her assistance with the magnetic measurements. I would also like to thank Professor B. Collinge, Mr. K. Aitchison and Mr. J. Share for there help and assistance with electronic equipment.

Mrs. D. Jones typed this thesis and I am extremely grateful to her.

My thanks are conveyed to the Natural Environment Research Council for providing a grant throughout the period of this research.

Finally I wish to thank my wife Joan for her patience, help and encouragement without which this thesis would not exist.

TABLE OF CONTENTS

CHAPTER 1. THE MAGNETIC RECORDING

1.1 Introduction

The direction and magnitude of the earth's magnetic field can be determined directly, with a directional magnetometer, or indirectly by measuring some other quantity that is related to the magnetic field. Clearly direct measurements apply only at the time that the measurement was taken. Indirect measurements, however, can be used to determine the magnetic field at some time in the past and so can provide a record of the time variation of both the magnitude and direction of the earth's magnetic field.

Many materials have a permanent magnetisation which disappears when the material is heated above its Curie temperature (T_c), and reappears when cooled in a constant magnetic field. Koenigsberger (1938) was able to show that when an igneous rock cooled through its Curie temperature in the earth's magnetic field (geomagnetic field), it acquired a thermoremanent magnetisation (TRM) in the same direction as the geomagnetic field at the time of cooling. This property of igneous rocks and other heated magnetic materials (pottery, brick, fireplaces etc.) has enabled workers to determine the direction of the ancient geomagnetic field (palaeofield) at different places on the earth's surface back to 2650 m.y. ago (McElhinny et al, 1968).

The magnitude of a laboratory TRM was found to be proportional to the magnitude of the applied constant magnetic field (B_{lab}) for small fields of up to 10^{-4} T (Nagata, 1943). Provided that the natural remanent magnetisation (NRM) was formed by cooling through the Curie temperature in the palaeofield (B_{anc}), and that the NRM has remained unaltered from the time of cooling, then the value of B_{anc} can be simply calculated by comparing the NRM to a laboratory TRM formed in the same specimen (eq.1).

$$\frac{NRM}{TRM} = \frac{B_{anc}}{B_{lab}} \qquad \text{eq.1}$$

when B_{anc} is the only unknown

Unfortunately the magnetic minerals often become chemically and magnetically altered when heated to high temperatures (400 to 700°C) to form the TRM. This means that eq.1 is no longer valid because the NRM and the TRM were not formed in the same set of magnetic minerals. This thesis describes how the alteration due to heating can be observed and in many cases isolated so that the correct value of B_{anc} can be obtained from thermally altered specimens.

1.2 The magnetic minerals

The magnetic minerals, which contain the NRM, carry with them a record of the direction and magnitude of the palaeofield.

The magnetic minerals contained in igneous rocks and pottery are the iron oxides and the iron sulphides. The iron oxides are by far the most common. They are within the F_eO - TiO_2 - Fe_2O_3 ternary system (figure 1) which can be generally divided into two types of magnetic minerals.

The first type of magnetic mineral varies in composition from Fe_2TiO_4 (ulvöspinel) to Fe_3O_4 (magnetite). This type is generally known as titanomagnetite and has a face-centred cubic crystal structure.

The second type of magnetic mineral varies in composition from $FeTiO_3$ (ilmenite) to Fe_2O_3 (haematite). This type is generally known as titanohaematite and has a rhombohedral crystal structure. Titanomagnetite is very strongly magnetic but is generally more easily demagnetised (is magnetically softer) than titanohaematite. These magnetic minerals can be magnetised in many different ways but, at present, thermally formed NRM's are usually used to determine the magnitude of the palaeofield.

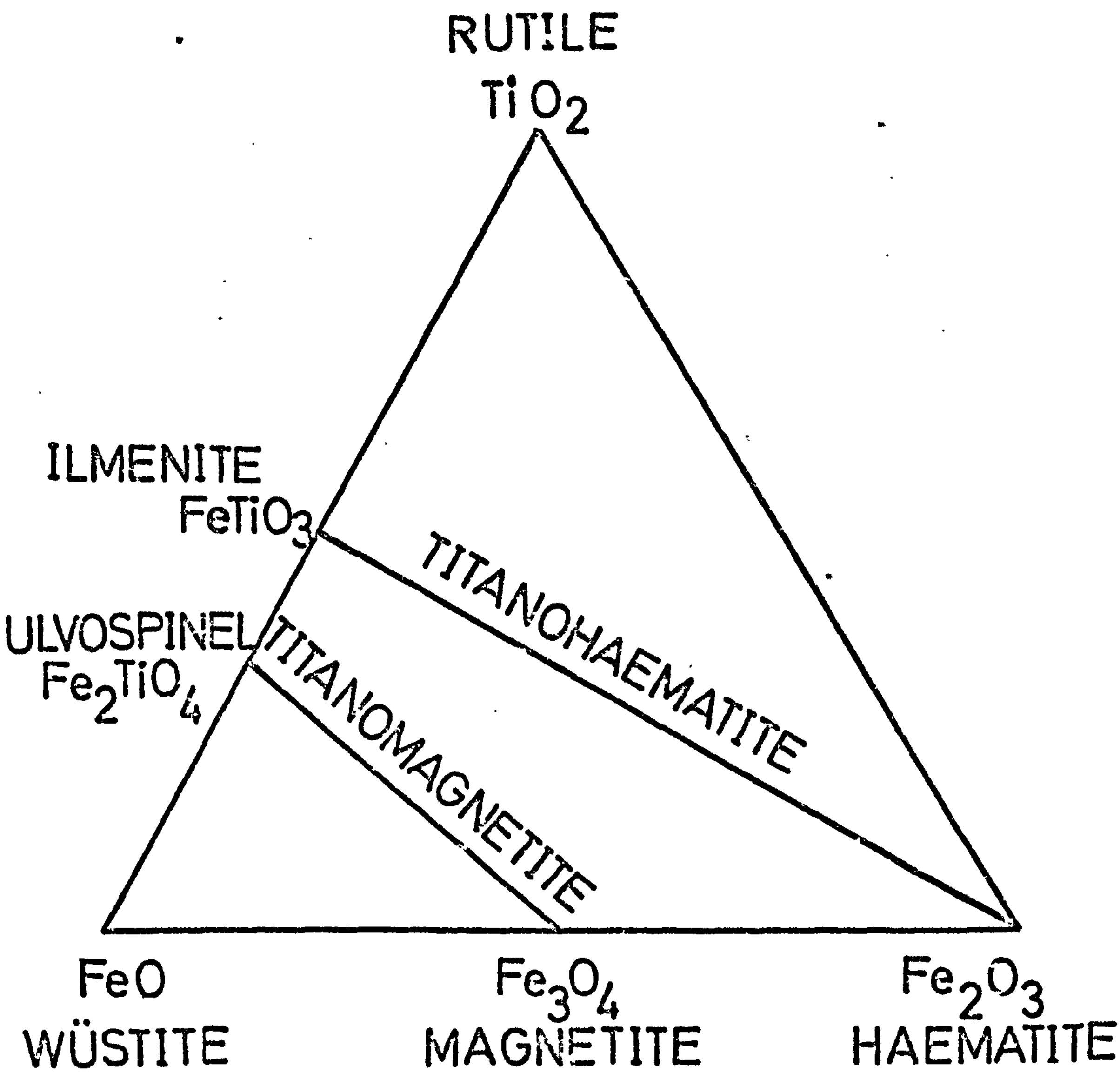
RUTILE
TiO_2
ILMENITE
$FeTiO_3$
ULVOSPINEL
Fe_2TiO_4
TITANOHAEMATITE
TITANOMAGNETITE
FeO
WÜSTITE
Fe_3O_4
MAGNETITE
Fe_2O_3
HAEMATITE

FIG 1.

1.3 Ways of magnetising the magnetic minerals

It is very important to know how the NRM of a specimen was formed. Different types of magnetisation must be interpreted in different ways so that reliable information may be obtained. In this section we shall see how the most common forms of magnetisation are created.

Thermal remanent magnetisation (TRM)

This is the most common form of NRM used in palaeomagnetic studies and is almost exclusively the only form of NRM from which the magnitude of the palaeofield can be determined.

A TRM is formed by heating a specimen to at least its Curie temperature, thus destroying any previously acquired magnetisation, and then allowing it to cool in a constant magnetic field. The acquired TRM is in the same direction as the constant magnetic field and the magnitude of the TRM is proportional to the magnitude of the constant magnetic field.

A specimen may be given a partial TRM (PTRM) by not heating it to its Curie temperature but only to some lower temperature T which exceeds the blocking temperatures of some of the grains of magnetic material within the specimen. The magnitude of a PTRM is always smaller than the magnitude of a full TRM for the same applied constant magnetic field and the same specimen.

We shall see later how PTRM's have been used to determine the magnitude of the palaeofield.

Chemical remanent magnetisation (CRM)

When a new magnetic mineral is formed chemically, below its Curie temperature, in a constant magnetic field, it acquires a C.R.M. in the direction of the applied field. This form of magnetisation often occurs in nature (e.g. in red sandstones) and has been used to determine the direction of the palaeofield.

Viscous remanent magnetisation (VRM)

When a magnetic specimen is placed in a weak constant magnetic field it slowly builds up a VRM in the same direction as the applied field. The VRM is proportional to the logarithm of the time of exposure to the magnetic field, and has been used to determine the age of the last major geomagnetic field reversal Heller and Markert, 1972).

Isothermal remanent magnetisation (IRM)

When a magnetic specimen is exposed to a constant magnetic field and is then retracted it has acquired an IRM in the direction of the applied field. For weak fields the IRM is very small but increases with increasing field strength up to a maximum value called the 'saturation IRM'.

Piezo remanent magnetisation (PRM).

A PRM is created when a specimen is stressed in a constant magnetic field. The stress allows the specimen to approach an equilibrium magnetisation in the applied field and it retains part of this magnetisation when the stress is removed. (Kawai et al 1959, Domen 1962).

Anhysteretic remanent magnetisation (ARM)

An ARM is given to a specimen by simultaneously applying a small constant magnetic field and an alternating field (a.f.). The a.f. is gradually increased to some maximum peak value, B_{max}, and then gradually reduced to zero. All the grains of magnetic material with coercive forces less than B_{max} will be influenced by the constant magnetic field and, when the a.f. is reduced to zero, will acquire a net ARM in the direction of the applied field.

Generally the a.f. is applied in the same direction as the constant field but we will see later that tumbling the specimen in the a.f., while keeping the constant field fixed in the frame of reference of the specimen, produces a larger ARM. This is because some grains of magnetic material have preferred directions of magnetisation.

The 'tumbling' ARM is formed in the laboratory and we will see later how it can be used as a powerful tool to determine the magnitude of the palaeofield.

Detrital remanent magnetisation (DRM)

This is formed when previously magnetised grains are deposited through water in a small constant magnetic field. The magnetic field tends to align the grains so that the sediment that is formed has a magnetisation parallel to the magnetic field.

As we have seen there are many ways in which a constant magnetic field can be recorded as a magnetisation. The direction of the magnetic field is easily retreived from most forms of magnetisation but the TRM is, at present, the form of magnetisation from which the magnitude of the magnetic field is usually determined. It is important to realise that while the origional NRM may have been thermally formed, the specimen may also have many other subsequently added components of magnetisations that must be removed before eq.1 can be applied.

1.4 Ways of demagnetising the magnetic minerals

We usually demagnetize specimens because they contain unwanted components of magnetisation. An unwanted component of magnetisation (eg. VRM) can often be preferentially demagnetised leaving some of the original NRM intact.

Demagnetising techniques can also be used to divide the NRM into small units that can be individually measured and used. In this way as many as twenty measurements of the direction and magnitude of the palaeofield can conveniently be made on one specimen.

This section describes the most common ways of demagnetising the magnetic minerals.

Thermal demagnetisation

When a specimen is thermally demagnetised it is heated to some temperature T and cooled in zero magnetic field. All the magnetic grains with blocking temperatures less than or equal to T will become magnetised as the specimen is cooled but, because there is no constant magnetic field to align the individual magnetic moments, they will become magnetised in different directions and the nett result is a decrease in the magnetisation of the specimen.

This process can be repeated to higher and higher temperatures until the specimen's Curie temperature is exceeded and the specimen is then completely demagnetised. This technique is particularly useful for removing PTRM's which were gained when the specimen was re-heated at some time, possibly by contact with another hot object or burial to some depth.

<u>Anhysteretic demagnetisation (or a.f. demagnetisation)</u>

If a specimen is placed in an a.f. of maximum amplitude B_{max}, all the magnetic moments with coercive forces less than B_{max} will become statistically aligned by any constant magnetic field as the a.f. is slowly reduced to zero. If there is no constant magnetic field to align the magnetisations of the grains, then the individual magnetisations will become randomly oriented and the total magnetisation of the specimen will be reduced.

Specimens are often tumbled while being a.f. demagnetised. This reduces the effects of any stray steady magnetic fields.

This technique can be used to remove unwanted VRM, IRM, CRM, and ARM. We will see later how it can be used to divide the total magnetisation (NRM or TRM) into components from which B_{anc} can be calculated.

<u>Chemical demagnetisation</u>

Chemical demagnetisation is usually carried out on red sediments (Collinson 1965). The specimens are placed in cold concentrated hydrochloric acid which dissolves away the red cement. This technique is used to remove chemically grown remanences.

Low temperature demagnetisation

When a magnetised specimen is repeatedly cooled to liquid nitrogen temperatures the magnetisation is partially demagnetised. Ozima et al (1964) have demonstrated that IRM is preferentially demagnetised in this way. However, no subsequent worker has demonstrated that this is a useful demagnetisation technique for palaeomagnetic purposes.

In this chapter we have seen how a magnetic specimen can carry a recording of the direction and magnitude of the palaeofield. We have observed how a stable magnetisation can be formed and how unwanted components can possibly be removed. With this knowledge we can now examine the techniques that have been used to determine the magnitude of the palaeofield and then go on to develop a new technique that will overcome the problem of magnetic changes that occur when a specimen is heated to give it a TRM in the laboratory.

CHAPTER 2. TECHNIQUES THAT ARE USED TO DETERMINE THE MAGNITUDE OF THE PALAEOFIELD

2.1 Introduction

In chapter one we observed that both the magnitude and the direction of the palaeofield are recorded as the NRM of some specimens. We know that if the NRM is a TRM then equation 1 can be applied to determine B_{anc}, because the NRM can be directly compared to a laboratory TRM given in a known field, B_{lab}.

$$\frac{NRM}{TRM} = \frac{B_{anc}}{B_{lab}} \qquad \text{eq.1}$$

This only applies if no chemical or magnetic alteration has occurred due to the heating of the sample when the TRM was formed.

There are many ways in which B_{anc} has been determined in the past. Most of these techniques use equation 1 combined with some method for detecting if any thermal alteration has occurred during the TRM heating.

This chapter describes how these techniques are used to determine B_{anc}.

2.2 Thermal methods

Koenigsberger (1938) and later Momose (1963) compared the total NRM to the total TRM formed in the laboratory. This method gives only one ratio of $\frac{NRM}{TRM}$ per specimen, will not detect any thermal alteration, and assumes that the NRM has remained unaltered from the time of formation. Results obtained in this way cannot now be considered to be very reliable estimates of the magnitude of the palaeofield.

Thellier and Thellier (1959) developed a technique that divides the NRM and the TRM into small units, each unit giving a value of the ratio $\frac{NRM}{TRM}$. The technique involves heating the specimen to successively higher temperatures T1, T2, T3 ...... up to the Curie temperature Tc. The NRM is first thermally demagnetised to T1 and measured (NRM (T1)).

The specimen is then given a PTRM in the region below temperature T1 (PTRM (T1)). This is repeated for higher temperatures until Tc is exceeded.

By plotting a graph of the NRM remaining against the TRM gained, at different temperatures, the mean $\frac{NRM}{TRM}$ ratio can be calculated.

When the specimen has been heated to say 300°c then all the data determined below this temperature are redetermined to ensure that no mineral change has occurred. This procedure is very time consuming but the repeated comparison of data is a very good check that no mineralogical changes have occurred.

Unfortunately mineral changes usually do occur at high temperatures and so the estimate of B_{anc} must frequently be made only on the low temperature region of the graph. This is the region that is most affected by other secondary magnetisations (VRM) which can cause errors when determining B_{anc}, and therefore it is not the ideal region of temperature for study. Nevertheless, this method has been extensively applied by many people and is considered to be one of the most reliable methods available. The Thelliers' method has been most successful when applied to archaeological specimens. Attempts have been made to apply it to igneous rocks (Coe 1967 , Kono 1974) but the "success rate" has been very low even when samples are carefully selected.

Wilson (1961) developed a faster thermal technique. He progressively thermally demagnetised the NRM, measuring it at the temperatures concerned. He then gave each specimen a TRM and this was also thermally demagnetised and measured at the same temperatures as the NRM.

Equation 1 was applied to each temperature interval and a series of values of B_{anc} determined. This technique will not detect any thermal alteration of the magnetic minerals unless the alteration is such that the apparent values of B_{anc} continuously increase or decrease with increasing temperature. This indicates a change in the shape of the blocking temperature spectrum.

As we shall see later, thermal alteration can often alter very deceptively the magnitude of a TRM without noticeably altering the shape of the TRM demagnetising curve.

Of these three methods the later two are the most useful. They both divide the NRM and TRM into thermal intervals and so B_{anc} can be determined from PTRM's of the type found in naturally baked rocks.

Wilson's method is fast but the Thelliers' method has more checks to detect and isolate thermal alterations so that B_{anc} can often be calculated from the low temperature part of the blocking temperature spectrum. Unfortunately the Thelliers' method requires many heatings of the specimen and this tends to increase the degree of alteration.

Let us now go on to consider some of the techniques that use a.f. demagnetisation as a means of dividing up the NRM and TRM into smaller units, that can each be used to determine B_{anc}.

2.3 Alternating field methods

Van Zijl (1961) and later Smith (1967(a)), Carmichael (1968), McElhinny et al (1968) and Abranson (1970) all used the basic technique of a.f. demagnetisation to divide the NRM and TRM into small units that can be used in equation 1.

Van Zijl (1961) used only one $\frac{NRM}{TRM}$ ratio after demagnetising both the NRM and the TRM in a 2.19×10^{-2}T peak a.f.. This method, like that of Koenigsberger (1938), has no alteration checks although the a.f. demagnetisation will probably remove most of the VRM acquired since the time of formation of the specimen.

Smith 1967(a)) Carmichael (1968) and Abranson (1970) used a number of a.f. intervals in which B_{anc} was determined. This technique, like Wilson's method, will detect any change in the shape of the TRM demagnetising curve. Thermal alterations, as we shall see later, usually result in a change in the magnitude of the TRM without changing much the shape of the TRM demagnetising curve. This type of alteration will give a consistently wrong value of B_{anc}, which cannot be detected.

Smith used several tests in an attempt to isolate thermally altered specimens.

He looked for changes in:-

a) High field (0.5T) Curie temperatures before and after heating.

b) Saturation magnetisation before and after heating.

c) Repeatability of saturation magnetisation heating curves.

d) The temperature at which the remanent magnetisation is completely demagnetised.

e) Shape of the NRM and TRM curves during a.f. demagnetisation.

Using the checks he was able to observe that some specimens were thermally altered. He was not able to isolate the alteration in any particular specimen and so he only used those specimens that were apparently almost completely unaltered. This restriction makes the method time consuming without improving on the reliability of the Thelliers' method.

McElhinny and Evans (1968) used the same a.f. demagnetisation of both the NRM and the TRM to determine a series of values of B_{anc}. One of their alteration tests involved the comparison of saturation IRM before the after heating. Each IRM was a.f. demagnetised and the two curves compared. If no change has occurred the curves will be identical. In some cases however they detected changes in the IRM's but no change in the $\frac{NRM}{TRM}$ ratios. This indicates that the TRM and saturation IRM are not closely related and that an observed change in one cannot be used to isolate a change in the other.

All the a.f. techniques described here can only be used on specimens that do not alter when heated. The tests are used simply to reject those which do alter.

There is a great need for a technique that is fast, requires only one heating (to minimise alteration), and can detect and isolate thermal alterations so that reliable results can be obtained even from thermally altered specimens. This technique would increase the 'yield' of results for a given amount of work, by several times. Such a method has been developed and is described in the next chapter.

CHAPTER 3. A NEW WAY OF DETERMINING THE MAGNITUDE OF THE PALAEOFIELD

3.1 Introduction

Several techniques for determining the magnitude of the palaeomagnetic field have been described. They all assume that the NRM was thermally formed and so equation 1 can be used to determine B_{anc}.

$$\frac{NRM}{TRM} = \frac{B_{anc}}{B_{lab}} \qquad \text{eq.1}$$

The most successful techniques use a series of values of the ratio $\frac{NRM}{TRM}$ to determine a mean value of B_{anc} for one specimen. The NRM and the TRM can be divided into smaller units by either a.f. or thermal step-wise demagnetisation. If all the individual units give the same $\frac{NRM}{TRM}$ ratio then most workers have assumed that the TRM was formed without any alteration occurring to the magnetic minerals.

In this chapter we will see that alteration of the magnetic minerals during the TRM process can produce a consistently wrong $\frac{NRM}{TRM}$ ratio. We will then go on to develop a technique for detecting and isolating all forms of thermal alteration.

3.2 A typical case of thermal alteration

I was very fortunate in being able to obtain a piece of the 1910 Etna lava from Dr. J.C. Tanguy. This lava had cooled in the known constant geomagnetic field of 0.42×10^{-4}T.

I compared the values of NRM and TRM, after a.f. demagnetisation, by plotting the NRM against the TRM using the peak a.f. value as a parameter (figure 2). The TRM was given in a constant magnetic field of 0.5×10^{-4}T. The points fall on a straight line but the derived value of B_{anc} is only 0.28×10^{-4}T, two thirds of the correct value. It is not likely that the specimen has become altered from the time of formation (only 64 years), and so it would seem that this incorrect value of B_{anc} is the result of thermal alteration that occurred during

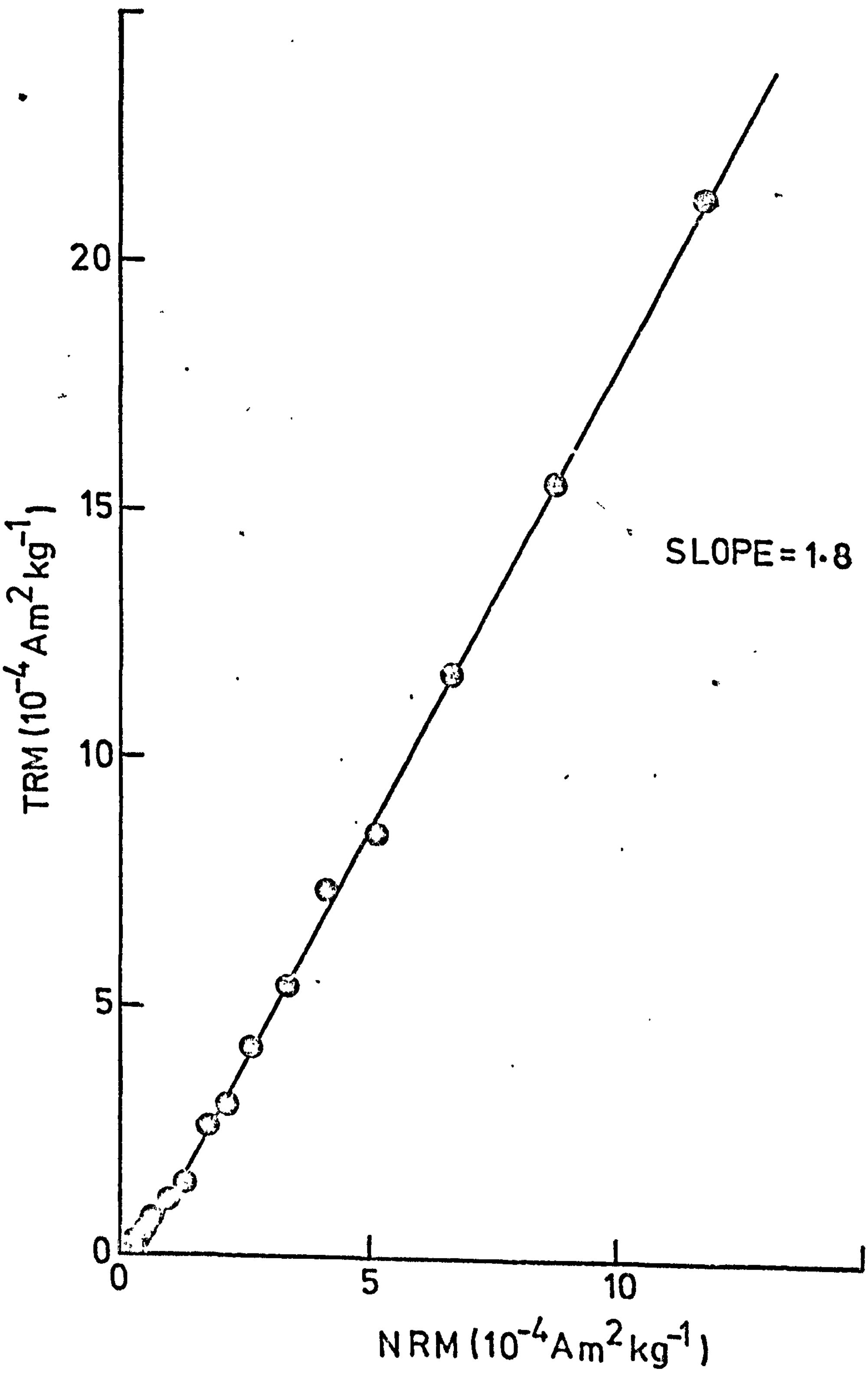

FIG 2.

the TRM heating.

This form of thermal alteration changes the magnitude of the TRM but changes very little the shape of the TRM A.F. demagnetisation curve and so we will call it "consistent alteration".

It would seem likely that the large errors previously associated with most studies of the magnitude of the palaeofield may be due to consistent alteration. This form of alteration cannot be detected by simply comparing the NRM and the TRM because the NRM and the TRM demagnetisation curves have nearly the same shape and so always give the same consistent answer.

3.3. A way of detecting and isolating all forms of thermal alteration

We have seen that consistent alteration can be detected if we know both B_{anc} and B_{lab}. This is clearly not much help in cases where B_{anc} is unknown.

One solution would be to a.f. demagnetise the NRM and then re-magnetise the specimen in some way that would not alter the magnetic minerals (call it XRM(1)). We could then give the specimen a TRM and a.f. demagnetise it, and then give the specimen a further magnetisation, XRM(2).

If XRM(1) and XRM(2) are created under the same conditions and in the same constant magnetic field then, if no thermal alteration has occurred, both XRM(1) and XRM(2) will have the same magnitude and shape of demagnetization curve. If consistent alteration has occurred then the XRM(1) and XRM(2) demagnetization curves will not be identical.

This technique will detect consistent alteration but, if we demagnetise both XRM(1) and XRM(2) and plot a graph of XRM(1) against XRM(2) using the peak a.f. value as a parameter, we may be able to see if there is some unaltered a.f. interval where the slope of the line is 1.0. If we can find a suitable form of magnetisation for the XRM we may be able to relate a particular unaltered a.f. region of the XRM to the equivalent a.f. region of the TRM and, in this way, use an unaltered region of the TRM demagnetisation curve to determine the correct value of B_{anc}.

Clearly the XRM must be a very special type of magnetisation which is not too dissimilar to a TRM and yet it must be formed in such a way that its a.f. demagnetisation curve can be directly associated with the a.f. demagnetisation curve of the NRM and the TRM. The XRM and the TRM do not necessarily need to have the same shape of demagnetisation curve, but it the magnetic minerals become altered in such a way that in the TRM only a particular a.f. interval is affected, then the XRM must somehow demonstrate the alteration within that same a.f. interval. I have chosen an ARM as having the best properties for use as an XRM.

3.4 The tumbling ARM

When the TRM (or NRM) has been a.f. demagnetised it can be replaced by heating the specimen and giving it another TRM. Another way of "replacing" the TRM (or NRM), after a.f. demagnetisation, is to reverse the demagnetising process.

The precise inverse of the demagnetising process is to tumble the sample in an a.f. field while applying a constant magnetic field along one axis of the specimen. This means that the specimen and the constant magnetic field are tumbled together. The a.f. is then raised to some high value and then reduced to zero. The magnetisation produced in this way is a type of ARM but, because the specimen and the constant magnetic field were being tumbled, we will call it a tumbling ARM to distinguish it from the usual stationary ARM. This tumbling ARM will not alter the magnetic minerals and can therefore be used as XRM.

Another 1910 Etna specimen was given a tumbling ARM after the NRM was a.f. demagnetised (call this ARM(1)) and another after the TRM was a.f. demagnetised (call this ARM(2)) so that we have four sets of demagnetisations all carried out under the same conditions on the same specimen, and in the same a.f. intervals.

The ARM(1), ARM(2) and TRM were all given in a 0.5×10^{-4}T constant magnetic field.

If we plot ARM(1) against ARM(2) and fit a straight line of gradient 1.0 to the points, rejecting those points that do not fit the line (marked R for rejected) we can see in figure 3 that the high a.f. region (0.045 to 0.130T) fits the line very well and that therefore it is reasonable to suppose that the magnetic minerals with coercive forces in the range 0.045 to 0.130T have remained unchanged by the heating to give the TRM. If we then plot NRM against TRM (figure 4) rejecting those points which correspond to the altered region of figure 3 (also marked R for rejected), and fit a straight line to only the accepted a.f. region (inset figure 4); then we obtain the already known correct value of B_{anc} (0.42×10^{-4}T) because this a.f. region is unaltered.

Because the unaltered region is continuous from 0.045T peak a.f. up to the maximum value of 0.130T peak a.f., we assume that the graph of NRM against TRM passes through the origin. This corresponds to an infinite demagnetising field. We have constrained the straight line to pass through the origin, therefore.

Using this new technique we can attempt to detect and isolate any thermal alteration of the TRM demagnetising curve. If the NRM is thermally formed and has remained unaltered, at least in some a.f. region, then we can determine B_{anc} provided that the alteration is limited to a particular a.f. region.

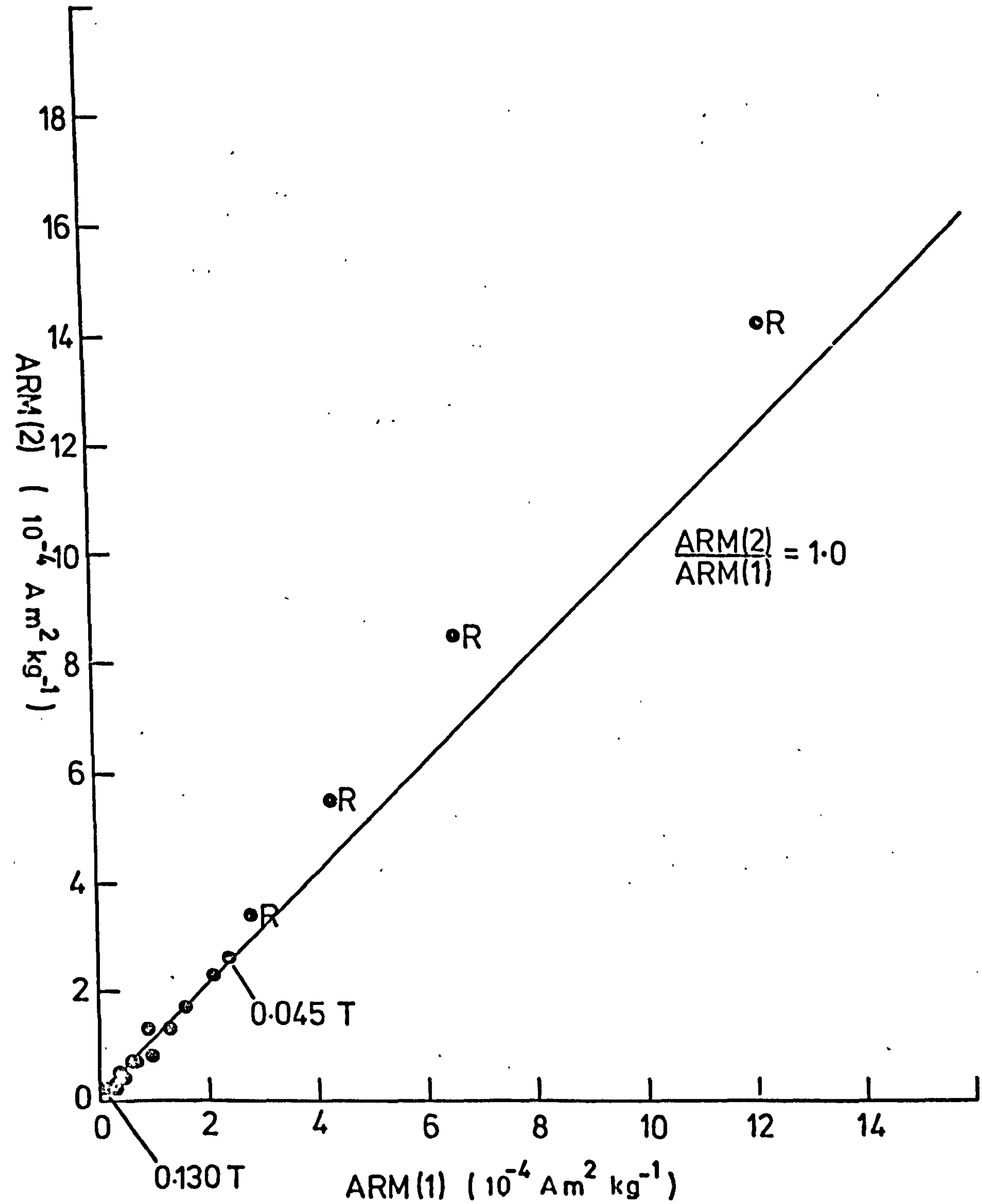

ARM(2) (10⁻⁴ A m² kg⁻¹)
18
16
14
12
10
8
6
4
2
0
R
R
R
R
$\frac{ARM(2)}{ARM(1)} = 1{\cdot}0$
0·045 T
0·130 T
0
2
4
6
8
10
12
14
ARM(1) (10⁻⁴ A m² kg⁻¹)

FIG 3.

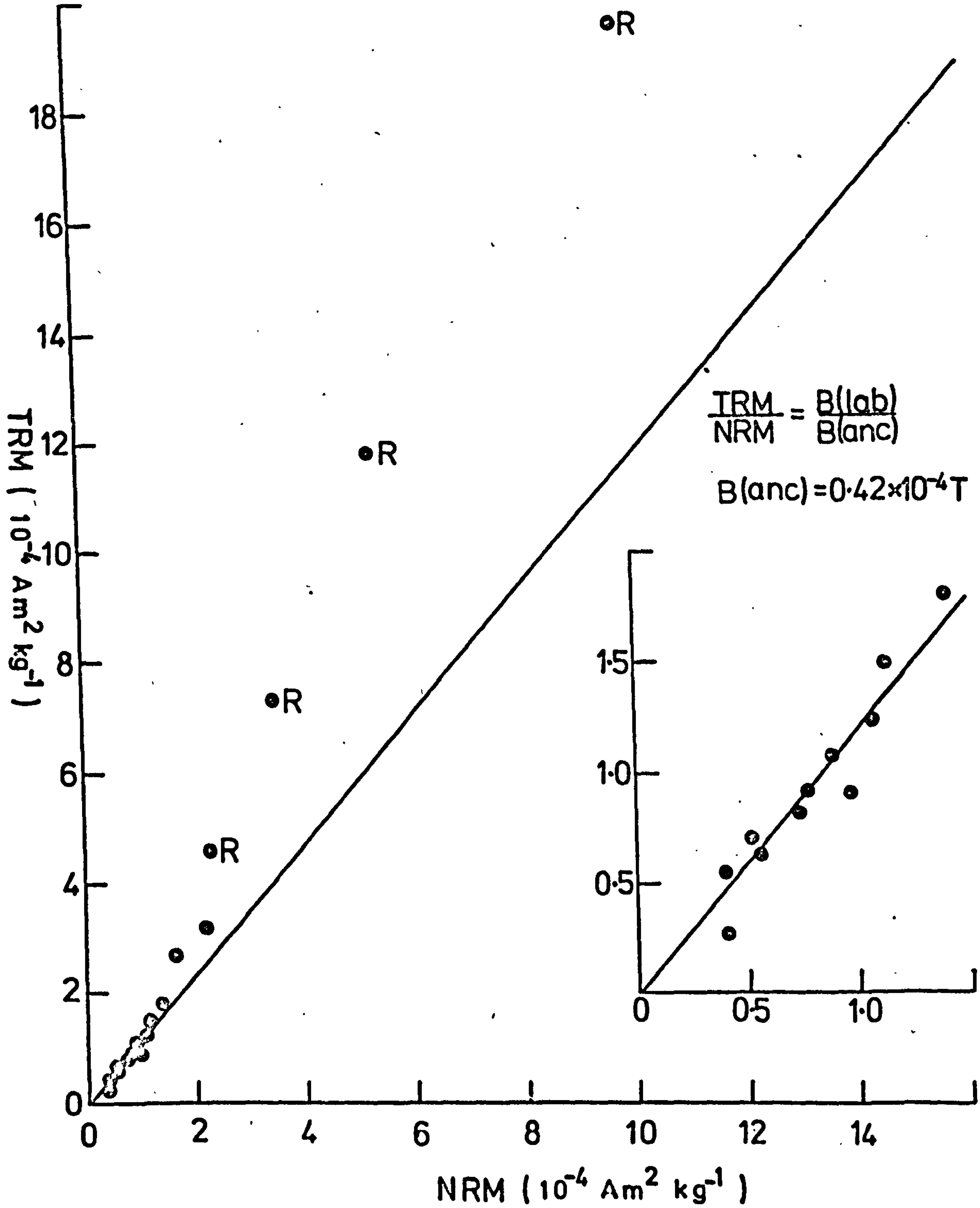

TRM (10^{-4} Am^2 kg^{-1})
NRM (10^{-4} Am^2 kg^{-1})
R
R
R
R
$\frac{TRM}{NRM} = \frac{B(lab)}{B(anc)}$
B(anc) = 0·42×10^{-4}T
0
2
4
6
8
10
12
14
16
18
0·5
1·0
1·5

FIG 4.

CHAPTER 4. EXPERIMENTAL PROCEDURE

4.1 Introduction

We have seen, in chapter 3, how thermal alteration may be detected and isolated in some a.f. region of the TRM a.f. demagnetisation curve. This chapter is a detailed description of how the magnitude of the palaeomagnetic field can be experimentally determined.

4.2 Producing a tumbling ARM

In order to produce an ARM (tumbling) I built a small set of five Rubens coils (Rubens 1945) around a perspex specimen holder (inset figure 5). Brass contact plates were glued to the ends of the holder. These brass plates were in electrical contact with the copper tumbling shafts. Current was passed into the system via two spring loaded carbon brushes in contact with the tumbling shafts. A constant current power supply was used to supply current to the coils. It was isolated from any induced currents by a filter circuit.

The magnetic field distribution within the coil system was calculated by Rubens. I checked the distribution along the axis of the coils by giving a thin (3 m.m.) slice of magnetic material an ARM, measuring the magnetisation produced at different places along the axis of the coils (figure 5). The magnetic field was very constant over the normal maximum specimen length (2.5 c.m.), and so the positioning of the specimen within the coils is not critical.

Tests were carried out using a 0.5×10^{-4} T constant magnetic field in the coils, to determine the relationship between a rotating and a static ARM (figure 6). They do not have the same shape a.f. demagnetisation curves and are therefore not equivalent. We can now produce a rotating ARM, which we will just call an ARM, and can go on to examine the experimental procedure for determining the magnitude of the palaeomagnetic field.

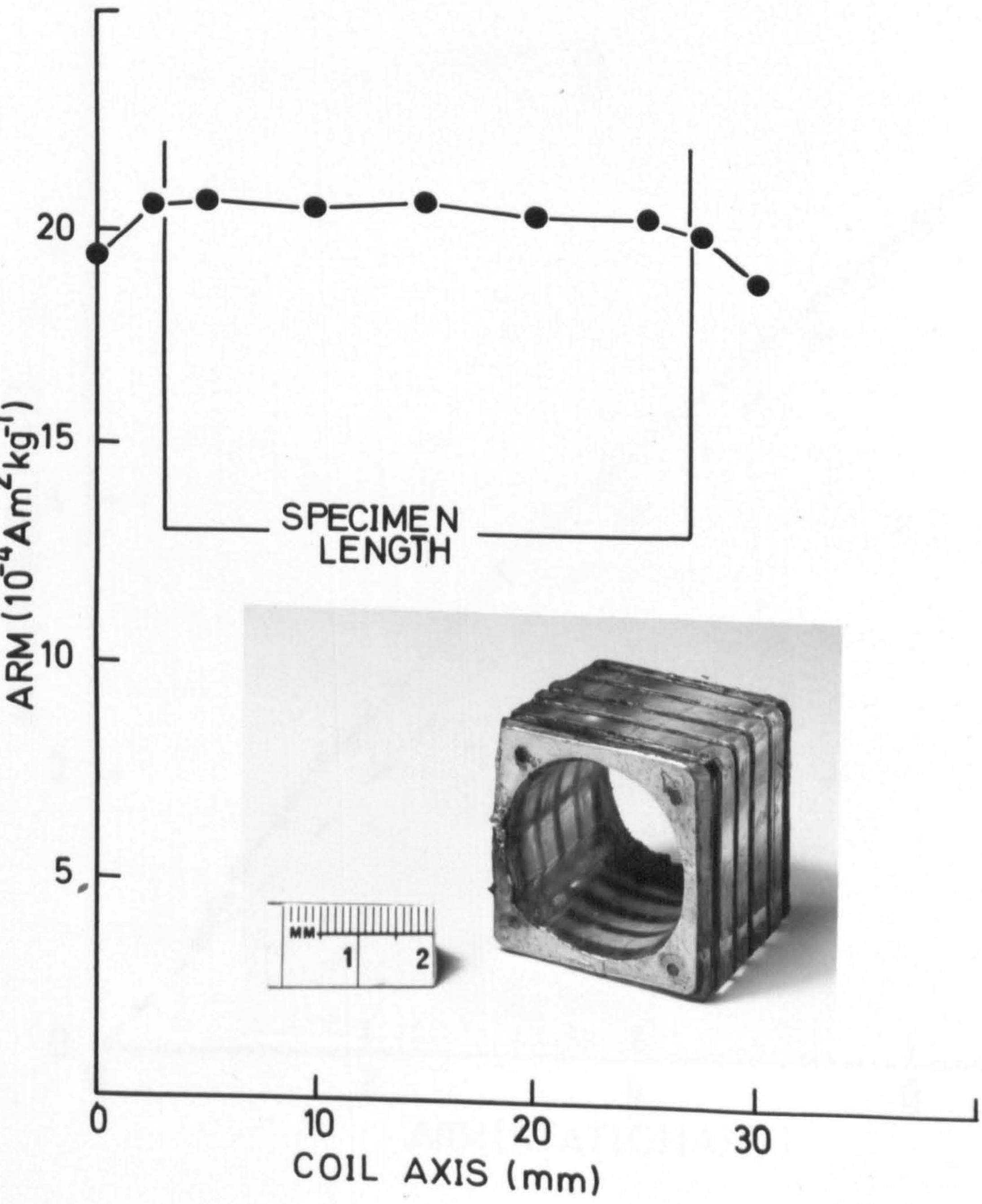
20
15
10
5
ARM (10^{-4} Am^2kg^{-1})
SPECIMEN LENGTH
MM
1
2
0
10
20
30
COIL AXIS (mm)

FIG 5.

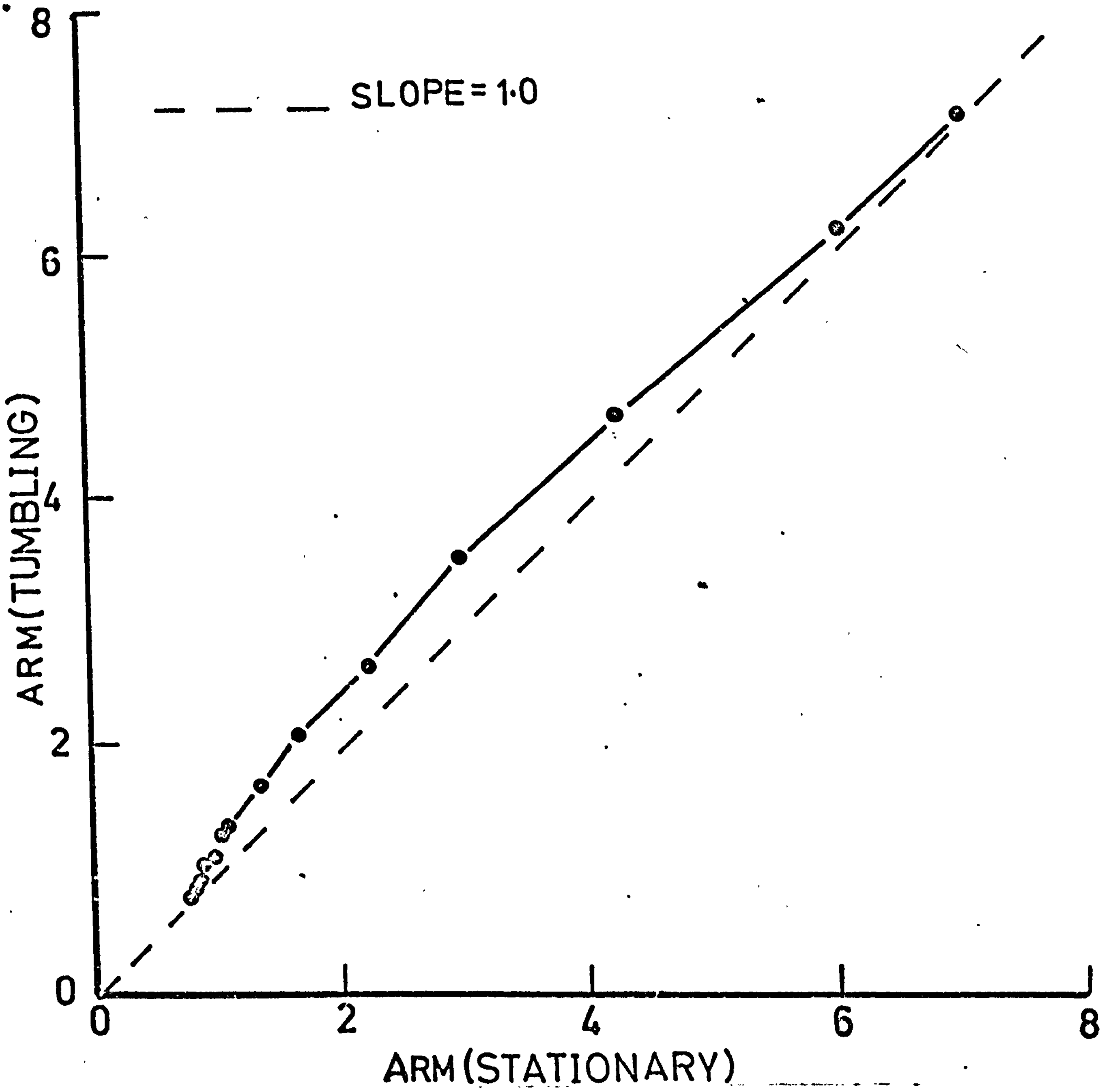

FIG 6. A graph of ARM(tumbling) against ARM(stationary) using the a.f. demagnetising field as a parameter.

4.3 Experimental procedure

The magnitude and direction of the palaeofield are determined in the following way:-

1. The Curie temperature (Tc) is determined (figure 7) from a small piece of the specimen, on a high field Curie balance. This value agrees with the Curie temperature determined from the magnitude of the PTRM gained with increasing temperature (figure 8), which I have assumed to be the same as the Tc of the NRM.

2. The NRM is a.f. demagnetised with increasing values of the peak a.f. The remaining NRM is measured after each successive demagnetisation up to the maximum demagnetising field. The same demagnetising intervals are used in all later demagnetisations of the specimen.

3. The specimen is then given an ARM (called ARM(1)) in the maximum peak a.f. used in 2. The ARM(1) is given along the axis of the cylindrical specimen and so only the one component of magnetisation need be measured after each demagnetisation.

The ARM(1)) is completely removed after a.f. demagnetisation in the maximum peak a.f. used in 2. When the ARM(1) has been completely removed that part of the NRM that has not been a.f. demagnetised in 2 still remains, and the axial component of this remaining NRM will be measured with the ARM(1) and will remain even after the ARM(1) has been completely a.f. demagnetised. Thus the measured magnetisation after a.f. demagnetisation in the maximum peak a.f. is always less than or equal to the total remaining NRM finally measured in 2.

4. The specimen is then given a TRM, by heating it above its Tc (determined in 1) and allowing it to cool to room temperature, in a constant magnetic field of 0.50×10^{-4} T along one axis of the specimen. This TRM is a.f. demagnetised and measured in the same way as ARM(1).

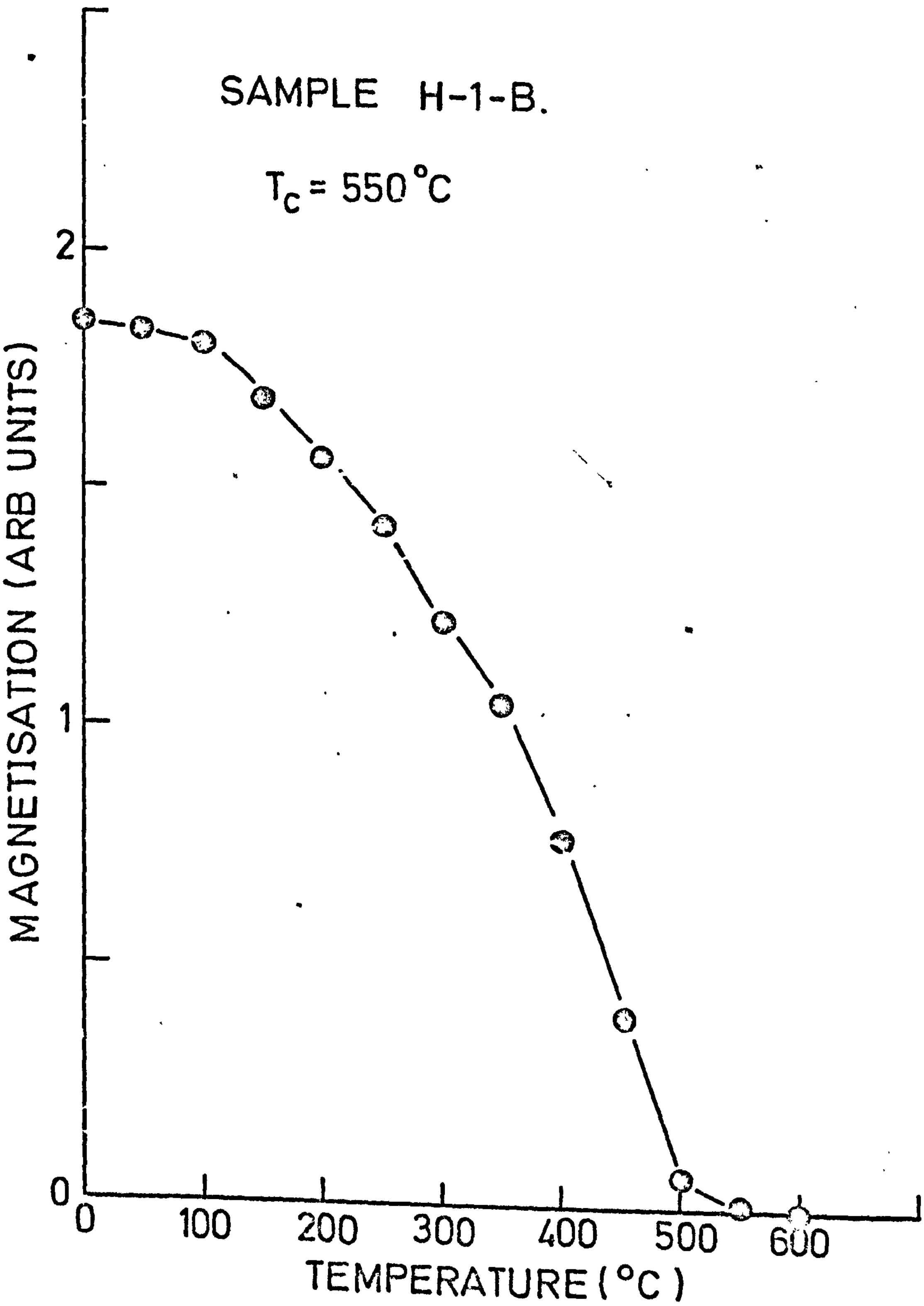
SAMPLE H-1-B.
T_c = 550°C
MAGNETISATION (ARB UNITS)
0
1
2
0
100
200
300
400
500
600
TEMPERATURE (°C)

FIG 7.

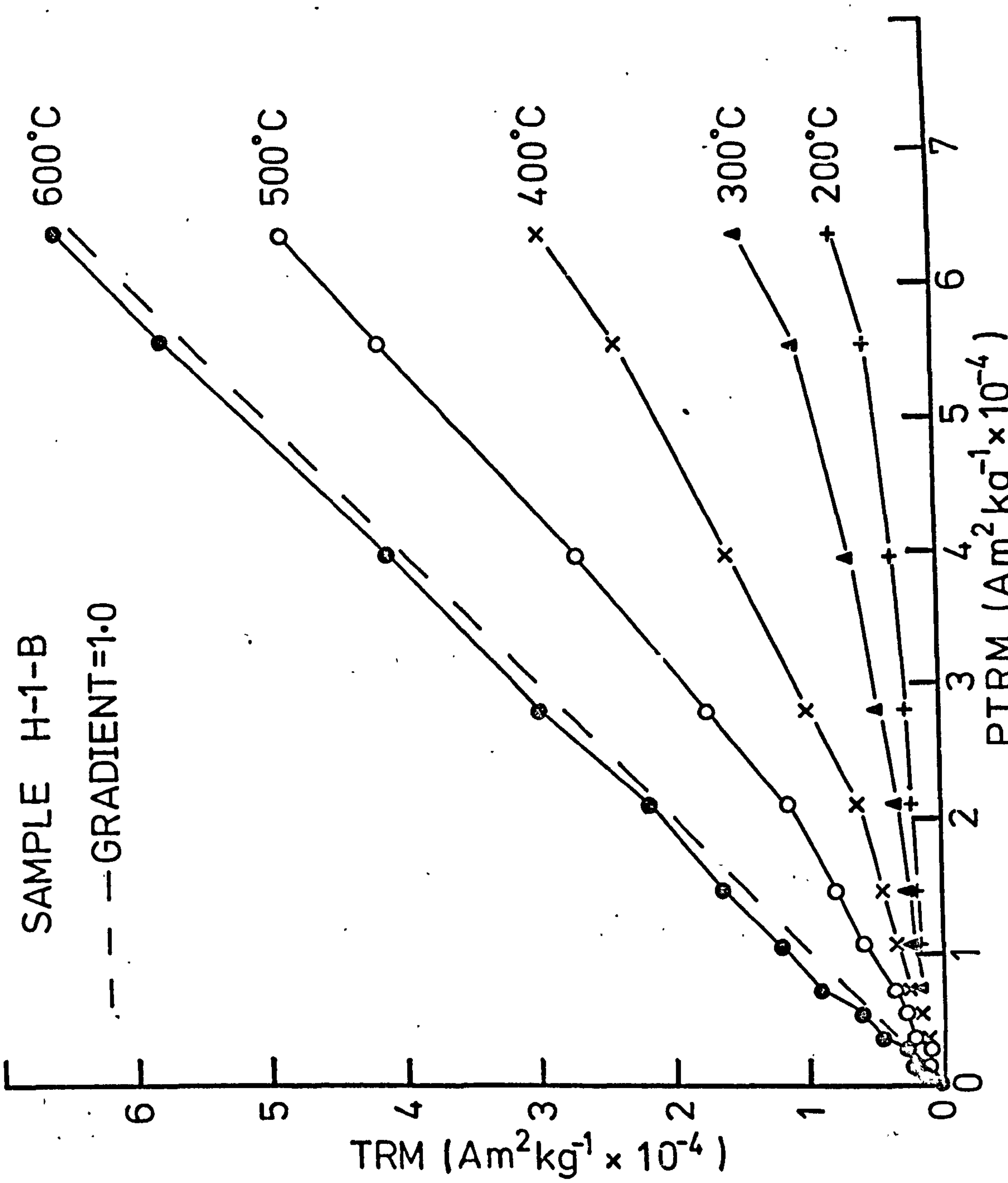

FIG 8.A graph of TRM given in a 0.5×10^{-4}T field at 700°C against PTRM given in a 0.5×10^{-4}T field at various temperatures. Tc is between 500 and 600°C.
ARM checks for thermal alteration were made after each heating.

5. The specimen is then given ARM(2) under the same conditions and in the same constant magnetic field that ARM(1) was given. This ARM(2) is a.f. demagnetised and measured as in 3.

6. A plot of ARM(2) against ARM(1), using the a.f. demagnetising field as a parameter, will give a straight line with gradient = 1.0 if the specimen is unaltered after heating.

A line of gradient = 1.0 is fitted to the points by the method of least squares. If the points do not fit the line within the 95% confidence level of the chi-squared distribution then the point with the largest deviation is rejected and the line re-fitted to the remaining points. This process is repeated until the remaining points fit the line within the 95% confidence level.

Empirically, only those data at the low a.f. end of the a.f. demagnetisation curve were rejected by this test, for any specimens so far investigated.

Within the remaining high coercive force range the ARM(1) and ARM(2) are identical and therefore this region of the a.f. demagnetisation curve has not been altered.

7. The TRM is plotted against the NRM using the a.f. demagnetising field as a parameter. The best straight line is fitted only to those points corresponding to the unaltered a.f. region determined in 6. The line is constrained to pass through the origin, which is the point corresponding to an infinite demagnetising field, and is fitted to the points by the method of least squares. If the points do not fit the line within the 95% confidence level of a chi-squared distribution, then the point with the largest deviation is rejected and the line re-fitted to the remaining points. This process is repeated until the remaining points fit the line within the 95% confidence level.

If more than one specimen is used from each sample, a mean value of B_{anc} is calculated by weighting each individual value of B_{anc} by the inverse variance of the NRM against TRM straight line determined for that specimen. In this way the best fitting straight lines are more strongly weighted.

A computer program was developed to analyse the data and draw the graphs (appendix 1). The computer is instructed first to plot all the points (NRM against TRM and ARM(1) against ARM(2). These graphs are then repeated with the accepted data only. The accepted data must be in a continuous a.f. region preferably terminating in the maximum a.f. used so that the origin of the NRM/TRM graph can be used to constrain the slope of the NRM/TRM graph.

In the next chapter we will go on to test this new technique on both lavas and man-fired artifacts which cooled in known fields (except in one case), to test that the derived values of B_{anc} are correct.

CHAPTER 5. TEST RESULTS

5.1 Introduction

In the last chapter be described how the magnitude of the palaeomagnetic field could be empirically determined. In this chapter we will test the method to ensure that the derived results are consistent and correct.

5.2 Application to a single lava

I was very fortunate in being able to obtain a continuous 30m core drilled through a fairly recent lava (8000 years old) near Arhram, Iceland. I selected eight specimens at 3m intervals across the middle of the lava. These specimens should all give the same value for the palaeofield magnitude, even though we do not know that value

The Curie temperatures were measured and found to be very low (figure 9b). On the assumption that the NRM resides in the material with this Curie point, all eight specimens were heated to 300°C in order to produce a TRM.

Table 1 lists all the data for one specimen (typical case) and figure 10 is the plotted data obtained from the computer, The ARM's and TRM's were all given in a constant magnetic field of 0.50×10^{-4}T (accurate to $\pm$ 0.005 T). In all eight cases the region of thermal alteration was isolated to the low a.f. region. A value for B_{anc} was determined from each specimen (figure 9a). All the results are quite consistent giving a mean value of $0.54 \pm 0.04 \times 10^{-4}$ T.

This lava is not typical because of its low Curie temperature and so very little thermal alteration occurred when it received a TRM at only 300°C.

5.3 Baked contact test

If a hot lava is extruded on to a sediment, the sediment may be heated above its Curie temperature and therefore

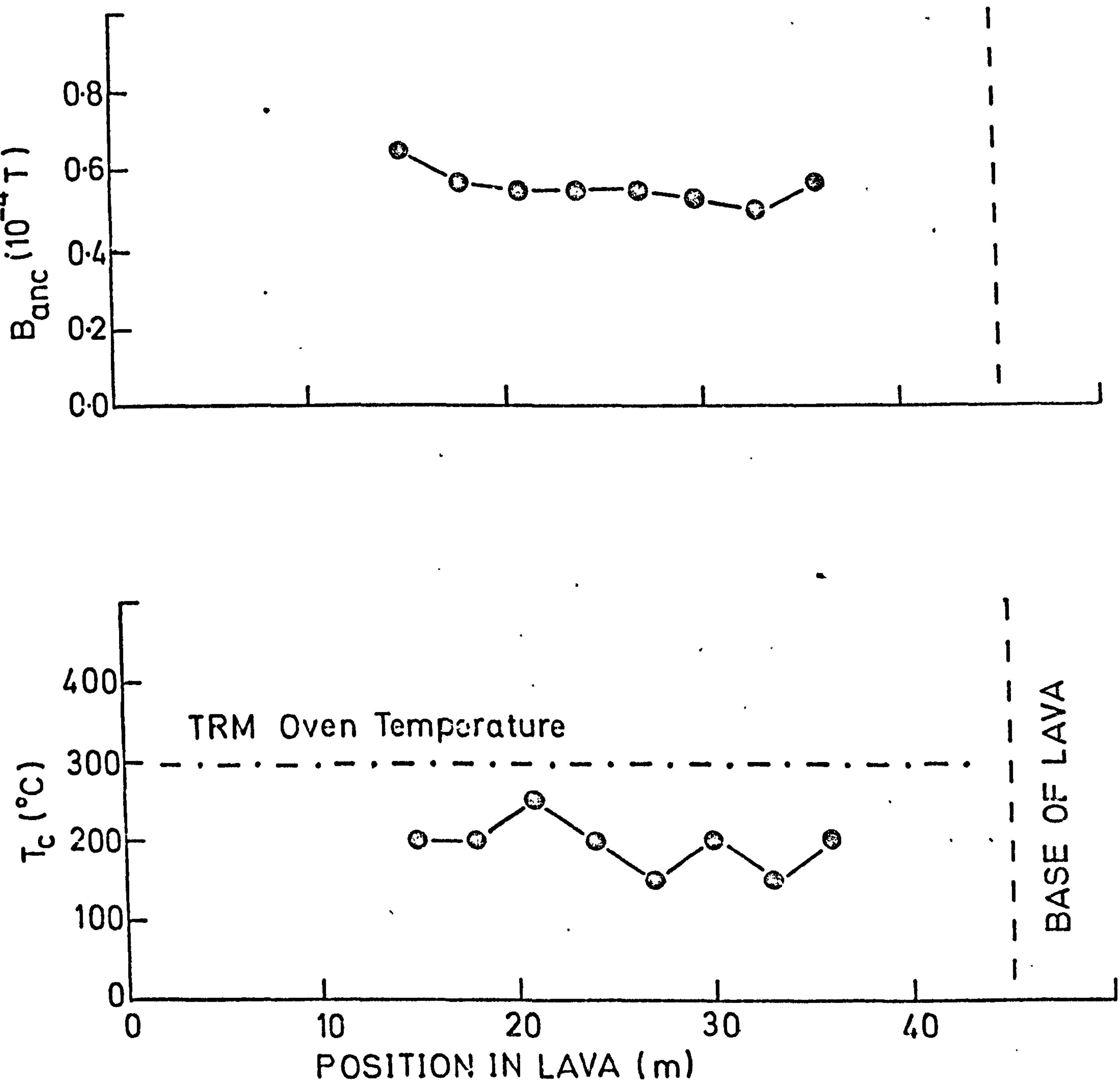

0.8
0.6
0.4
0.2
0.0
B_{anc} (10^{-4} T)
400
300
200
100
0
T_c (°C)
TRM Oven Temperature
BASE OF LAVA
0
10
20
30
40
POSITION IN LAVA (m)

FIG 9.

a.f.	NRM	ARM(1)	ARM(2)	TRM	A = accepted
10^{-4}T		10^{-5} Am^2	kg^{-1}		R = rejected
0	151.88	167.80	229.40	852.95	R
100	217.67	87.98	121.93	335.56	R
200	165.81	60.47	56.94	147.55	A
300	119.35	44.02	39.93	104.34	A
400	86.65	32.11	30.78	77.37	A
450	74.52	28.58	26.30	66.98	A
500	64.21	25.56	23.82	54.06	A
550	54.74	22.77	20.93	51.66	A
600	47.59	21.47	18.30	41.65	A
650	42.28	20.31	16.83	35.66	A
700	36.92	17.46	15.36	36.03	A
750	32.61	16.08	14.26	27.37	A
800	28.71	14.73	13.45	25.05	A
900	25.57	15.09	12.41	25.37	A
1000	20.36	14.73	10.05	20.82	A
1100	17.44	11.74	8.92	14.90	A
1200	14.53	12.27	9.64	14.05	A
1300	13.43	10.16	8.29	11.23	A
1400	12.05	11.71	7.97	9.56	A

Table 1

ICL - 36. All the data used to calculate B_{anc} (typical case). The first two sets of data are rejected because the ARM's are not equivalent.

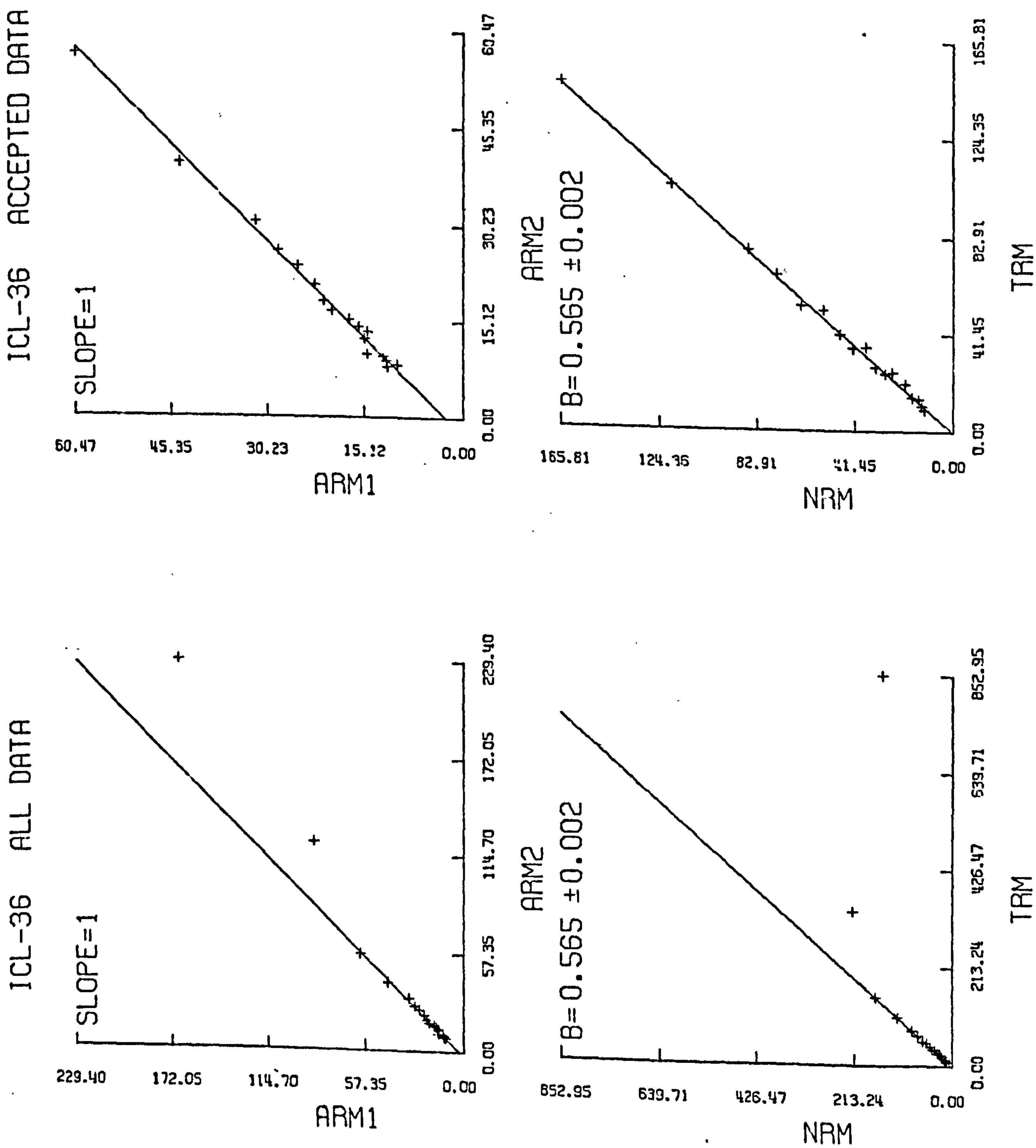
ICL-36 ACCEPTED DATA
SLOPE=1
ARM1
ARM2
B= 0.565 ±0.002
NRM
TRM
ICL-36 ALL DATA
SLOPE=1
ARM1
ARM2
B= 0.565 ±0.002
NRM
TRM

FIG 10.

acquire a full TRM at the same time and in the same field as the extruded lava. When analysed, both the lava and the baked contact (sediment) should give the same value for B_{anc}.

Two specimens, taken from a baked contact zone on the island of Mull, were made available to me. One specimen (C64 - 3b) was taken from the baked contact close to the overlying lava. The second specimen (C64 - 4b) was taken from the overlying lava.

Both specimens were heated to 620°C (when receiving a TRM) which is about 50°C above their observed Curie temperatures. The results are given in table 2 and the graphs of the data are plotted in figure 11 and 12.

Specimen	B_{anc} 10^{-4}T	S.D. 10^{-4}T	Tc °C	D	I
C64 - 3b	0.239	0.003	575	219°	-43°
C64 - 4b	0.245	0.023	575	224°	-50°

Table 2

The values of B_{anc} agree very well but only two specimens were used and although the two results agree it is clear from the graphs that some alteration has occured even in the accepted data.

We have now experimentally determined that the new method gives consistent results when applied to a single lava and to a baked contact where two different materials were used (igneous rock and sediment). We have not been able to show experimentally that the derived values of B_{anc} are correct. This can only be done by applying the technique to very recent specimens that have cooled in a known field.

5.4 Application to five historic lavas

In order to check that the new technique gives the correct results, and not just consistent results, experiments were carried out on five historic lavas that were extruded and cooled in a known magnetic field.

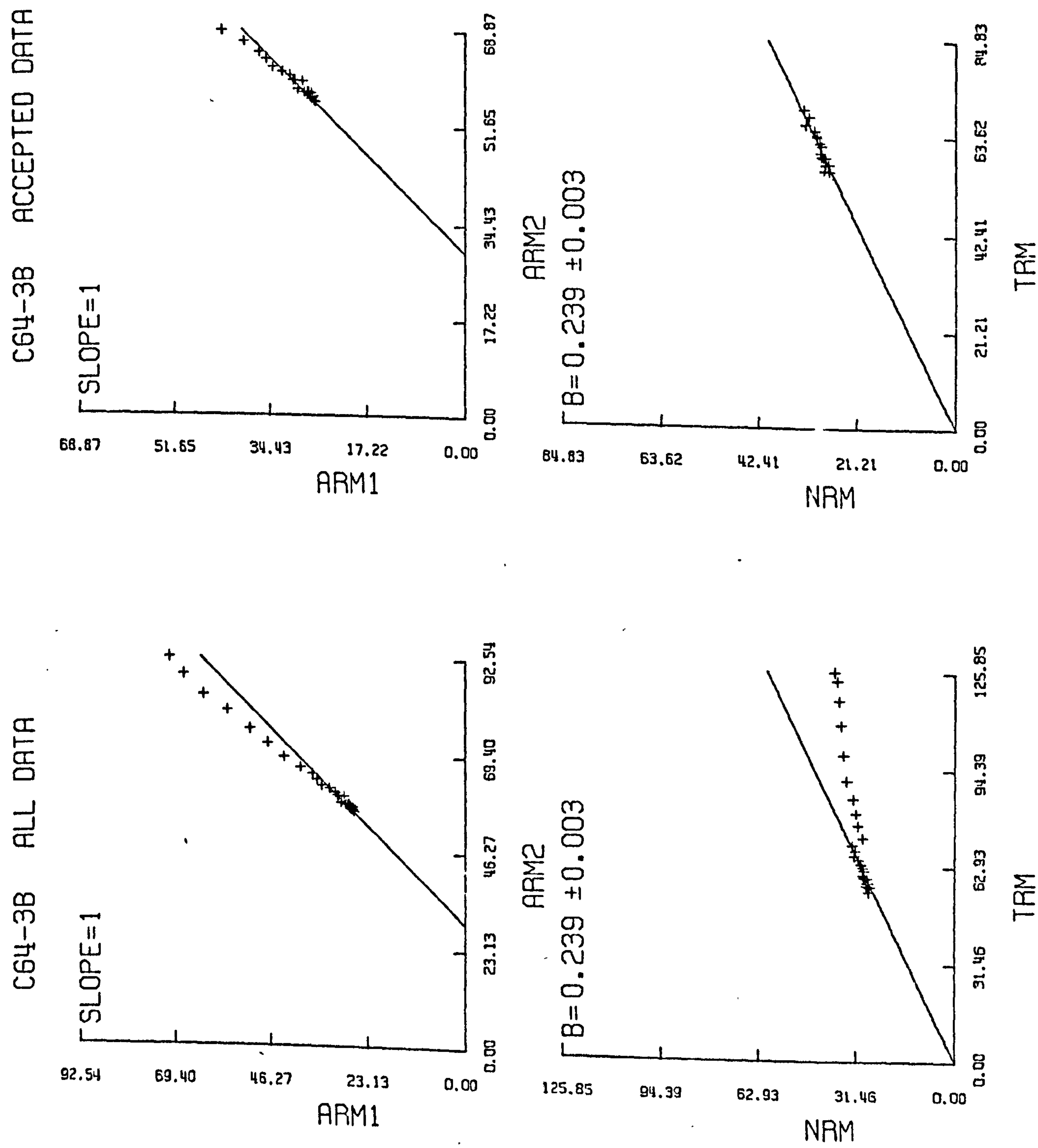
C64-3B ACCEPTED DATA
SLOPE=1
ARM1
ARM2
B= 0.239 ±0.003
NRM
TRM
C64-3B ALL DATA
SLOPE=1
ARM1
ARM2
B= 0.239 ±0.003
NRM
TRM

FIG 11.

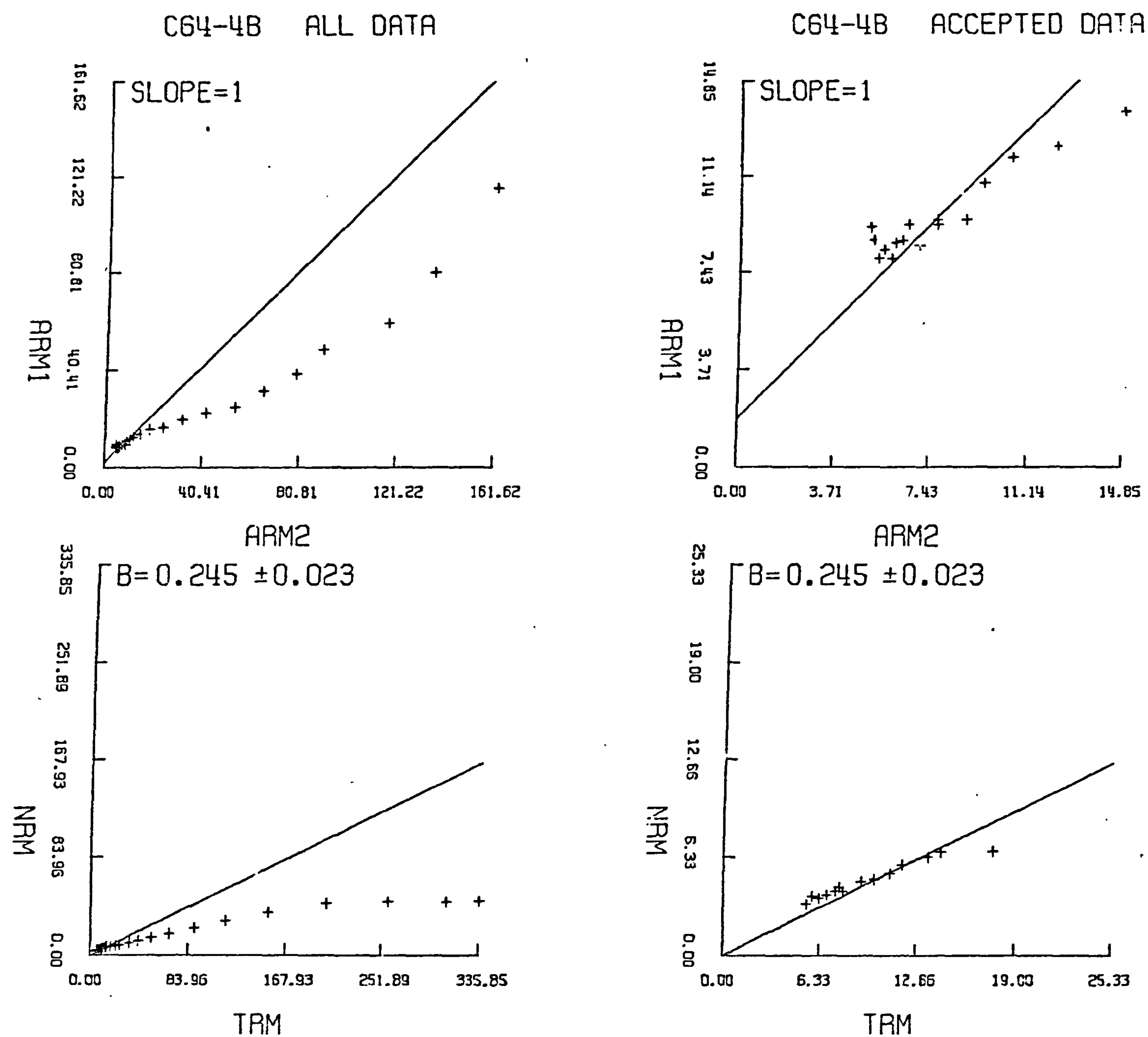
C64-4B ALL DATA
SLOPE=1
ARM1
ARM2
0.00
40.41
80.81
121.22
161.62
C64-4B ACCEPTED DATA
SLOPE=1
ARM1
ARM2
0.00
3.71
7.43
11.14
14.85
B=0.245 ±0.023
NRM
TRM
0.00
83.96
167.93
251.89
335.85
B=0.245 ±0.023
NRM
TRM
0.00
6.33
12.66
19.00
25.33

FIG 12.

The results are given in table 3. The 1973 Heimaey lava was totally altered by the laboratory heating within the observable region of the a.f. demagnetisation curve (up to 0.13T) and consequently the magnitude of the palaeofield was not determined.

The three Hawaiian lavas each gave internally consistent results. The maximum alteration occurred in the 1907 lava, which remained unaltered only above 0.08T a.f. demagnetising field, and consequently only four or five points could be used from each specimen from this lava. The magnetic field at Hawaii is not accurately known. The value quoted in table 3 is the measured magnetic field at Honolulu, which is 300 km northwest of Hawaii. It is therefore likely that the discrepancies in table 3, between the deduced and the known fields are in part due to the uncertainty of the known field at Hawaii.

The 1910 Etna lava has been used for palaeofield studies by Angenheister et al (1971), who were unable to obtain any results from it; and also by Tanguy (personal communication), who has derived consistent results from it by the application of another new technique. This lava, while producing the largest scatter of individual results, also produced a mean palaeofield which was closest to the known 1910 magnetic field, probably because of the large number (7) of specimens used. The magnetic field at Etna is accurately known.

These results are very encouraging and it is clear the new technique used to determine the magnitude of the palaeofield produces, for lavas, results which are accurate to about 10%, and whose reliability can be assessed from the data diagrams. The ability to assess the result is a very good aspect of this technique.

5.5. Application to five Archaeomagnetic specimens

A more detailed analysis of the palaeofield in recent times (the last 30,000 years) can be made by examining man fired artefacts such as pottery, bricks and even primitive fireplaces (Barbetti et al 1972). In order to check that the new technique could be applied to man fired artefacts (archaeomagnetic specimens), five specimens were obtained

LAVA		CODE	Numbers of specimens	Tc °C	B_{anc} 10^{-4}T	Standard deviation 10^{-4}T	Known field 10^{-4}T
1907	HAWAII	2L148	3	550	0.31	0.03	0.38
1910	ETNA	E1	7	570	0.42	0.05	0.42
1926	HAWAII	2L152	3	550	0.34	0.02	0.37
1955	HAWAII	2L025	3	570	0.42	0.02	0.37
1973	HEIMAEY	W	4	600	NO ACCEPTABLE DATA		0.51

Table 3

The mean results from five historic lavas. The Hawaiian 'known field' is the field measured at Honolulu (300 km away) as no measurements were taken on Hawaii Island. The individual graphs of each specimen (40 graphs) are included in appendix 2.

from Dr. M. Aitken at The Research Laboratory for Archaeology and the History of Art, Oxford.

In order to increase the magnitude of the induced ARM's I increased the current through the coils to 100 ma. This corresponds to a constant magnetic field of 1.35×10^{-4}T. I also increased the maximum a.f. value from 0.13 to 0.14T. These values are used throughout the remaining part of this thesis.

By increasing the magnitude of the ARM any small deviation of the graph of ARM(1) against ARM(2) will be more easily measured. The increased a.f. value allows an extra NRM/TRM ratio to be determined.

Three of the five archaeomagnetic specimens were taken from samples which had already been used for palaeofield determinations by Weaver (1966) who used the method developed by the Thelliers. The experimental results are given in table 4 and Weaver's results are listed in the comparison section.

The 103-A pottery sample was fired in 1965. The derived value of the magnetic field is in very good agreement with the observed magnetic field at the time.

The S2-1 brick came from a Sheffield glass furnace. Weaver had applied the Thelliers method to part of this brick. Although our two mean values agree within the errors, the new palaeofield method reduced the error by a factor of 9.

The 5PT tile came from a mediaeval tile kiln at Boston. In this case I did not use the same tile but used a brick from the same kiln. The mean results are in agreement and the error from the new palaeofield method is an order of magnitude better than Weaver's error.

The H1 tile was from a fourth century grain drier at Hampstead Marshall (Berkshire). In this case the new method produced a large error (12%). This tile was highly oxidised on the outside (red) and light grey on the inside. Experiments were carried out on a red only and a grey only specimen. The red specimen NRM was very hard (hematite) while the grey NRM was quite soft (magnetite). The red specimen gave a value for B_{anc} of 1.21 ± 0.10 and the grey a value of $0.98 \pm 0.05 \times 10^{-4}$T. Both values are within the limits of the three whole specimen values and are included among the five samples in table 4. Weaver applied the Thelliers method to this tile but failed to obtain any result from it.

The 48 - A3 pottery specimen came from Stibbington (Huntingdon). The pottery was white throughout and the total NRM was considerably weaker than the other four samples. This specimen gave an acceptable result although the error was fairly large (6%).

These five English archaeomagnetic results are compared with the Thelliers' results from French material (Thellier and Thellier, 1959) by converting the palaeofield to an "assumed" or virtual dipole moment (VDM; Smith, 1967), the calculation of VDM is discussed in appendix 3. The results are plotted in figure 13. The agreement between the two sets of data is very good. The data and associated graphs are included in appendix 2.

We have seen that the new method agrees with the Thelliers' method and also that it gives the correct result when applied to both lavas and archaeomagnetic specimens (103 - A pottery sample was fired in 1965 in a known field).

The new method requires that the specimen was heated to at least its Curie temperature when the NRM was formed and so, unlike the Thelliers' method, it cannot be used to determine B_{anc} from a specimen that only has a PTRM. On the other hand this new method is quicker, requiring only one heating, and apparently more accurate than the Thelliers' method. It also has the advantage that the high

Sample	Description	Number of specimens	Date Yrs. A.D.	Banc 10^{-4}T	Standard Deviation 10^{-4}T	Comparisons: Banc 10^{-4}T	Comparisons: Standard Deviation 10^{-4}T	Comparisons: Investigator
103-A	Pottery	3	1965	0.49	0.03	0.485		Direct observations
S2-1	Brick	3	1900	0.53	0.01	0.49	0.09	Weaver (Thellier's method)
5.PT	Tile	3	1356	0.62	0.02	0.68	0.26	Weaver (Thellier's method)
H-1	Tile	5	350	0.94	0.12	No acceptable result		Weaver (Thellier's method)
48-A1	Pottery	3	150	0.68	0.04			

Table 4

The results from five archaeological samples

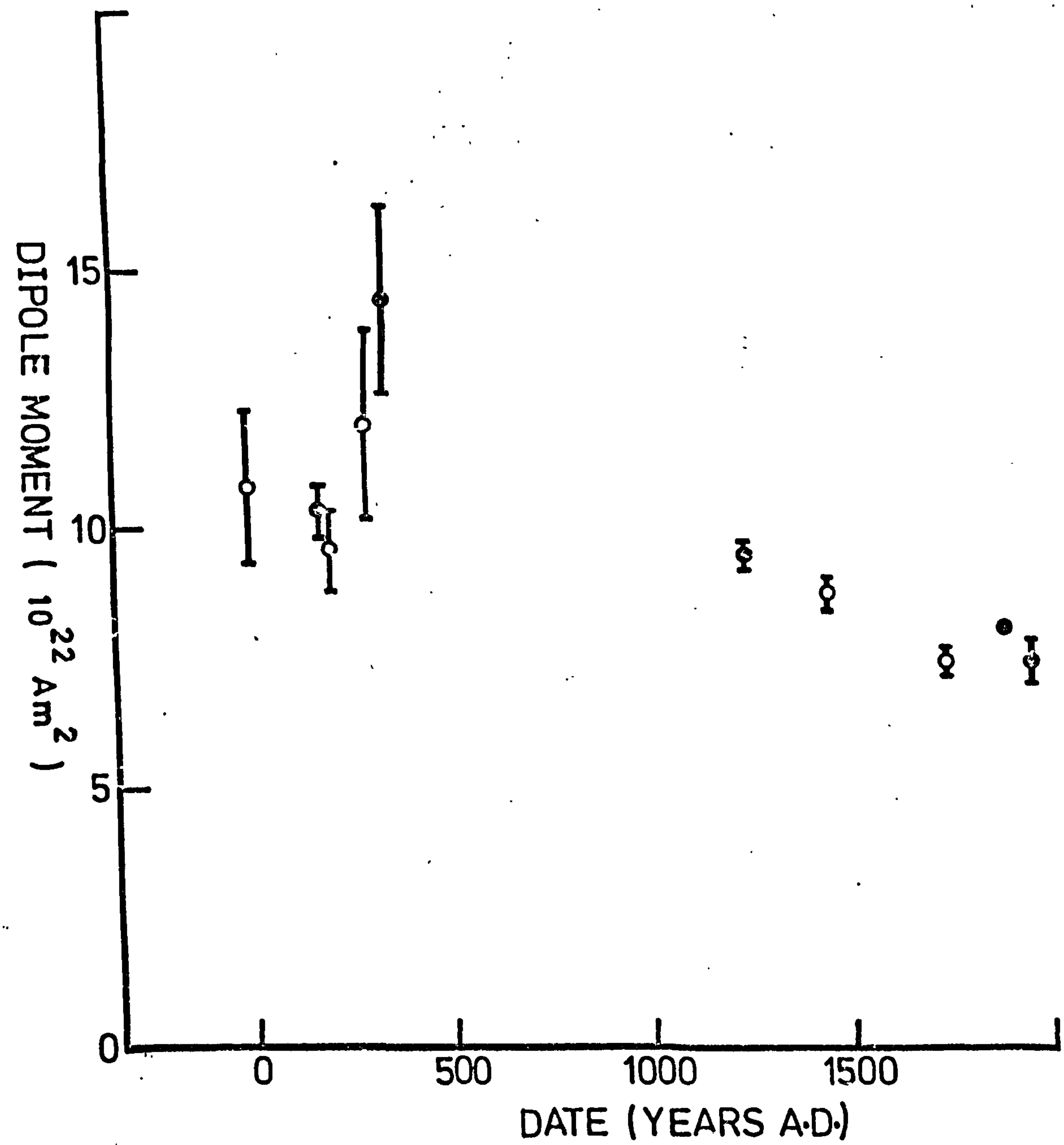

FIG 13. A graph of virtual geomagnetic dipole moment against time. Closed circles represent English data (this thesis), open circles represent European data (Thellier and Thellier 1959). The standard deviation is plotted for both sets of data.

a.f. region is used to determine B_{anc}. This region is not as likely to have been affected by VRM and so the new method may produce valid results when applied to much older specimens.

The new method has been tested on both lavas and man fired artefacts. Let us now go on to use it as a tool with which to examine how the earth's magnetic field changes during a field reversal.

The results discussed in this chapter have been published (Shaw 1974(a)). A copy of the published paper is included in the back of this thesis.

CHAPTER 6. A PALAEOMAGNETIC FIELD REVERSAL

6.1 Introduction

The generating mechanism of the geomagnetic field is not clearly understood although most workers favour some form of dynamo action within the liquid core of the earth (Bullard and Gellman, 1954). No one has yet provided a complete description of the assumed dynamo, mainly because of difficult mathematics and of insufficient information around which a theory can be constructed. One of the most constraining phenomena that any theory must account for is the fact that the earth's magnetic field has, in the geological past, reversed its polarity.

A well documented field reversal is the R_3 to N_3 transition of Western Iceland which was first discovered by Einarsson (1957) and explored in detail by Sigurgeirsson (1957), Brynjolfsson (1957) and later by Wilson et al (1972(a)). This chapter describes the results that were obtained when the new palaeofield technique was applied to lavas that were extruded during this transition. These results place certain further restrictions on any proposed dynamo theories.

6.2 Representation of results

Anomalous directions of magnetisation have been encountered by many workers. One way of formally representing anomalous directions is to 'assume' that, even in an anomalous state, the geomagnetic field can be represented by a non-axial centred dipole. This assumption has been made whenever anomalous 'virtual geomagnetic poles' (V.G.P's Cox and Doell, 1960) are calculated. The same assumption can be made when considering the magnitude of the geomagnetic field (Wilson et al 1972(b)) which allows us to represent the magnitude of the geomagnetic field as a 'virtual dipole moment' (V.D.M. Smith (1967(b)). The calculation of V.D.M. is discussed in appendix 3.

6.3 The R_3 to N_3 transtion

In July 1974 I sampled six lava sequences in the Hvalfjordur district just north of Reykjavik in Western Iceland (figure 14). 289 oriented cores were taken from 38 lavas. Measurements of the directions of magnetisation of two cores from each lava revealed that 32 lavas from five sections (P,R,S,T and U sections) contained the R_3 to N_3 transition. Oriented cores from these 32 lavas were used for palaeofield determinations.

The magnitude of the palaeofield was determined from 21 lavas. Of the remaining 11 lavas that did not produce a value, the specimens from 2 lavas exploded on heating, the specimens from another 2 lavas were magnetically unstable when a.f. demagnetised in high fields and the specimens from 7 lavas underwent severe thermal alteration. The magnitude of the palaeofield was also determined from specimens from 2 lavas sampled by Wilson et al (1972(a)) thus making a total of 23 determinations of the magnitude of the palaeofield during the R_3 to N_3 transition (table 5). Each palaeofield value was determined from at least 2 specimens. As a measure of the work done, more than 2500 a.f. demagnetisations were carried out to achieve these 23 results.

The transition zone between R_3 and N_3 is represented by V.G.P. positions in figure 15(a) (results from this work) and figure 15(b) (from Wilson et al, 1972(a)). The two independent sets of results agree very well and it seems likely from the number of intermediate lavas that the assumed geomagnetic dipole must have remained in a fixed equatorial orientation for a considerable length of time.

Previous determinations of the virtual dipole moment magnitude for anomalous palaeomagnetic pole positions, have indicated that the V.D.M. is much weaker than in the more usual 'normal' and 'reversed'

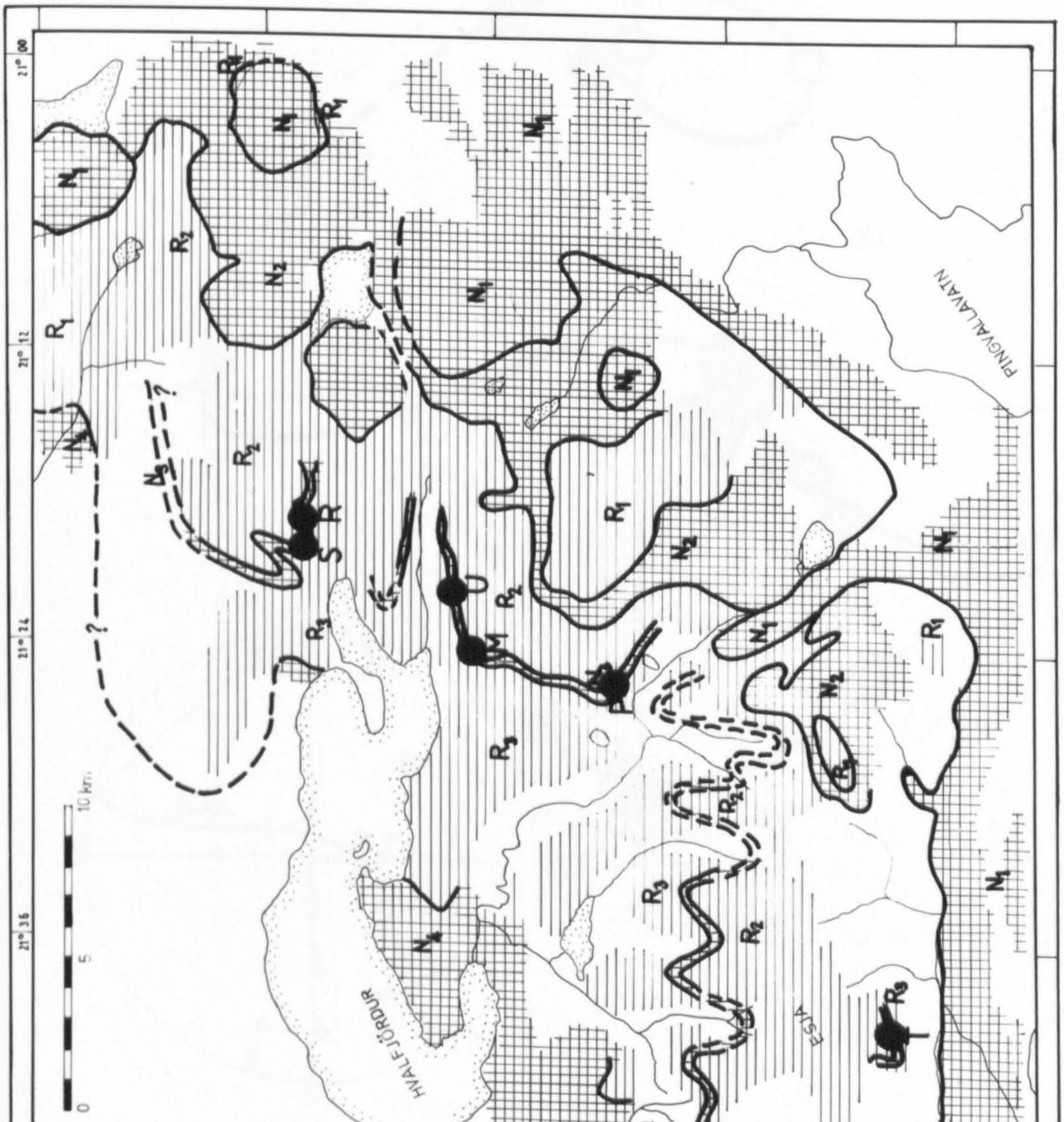

FIG 14. A map of the collecting area showing the six sampled lava sequences (after Sigurgeirsson 1957.)

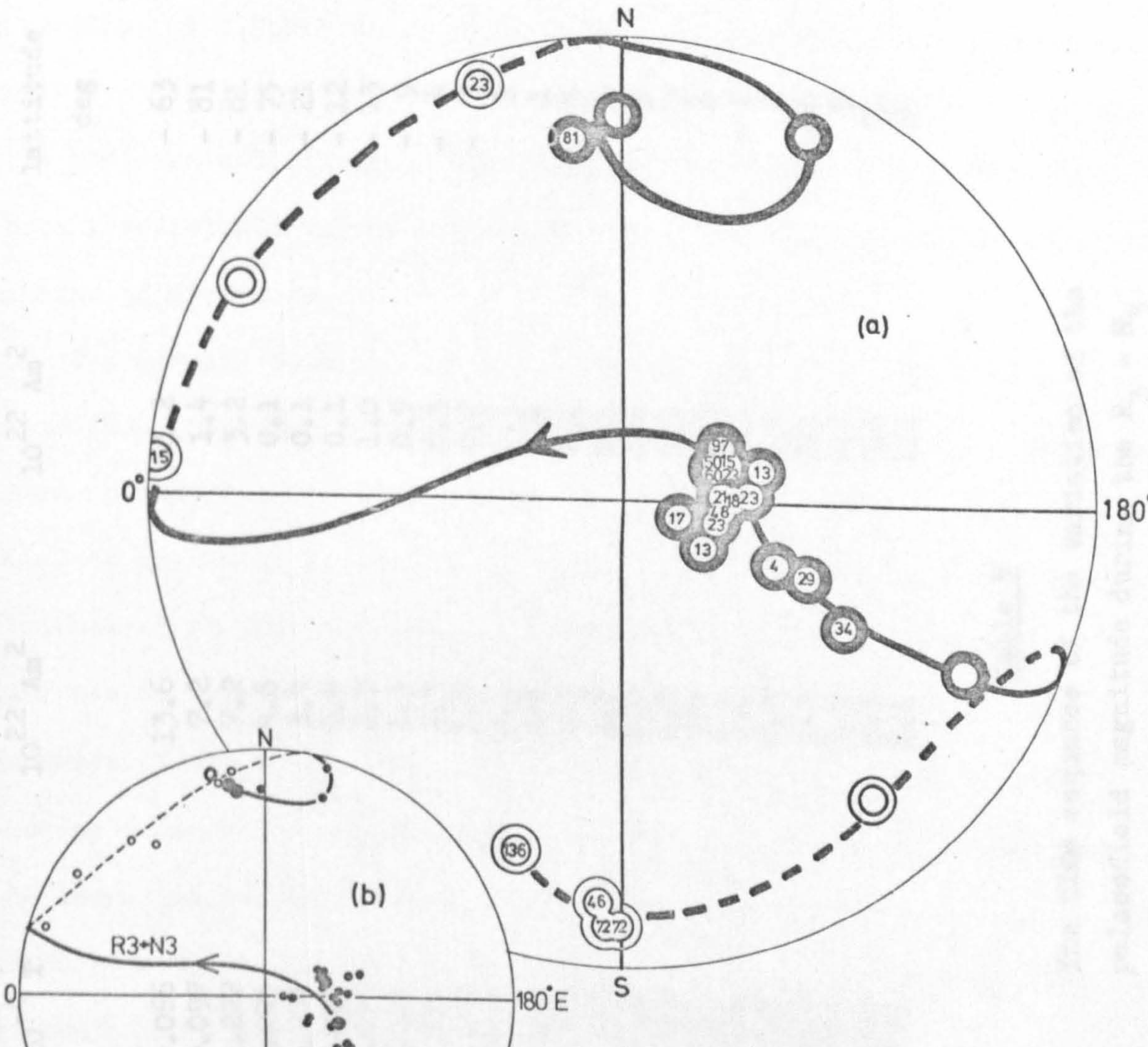

FIG 15.

TIME ↓

Magnetic field 10^{-4} T	Standard deviation 10^{-4} T	V.D.M. 10^{22} Am^2	Standard deviation 10^{22} Am^2	V.G.P. lattitude deg	V.G.P. longitude deg East	α_{95} deg
0.777	0.066	13.6	1.2	- 63	306	4
0.501	0.097	7.2	1.4	- 81	273	1
0.497	0.222	7.2	3.2	- 81	278	3
0.303	0.005	4.6	0.1	- 75	284	4
0.202	0.006	3.4	0.1	- 21	131	2
0.018	0.005	0.4	0.1	- 12	117	4
0.155	0.053	2.9	1.0	- 13	122	2
0.061	0.025	1.3	0.5	- 9	114	2
0.105	0.012	2.3	0.3	- 4	114	4
0.075	0.009	1.7	0.2	- 3	110	5
0.095	0.003	2.1	0.1	1	117	9
0.083	0.019	1.8	0.4	1	107	4
0.054	0.003	1.3	0.1	5	114	4
0.062	0.002	1.5	0.1	6	108	2
0.204	0.008	5.0	0.2	5	106	2
0.246	0.003	6.0	0.1	3	107	1
0.386	0.013	9.7	0.3	8	107	2
0.208	0.011	4.8	0.3	- 2	107	8
0.099	0.915	2.3	0.4	2	112	9
0.095	0.002	2.3	0.1	6	107	1
0.076	0.012	1.5	0.2	5	359	12
0.175	0.005	2.3	0.1	71	339	3
0.537	0.071	8.1	1.1	65	72	2

Table 5

The time sequence of the variation of the palaeofield magnitude during the $R_3 - N_3$ transition.

states (Momose, 1963; Prevot and Watkins, 1969; Lawley, 1970).

Because anomalous V.D.M's have been assumed to be small, little importance has been placed on the magnetic stability of rocks which record some intermediate directions.

Wilson et al (1972(b)) presented a statistical analysis of the dependance of V.D.M's on colatitude of pole position (figure 16(a)). Their results indicated the possibility of large V.D.M's at intermediate pole position colatitudes. The 'spread' of results associated with these intermediate values were very large, ostensibly because of small numbers of specimens.

The results obtained by using the new technique on the R_3 to N_3 transition are shown in figure 16(b) and listed in table 5. The error shown in figure 16(b) is the standard deviation (the error in figure 16(a) is the error on the mean). The results agree with the Wilson et al statistical results and it is clear that the V.D.M. can sometimes increase to large values at intermediate colatitudes. The sharp increase of the V.D.M. will not be easily detected in figure 16(a) because these V.D.M's are averaged over 5^{o} colatitude intervals and so the large intermediate values will be combined with smaller values. This probably explains the large spread of results associated with three of Wilson's intermediate values (90 to 110^{o} colatitude).

Although only the R_3 to N_3 transition has been examined in detail, the statistical data of figure 16(a) also supports the possibility that the earth's magnetic field has a third metastable state (intermediate state). The 'intermediate' state would appear to have the same characteristics as the more usual 'normal' and 'reversed' states in that the direction of the V.G.P. remains fixed for large values of V.D.M., and that changes from one state to another can only be made when the V.D.M. is small. The minimum V.D.M. value, recorded during the R_3 to N_3 transition, was $0.35 \pm 0.10 \times 10^{22}$ Am^2). The

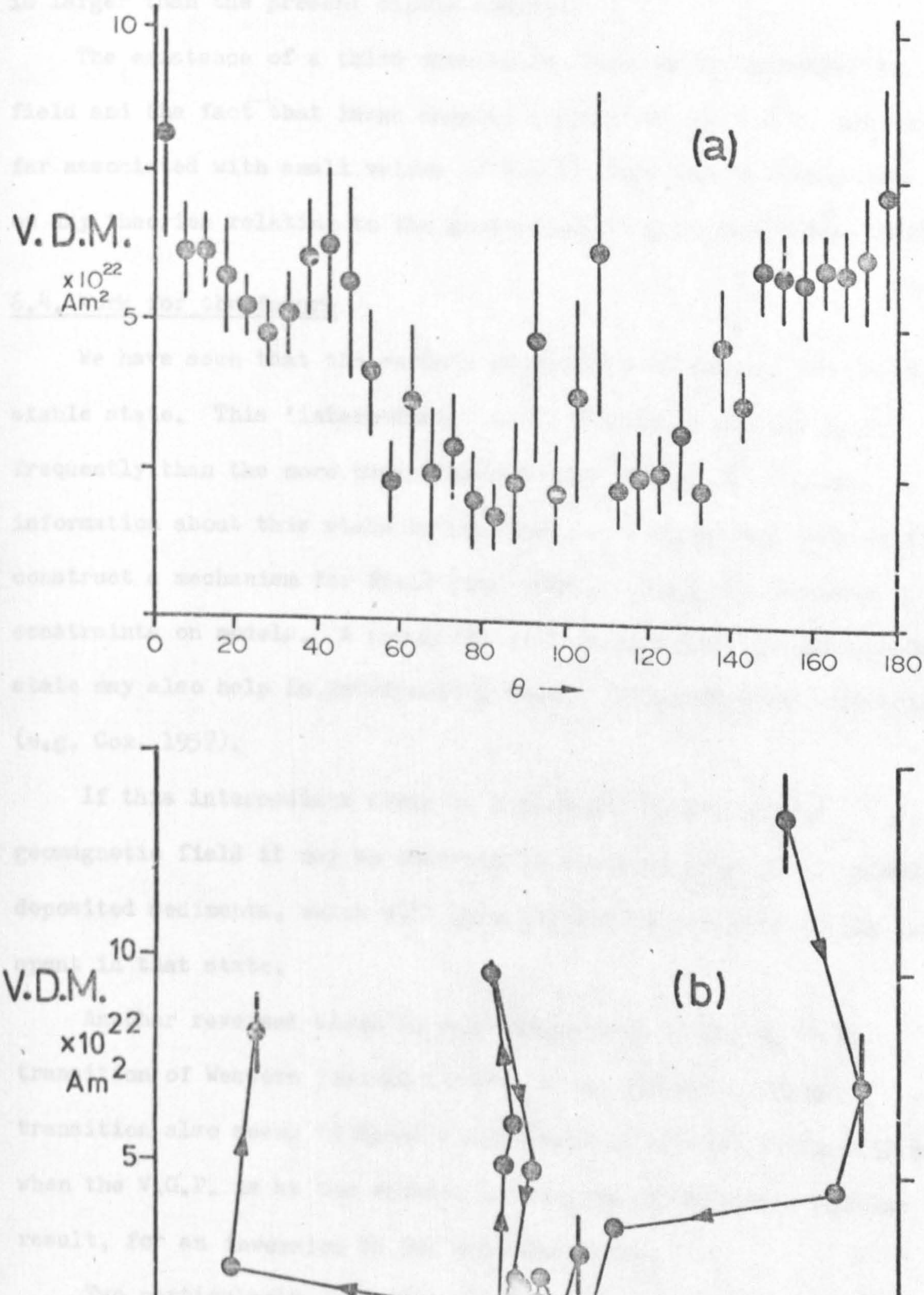
(a)
V.D.M.
x10^22 Am^2
10
5
0
20
40
60
80
100
120
140
160
180
θ →
(b)
V.D.M.
x10^22 Am^2
10
5
0
20
40
60
80
100
120
140
160
180
θ →

Fig 16.

maximum measured intermediate value was $9.7 \pm 0.3 \times 10^{22}$ Am^2, which is larger than the present dipole moment.

The existence of a third metastable state of the geomagnetic field and the fact that large angular changes of the V.G.P. are so far associated with small values of V.D.M. must impose constraints on any theories relating to the generation of the geomagnetic field.

6.4. Work for the future

We have seen that the earth's geomagnetic field may have a third stable state. This 'intermediate' state obviously happens less frequently than the more usual 'normal' and 'reversed' states. As information about this state accumulates, it will assist workers to construct a mechanism for field generation, if only by imposing constraints on models. A knowledge of this intermediate metastable state may also help in interpreting unusual palaeomagnetic directions (e.g. Cox, 1957).

If this intermediate state is a general feature of the geomagnetic field it may be observed in detailed studies of quickly deposited sediments, which will also provide an estimate of the time spent in that state.

Another reversal which is well documented is the N_4 to R_3 transition of Western Iceland (Wilson et al 1972(a)). This transition also seems to spend a considerable period of time (12 lavas) when the V.G.P. is at the equator and may possibly give a similar result, for an inversion in the opposite sense.

Two particularly well documented North American transitions are the Steens Mountain transition (Watkins, 1965(a), (b), 1969; Goldstein, Larson and Strangway, 1969) and the Lousetown Creek transition (Heinrichs, 1967). If these transitions also give similar results then we will know that this phenomenon is not restricted to Iceland.

The results discussed in this chapter have been included in a published paper (Shaw, 1974(b)) a copy of which is included in the back of this thesis.

CHAPTER 7. SUMMARY OF THESIS

An ARM may be used to detect and isolate any changes in the TRM a.f. demagnetisation curve that occur when the specimen receives a laboratory TRM.

Empirically, changes in the a.f. demagnetisation curve start in the low a.f. region and progressively spread to the higher a.f. region as the specimen becomes more thermally magnetically altered. This means that in most cases the value of B_{anc} can be determined from the unaltered high a.f. region.

This new technique has many advantages over other methods:-

1. Only one heating is required, which minimizes the degree of thermal magnetic alteration and makes for a quick method.
2. The new technique, like some other methods, can detect changes in the shape of the TRM demagnetisation curve.
3. The new technique can detect "consistent alteration" (where thermal alteration changes the TRM magnitude by a constant factor) which has previously been undetectable.
4. The high a.f. region is used to determine B_{anc}. This region is not likely to be affected by VRM.

There is however one disadvantage. The new technique unlike the Thelliers' cannot be applied to PTRM's of the type found in partially fired pottery and open fireplaces.

We have observed that this new technique not only produces consistent results but correct results when applied to igneous rocks and archaeomagnetic specimens which cooled in known fields. This technique has proved itself to be a reliable procedure for determining the magnitude of the palaeofield.

Having developed and tested the technique we then applied it to a collection of lavas from Western Iceland which were extruded during a geomagnetic field reversal (the R_3 to N_3 transition). The results of this investigation were very good (small errors) and very surprising in that the earth's magnetic field apparently can have a third stable state when the north magnetic pole is near the geographic equator; a result which immediately constains any theories relating to the generation of the earth's magnetic field and may also explain many previously anomalcus groupings of V.G.P. positions.

APPENDIX 1.

This appendix contains a listing of the computer programe (written in fortran 4) which was developed to analyse the NRM, TRM and ARM data. The TRM is assumed to have been formed in a constant magnetic field of 0.5×10^{-4} T.

The graphs included in appendix 2 were obtained by using this programe.

```
FORTRAN IV G LEVEL  21                MAIN                DATE = 74262          16/01/34

                REAL NRM
                REAL*8 ALD(2),ACD(2)
                DATA ALD,ACD/'ALL DATA','        ','ACCEPTED',' DATA   '/
                DIMENSION TEST(30),W(30),COD(3)
                DIMENSION P(20),VAR(20)
                DIMENSION CODE(3)
                DIMENSION IF(30),NRM(30),ARM1(30),ARM2(30),TRM(30)
                DIMENSION U(30),V(30)
                DIMENSION X(30),Y(30)
                DIMENSION V1(30),V2(30),WZ(30),Z(30),P1(30),VAR1(30)
                LOGICAL*1 TARM1(34),TARM2(34),TNRM(34),TTRM(34),TTXA1(34),TNXA2(34
               1)
                DATA TARM1/15*' ','A','R','M','1',15*' '/
                DATA TARM2/15*' ','A','R','M','2',15*' '/
                DATA TNRM/15*' ','N','R','M',16*' '/
                DATA TTRM/15*' ','T','R','M',16*' '/
                DATA TTXA1/15*' ','T','X','A','1',15*' '/
                DATA TNXA2/15*' ','N','X','A','2',15*' '/
                NP=0
                READ(5,103) IPLOT
                IF(IPLOT.NE.1) GO TO 1
                CALL PLOTON
                CALL PLTLIM(200.0)
                CALL MOVE(1.0,0.0)
              1 CONTINUE
              5 B=1.0
                B1=1.0
                B2=1.0
                EPS=0.0001
                I=1
             10 READ(5,101,END=99) IF(I),NRM(I),ARM1(I),ARM2(I),TRM(I),(COD (J),J=
               11,3)
                IF(IF(I).EQ.1001) GO TO 20
                IF(IF(I).EQ.1002) GO TO 98
                IF(I.NE.1) GO TO 15
                WRITE(6,203)(COD(J),J=1,3)
                DO 12 J=1,3
                CODE(J)=COD(J)
             12 CONTINUE
             15 I=I+1
                GO TO 10
             20 N=I-1
                CALL ACCEPT (NRM,TRM,ARM1,ARM2,WZ,Z,X,Y,IF,TEST,N,M,C)
                DO 30 I=1,N
                U(I)=1.0
             30 V(I)=1.0
                WRITE(6,209)
                WRITE(6,205)
                DO 31 I=1,M
                V1(I)=X(I)
             31 V2(I)=Y(I)
                M1=M
             32 CALL HAFIT(V2,V1,M1,B,EPS,ITER,W,VAB,S)
                HANC=B*0.5
                SOD=SQRT(VAB)*0.5*B
                WRITE(6,214) HANC,SOD,B,VAB,ITER,S,M1
                CALL REJECT (V1,V2,M1,S,W,&32)
                CALL PLAT(ARM1,ARM2,TEST,N,1,TARM2,TARM1)
```

```
          CALL PLOT(NRM,TRM,TEST,N,2,TTRM,TNRM)
          CALL PRTPLT
          IF(IPLOT.EQ.0) GO TO 70
          CALL MOVE(1.0,0.0)
          CALL SETO
          C=-C
          CALL CALPLT(ARM1,ARM2,NRM,TRM,TEST,N,B,CODE,ALD,C,SOD)
          CALL CALPLT(HZ,Z,X,Y,TEST,M,B,CODE,ACD,C,SOD)
       70 CONTINUE
          NP=NP+1
          P(NP)=0.5*B
          VAR(NP)=SOD*SOD
          GO TO 5
       98 CALL WAITAV(P,VAR,NP,AVE,VARIAN)
          STD=SQRT(VARIAN)
          WRITE(6,210) AVE,STD
          NP=0.0
          GO TO 5
       99 IF(IPLOT.NE.0) CALL PLOTOF
          STOP
      101 FORMAT(I4,4F10.2,T69,3A4)
      102 FORMAT(80A1)
      103 FORMAT(I1)
      200 FORMAT(1H ,F5.3,5X,F5.3,2F10.3,2F10.5,I10,F10.3,I10)
      203 FORMAT(1H1,T50,'SAMPLE',2X,3A4)
      205 FORMAT('0BANC',T12,'STD',T22,'SLOPE',T40,'VAR(SLOPE)',T61,'ITERS',
         AT75,'S',T85,'N'/)
      207 FORMAT(/' ',                 T22,'SLOPE',T30,'INTERCEPT',T40,
         A'VAR(SLOPE)',T51,'VAR(INT)',T61,'ITERS',T75,'S',T85,'N'/)
      208 FORMAT(1H ,T18,2F10.3,2F10.5,I8,F10.3,I10)
      209 FORMAT(//T40,'NRM/TRM')
      210 FORMAT(//1H0,T30,'*** ANCIENT FIELD INTENSITY',F7.3,' STANDARD DEV
         1IATION',F7.3,' ***')
      214 FORMAT(1H ,F5.3,2F10.3,10X,F10.5,10X,I10,F10.3,I10)
          END
```

```
FORTRAN IV G LEVEL  21                  ACCEPT              DATE = 74262           16/01/34

0001            SUBROUTINE ACCEPT(NRM,TRM,ARM1,ARM2,W,X,Y,Z,IF,TEST,N,M,C)
0002            DIMENSION CHISQ(30)
0003            DIMENSION NRM(30),TRM(30),ARM1(30),ARM2(30),W(30),X(30),Y(30),Z(30
               1),IF(30),TEST(30)
0004            DIMENSION RW(30),RX(30),RY(30),RZ(30),RJF(30),BDEV(30),JF(30),GDEV
               1(30),DEV(30)
0005            DATA CHISQ/3.841,5.991,7.815,9.488,11.070,12.592,14.067,15.507,
               A16.919,18.307,19.675,21.026,22.362,23.685,24.996,26.296,27.587,
               B28.869,30.144,31.410,32.67,33.92,35.17,36.42,37.65,38.89,40.11,
               C41.34,42.56,43.77/
0006            REAL*4 NRM
0007            INTEGER RJF
          C
          C     INITALISE VECTORS
          C
0008            M=N
0009            IR=0
0010            DO 10 I=1,M
0011            W(I)=ARM1(I)
0012            X(I)=ARM2(I)
0013            Y(I)=NRM(I)
0014            Z(I)=TRM(I)
0015            JF(I)=IF(I)
0016            TEST(I)=0.0
0017         10 CONTINUE
          C
          C     FIND INTERCEPT OF FITTED LINE
          C
0018         20 SW=0.0
0019            SX=0.0
0020            DO 30 I=1,M
0021            SW=SW+W(I)
0022            SX=SX+X(I)
0023         30 CONTINUE
0024            C=(SW-SX)/M
          C
          C     CALCULATE DEVIATIONS SQUARED FROM LINE
          C
0025            SD=0.0
0026            DO 40 I=1,M
0027            DEV(I)=(W(I)-X(I)-C)**2
0028            SD=SD+DEV(I)
0029         40 CONTINUE
          C
          C     TEST FOR GOODNESS OF FIT
          C
0030            CHECK=1.0*CHISQ(M-1)
0031            IF(SD.GT.CHECK) GO TO 60
          C
          C     WRITE ACCEPTED AND REJECTED DATA
          C
0032            IF(M.NE.N) GO TO 45
0033            MAX=1000
0034            GO TO 64
0035         45 WRITE(6,206)
0036         50 DO 51 I=1,M
0037         51 WRITE(6,201) JF(I),Y(I),W(I),X(I),Z(I),GDEV(I)
0038            IF(IR.EQ.0) RETURN
```

```
FORTRAN IV G LEVEL  21                  ACCEPT              DATE = 74262           16/01/34

            DO 52 I=1,IR
         52 WRITE(6,202) RJF(I),RY(I),RW(I),RX(I),RZ(I),BDEV(I)
            DO 53 I=1,N
            DO 53 J=1,IR
            IF(IF(I).EQ.RJF(J)) TEST(I)=1.0E06
         53 CONTINUE
            RETURN
      C
      C     REJECT WORST POINT
      C
         60 AMAX=DEV(1)
            MAX=1
            DO 61 I=2,M
            IF (AMAX.GT.DEV(I)) GO TO 61
            MAX=I
            AMAX=DEV(I)
         61 CONTINUE
      C
      C     UPDATE VECTORS
      C
         64 K=0
            DO 63 I=1,M
            IF (I.EQ.MAX) GO TO 62
            K=K+1
            W(K)=W(I)
            X(K)=X(I)
            Y(K)=Y(I)
            Z(K)=Z(I)
            JF(K)=JF(I)
            SDEV(K)=SD
            GO TO 63
         62 IR=IR+1
            RW(IR)=W(I)
            RX(IR)=X(I)
            RY(IR)=Y(I)
            RZ(IR)=Z(I)
            RJF(IR)=JF(I)
            BDEV(IR)=SD
         63 CONTINUE
            IF(MAX.EQ.1000) GO TO 45
            M=K
            IF(M.GT.3) GO TO 20
            WRITE(6,200)
        200 FORMAT(1H0,T40,'***INSUFFICIENT ACCEPTABLE DATA POINTS***')
        201 FORMAT(1H ,I4,5F10.2)
        202 FORMAT(1H ,T60,'REJECTED',2X,I4,5F10.2)
        206 FORMAT(/' FIELD',T9,'NRM',T20,'ARM1',T30,'ARM2',T40,'TRM',T70,'FIE
           1LD',T78,'NRM',T88,'ARM1',T98,'ARM2',T108,'TRM',/)
            END
```

```
FORTRAN IV G LEVEL  21                 HAFIT              DATE = 74262           16/01/34

              SUBROUTINE HAFIT(X,Y,N,SLOPE,EPS,ITER,W,VAR,A)
              DIMENSION X(1),Y(1),W(1)
              REAL M
        C
        C     CALCULATE SUMS OF CROSS PRODUCTS OF X AND Y
        C
              A=0.0
              B=0.0
              C=0.0
              DO 10 I=1,N
              B=B+X(I)*Y(I)
              A=A+X(I)*X(I)
           10 C=C+Y(I)*Y(I)
              M=1.0
              ITER=0
           20 DF=3*M*M*B-4.0*A*M**3.0-B
              F=B*M**3.0+C-A*M**4.0-B*M
              SLOPE=M-F/DF
              ITER=ITER+1
              IF(ABS(SLOPE-M).LT.0.0001) GO TO 30
              SLOPE=ABS(SLOPE)
              M=SLOPE
              IF(ITER.GT.40) GO TO 40
              GO TO 20
        C
        C     CALCULATE VARIANCE OF SLOPE
        C
           30 A=0.0
              DO 50 I=1,N
              W(I)=0.5*((Y(I)-SLOPE*X(I))**2+(X(I)-Y(I)/SLOPE)**2)
           50 A=A+W(I)
              P=M**6*A-M**4*2*A+M**3*4*B+M**2*A-M*4*B+4*C
              Q=M**8*4*A+M**7*4*B+M**6*C-M**5*4*B-M**4*2*C+M**2*C
              U=(M**2*3*B+M**3*4*A-B)**2
              VAR=(P+Q)/U
              RETURN
           40 WRITE(6,200)
              GO TO 30
          200 FORMAT(1H0,'ITTERATION STOPPED AFTER 40 ITTERATIONS')
              END
```

```
FORTRAN IV G LEVEL  21                  REJECT              DATE = 74262          16/01/34

                SUBROUTINE REJECT(X,Y,M,S,W,*)
                DIMENSION X(M),Y(M),CHISQ(30),W(M)
                DATA CHISQ/3.841,5.991,7.815,9.488,11.070,12.592,14.067,15.507,
               A16.919,18.307,19.675,21.026,22.362,23.685,24.996,26.296,27.587,
               B28.869,30.144,31.410,32.671,33.924,35.172,36.415,37.652,38.885,40.
               C113,41.337,42.557,43.773/
                NU=M-2
                IF(NU.LT.1) RETURN
                IF(NU.GT.30) GO TO 30
                IF(S.LT.CHISQ(NU)) RETURN
                AMAX=W(1)
                K=1
                DO 10 I=2,M
                IF(W(I).LT.AMAX) GO TO 10
                K=I
                AMAX=W(I)
             10 CONTINUE
                J=0
                DO 20 I=1,M
                IF(I.EQ.K) GO TO 20
                J=J+1
                X(J)=X(I)
                Y(J)=Y(I)
             20 CONTINUE
                M=J
                RETURN1
             30 WRITE(6,200)
                RETURN
            200 FORMAT(1H+,T90,'TOO MANY DEGREES OF FREEDOM')
                END
```

```
      SUBROUTINE PLAT (X,Y,TEST,N,K,TIT2,TIT1)
      LOGICAL*1 ARRAY(34,56,2),BLANK,MINUS,LINE,STAR,R,TIT,TIT1,TIT2,TIT
     13,TIT4,SYMBOL
      DATA BLANK,MINUS,LINE,STAR,R/' ','-','|','*','R'/
      LOGICAL*1 TIT3(34,2),TIT4(56,2),TIT1(34),TIT2(56)
      DIMENSION X(1),Y(1),TEST(1)
      DO 1 I=1,34
    1 TIT3(I,K)=TIT1(I)
      DO 2 I=1,34
    2 TIT4(I,K)=TIT2(I)
      DO 3 I=35,56
    3 TIT4(I,K)=BLANK
      DO 10 J=2,56
      DO 10 I=2,34
   10 ARRAY(I,J,K)=BLANK
      DO 20 J=1,56
   20 ARRAY(1,J,K)=MINUS
      DO 30 J=1,34
   30 ARRAY(J,1,K)=LINE
      AMAX1=X(1)
      AMIN1=0.0
      AMAX2=Y(1)
      AMIN2=0.0
      DO 40 I=2,N
      IF(X(I).GT.AMAX1) AMAX1=X(I)
      IF(Y(I).GT.AMAX2) AMAX2=Y(I)
   40 CONTINUE
      SCALE1=33.0/(AMAX1-AMIN1)
      SCALE2=55.0/(AMAX2-AMIN2)
      DO 50 I=1,N
      SYMBOL=STAR
      IF(TEST(I).GT.5.0)SYMBOL=R
      IX=(X(I)-AMIN1)*SCALE1+1
      IY=(Y(I)-AMIN2)*SCALE2+1
      IF(IX.GT.33)IX=34
      IF(IY.GT.55)IY=56
   50 ARRAY(IX,IY,K)=SYMBOL
      RETURN
      ENTRY PRTPLT
      WRITE(6,102)
      DO 60 I=1,34
      L=35-I
      WRITE(6,100) TIT3(I,1),(ARRAY(L,J,1),J=1,56),TIT3(I,2),(ARRAY(L,J,
     12),J=1,56)
   60 CONTINUE
      WRITE(6,101) ((TIT4(I,K),I=1,56),K=1,2)
      RETURN
  100 FORMAT(1H ,A1,1X,56A1,5X,A1,1X,56A1)
  101 FORMAT(1H0,T3,56A1,7X,56A1)
  102 FORMAT(1H1)
      END
```

```
FORTRAN IV G LEVEL  21                    CALPLT               DATE = 74262            16/01/34

              SUBROUTINE CALPLT(Y1,X1,Y2,X2,TEST,N,B,CODE,ALD,C,ERR)
              INTEGER*2 TIT2
              REAL*8 ALD(2),TIT1
              DIMENSION Y1(30),X1(30),Y2(30),X2(30),TEST(30),CODE(3)
              REAL*4 LENGTH
              DATA ARM1,ARM2,ANRM,TRM/'ARM1','ARM2','NRM ','TRM '/
              DATA TIT1,TIT2/'SLOPE=1','B='/
        C
        C     CALCULATE MAXIMA AND SCALEING FACTORS
        C
              F=0.5*B
              S=C/ABS(C)
              AMAXX=0.0
              AMAXY=0.0
              DO 100 I=1,N
              IF(Y1(I).GT.AMAXY) AMAXY=Y1(I)
              IF(X1(I).GT.AMAXY) AMAXY=X1(I)
              IF(Y2(I).GT.AMAXX) AMAXX=Y2(I)
              IF(X2(I).GT.AMAXX) AMAXX=X2(I)
          100 CONTINUE
              LENGTH=4.0
              SCALEY=LENGTH/AMAXY
              SCALEX=LENGTH/AMAXX
        C
        C     PLOT NRM AGAINST TRM
        C
              CALL MOVE(0.5,0.5)
              CALL SETO
              CALL SYMBOL(0.2,3.8,0.2,TIT2,0.0,2)
              CALL NUMBER(0.5,3.8,0.2,F,0.0,3)
              CALL SYMBOL(1.6,3.8,0.2,23,0.0,-1)
              CALL NUMBER(1.8,3.8,0.2,ERR,0.0,3)
              CALL SYMBOL(-0.5,9.5,0.2,CODE,0.0,12)
              CALL SYMBOL(2.0,9.5,0.2,ALD,0.0,16)
              CALL MOVE(0.0,0.0)
              CALL PLOTIT(X2,Y2,TEST,SCALEX,SCALEX,ANRM,TRM,N,LENGTH)
              RAT=1.0
              IF(RAT.LT.B) GO TO 400
              Y=3*SCALEX*AMAXX
              CALL MOVE(0.0,0.0)
              CALL PLOT(LENGTH,Y)
              GO TO 450
          400 X=SCALEX*AMAXX/B
              CALL MOVE(0.0,0.0)
              CALL PLOT(X,LENGTH)
          450 CONTINUE
        C
        C     PLOT ARM1 AGAINST ARM2
        C
              CALL MOVE(0.0,5.0)
              CALL SETO
              CALL SYMBOL(0.2,3.8,0.2,TIT1,0.0,8)
              CALL MOVE(0.0,0.0)
              CALL PLOTIT(X1,Y1,TEST,SCALEY,SCALEY,ARM1,ARM2,N,LENGTH)
              IF(C.LT.0.0) GO TO 200
              X=SCALEY*C
              CALL MOVE(X,0.0)
              IF((AMAXY-C).LT.AMAXY) GO TO 220
```

```
          X=(C+AMAXY)*SCALEY
          CALL PLOT(X,4.0)
          GO TO 300
      220 Y=(AMAXY-C)*SCALEY
          CALL PLOT(4.0,Y)
          GO TO 300
      200 C=ABS(C)
          Y=C*SCALEY
          CALL MOVE(0.0,Y)
          IF((AMAXY-C).LT.AMAXY) GO TO 210
          Y=(C+AMAXY)*SCALEY
          CALL PLOT(4.0,Y)
          GO TO 300
      210 X=(AMAXY-C)*SCALEY
          CALL PLOT(X,4.0)
      300 CONTINUE
C
C         RESET PLOTTER FOR NEXT SET
C
          CALL MOVE(6.0,-5.5)
          CALL SETO
          C=C*S
          RETURN
          END
```

FORTRAN IV G LEVEL 21 PLOTIT DATE = 74262 16/01/34

```
      SUBROUTINE PLOTIT(X,Y,TEST,SCALEX,SCALEY,ORD,ABS,N,LENGTH)
      DIMENSION X(30),Y(30),TEST(30)
      REAL*4 LENGTH
C
C     PLOT AXES
C
      CALL PLOT(LENGTH,0.0)
      CALL MOVE(0.0,0.0)
      CALL PLOT(0.0,LENGTH)
      CALL MOVE(0.0,0.0)
      DO 200 I=1,5
      AI=I-1
      VX=AI/SCALEX
      CALL SYMBOL(AI,0.0,0.2,16,0.0,-1)
      CALL NUMBER(AI-0.2,-0.3,0.1,VX,0.0,2)
  200 CONTINUE
      DO 300 I=1,5
      AI=I-1
      VY=AI/SCALEY
      CALL SYMBOL(0.0,AI,0.2,15,0.0,-1)
      CALL NUMBER(-0.4,AI+0.2,0.1,VY,-90.0,2)
  300 CONTINUE
C
C     LABEL AXES
C
      CALL SYMBOL(-0.8,1.5,0.2,ORD,-90.0,4)
      CALL SYMBOL(1.5,-0.8,0.2,ABS,0.0,4)
C
C     PLOT POINTS
C
      DO 400 I=1,N
      VX=X(I)*SCALEX
      VY=Y(I)*SCALEY
      ICHAR=3
      CALL SYMBOL(VX,VY,0.1,ICHAR,0.0,-1)
  400 CONTINUE
      RETURN
      END
```

```
      SUBROUTINE WAITAV(P,VAR,N,AVE,VARIAN)
      DIMENSION P(N),VAR(N),W(30)
      SUM=0.0
      DO 10 I=1,N
      W(I)=1.0/VAR(I)
   10 SUM=SUM+W(I)
      AVE=0.0
      VARIAN=0.0
      DO 20 I=1,N
      A=W(I)/SUM
      AVE=A*P(I)+AVE
   20 CONTINUE
      IF(N.EQ.1) GO TO 40
      SUM1=0.0
      DO 30 I=1,N
      SUM1=SUM1+W(I)*(P(I)-AVE)*(P(I)-AVE)
   30 CONTINUE
      VARIAN=N*SUM1/((N-1.0)*SUM)
      RETURN
   40 VARIAN=0.0
      RETURN
      END
```

APPENDIX 2.

This appendix contains all the data discussed in chapter 5 but not included in chapter 5 (test results).

The graphs are in the following order:-

Description		Code
Single lava		ICL
Baked contact		C64
Historic lavas	(1907 Hawaii	2L148
	(1910 Etna	E1
	(1926 Hawaii	2L152
	(1955 Hawaii	2L025
	(1973 Heimaey	W
Archaeomagnetic specimens	(1965 Pottery	103 A
	(1900 Brick	S2 1
	(1356 Tile	5PT
	(350 Tile	HAMA1
	(150 Pottery	48A1

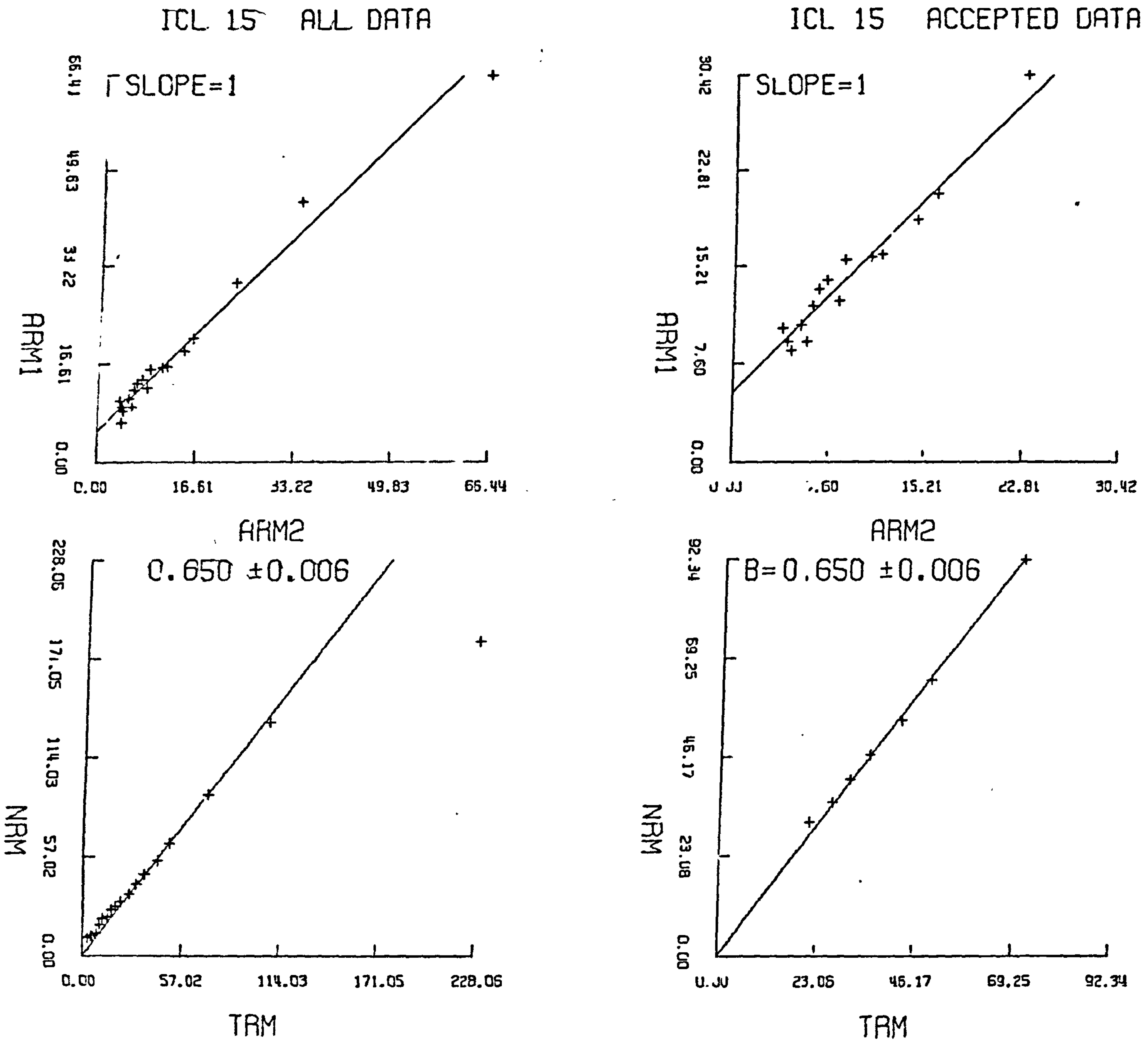
ICL 15 ALL DATA
SLOPE=1
ARM1
ARM2
0.00
16.61
33.22
49.83
66.44
C.650 ±0.006
NRM
TRM
0.00
57.02
114.03
171.05
228.06
ICL 15 ACCEPTED DATA
SLOPE=1
ARM1
ARM2
0.00
7.60
15.21
22.81
30.42
B=0.650 ±0.006
NRM
TRM
0.00
23.08
46.17
69.25
92.34

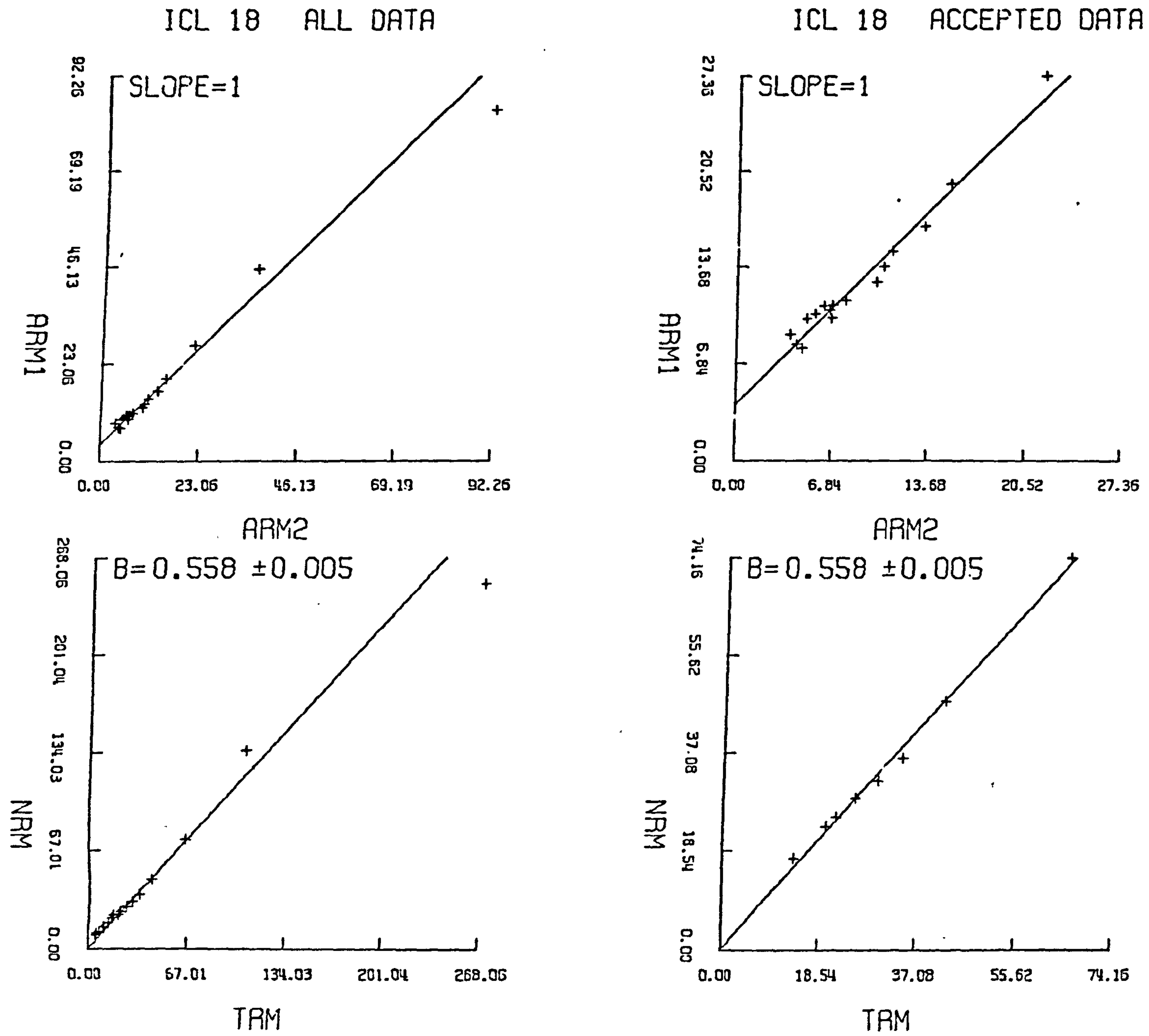
ICL 18 ALL DATA
ICL 18 ACCEPTED DATA
SLOPE=1
SLOPE=1
ARM1
ARM2
ARM1
ARM2
0.00
23.06
46.13
69.19
92.26
0.00
6.84
13.68
20.52
27.36
B=0.558 ±0.005
B=0.558 ±0.005
NRM
TRM
NRM
TRM
0.00
67.01
134.03
201.04
268.06
0.00
18.54
37.08
55.62
74.16

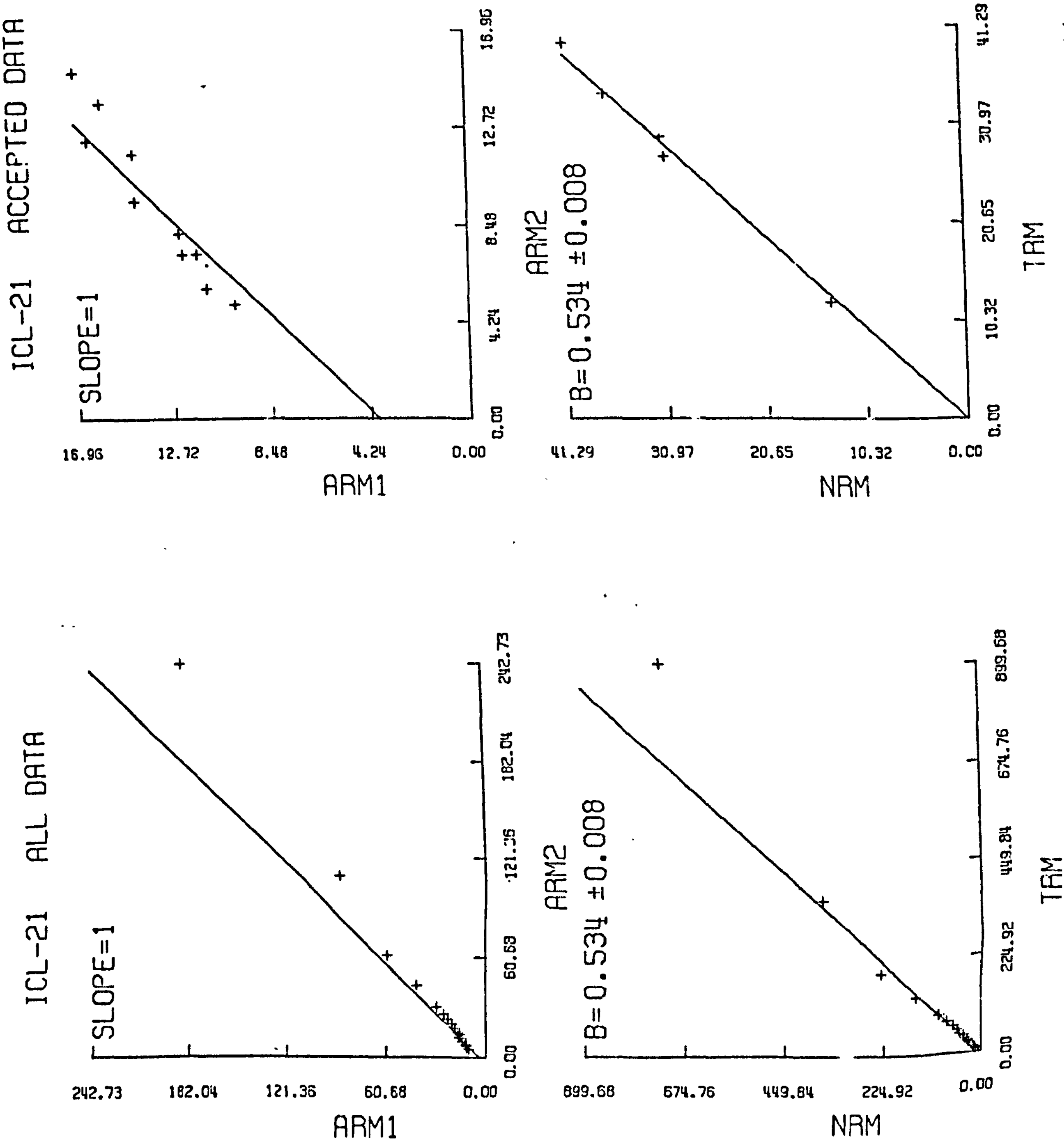
ICL-21 ACCEPTED DATA
SLOPE=1
ARM1
ARM2
B=0.534 ±0.008
NRM
TRM
ICL-21 ALL DATA
SLOPE=1
ARM1
ARM2
B=0.534 ±0.008
NRM
TRM

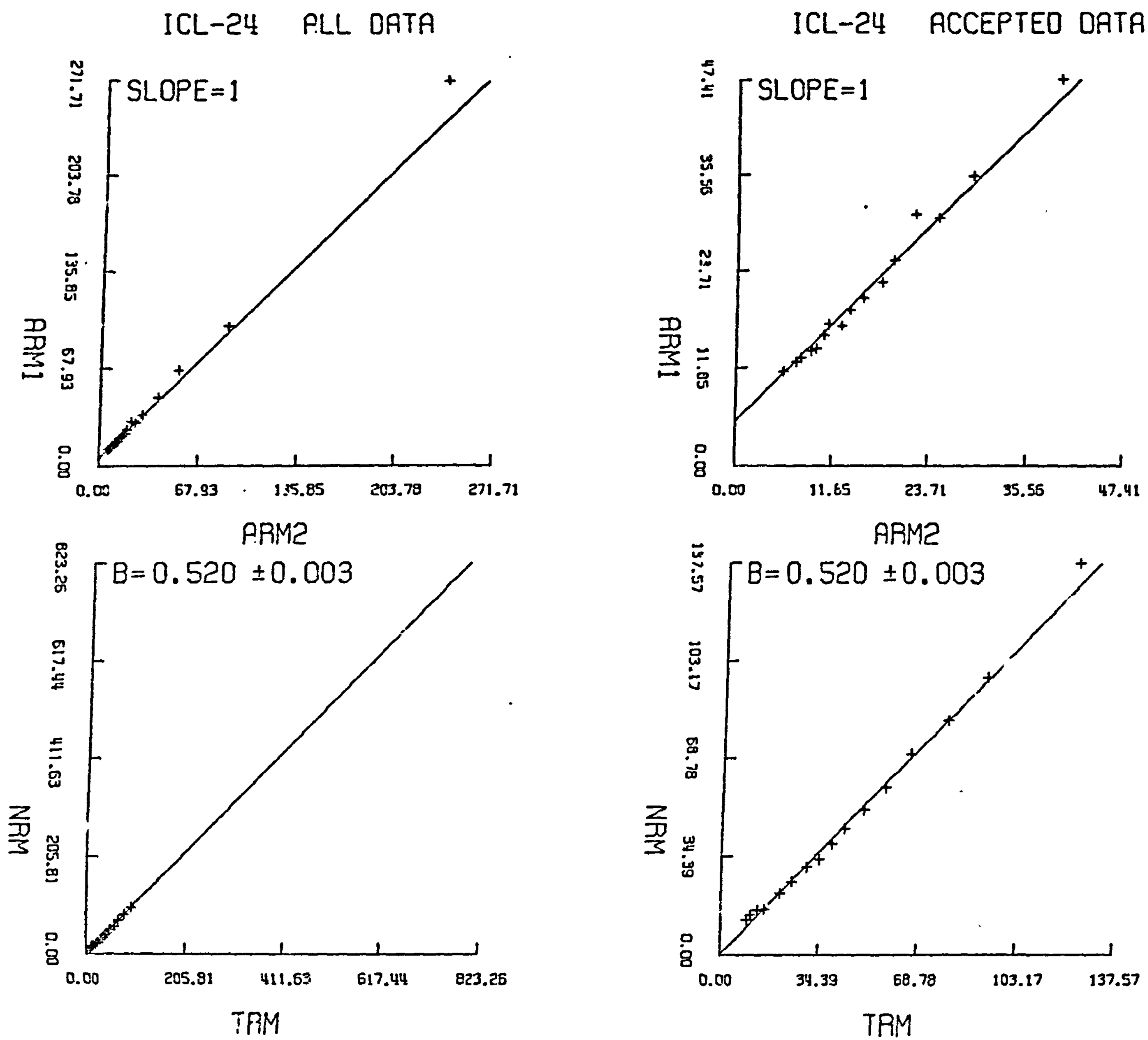
ICL-24 ALL DATA
ICL-24 ACCEPTED DATA
SLOPE=1
SLOPE=1
ARM1
ARM1
ARM2
ARM2
0.00
67.93
135.85
203.78
271.71
0.00
11.85
23.71
35.56
47.41
B=0.520 ±0.003
B=0.520 ±0.003
NRM
NRM
TRM
TRM
0.00
205.81
411.63
617.44
823.26
0.00
34.39
68.78
103.17
137.57

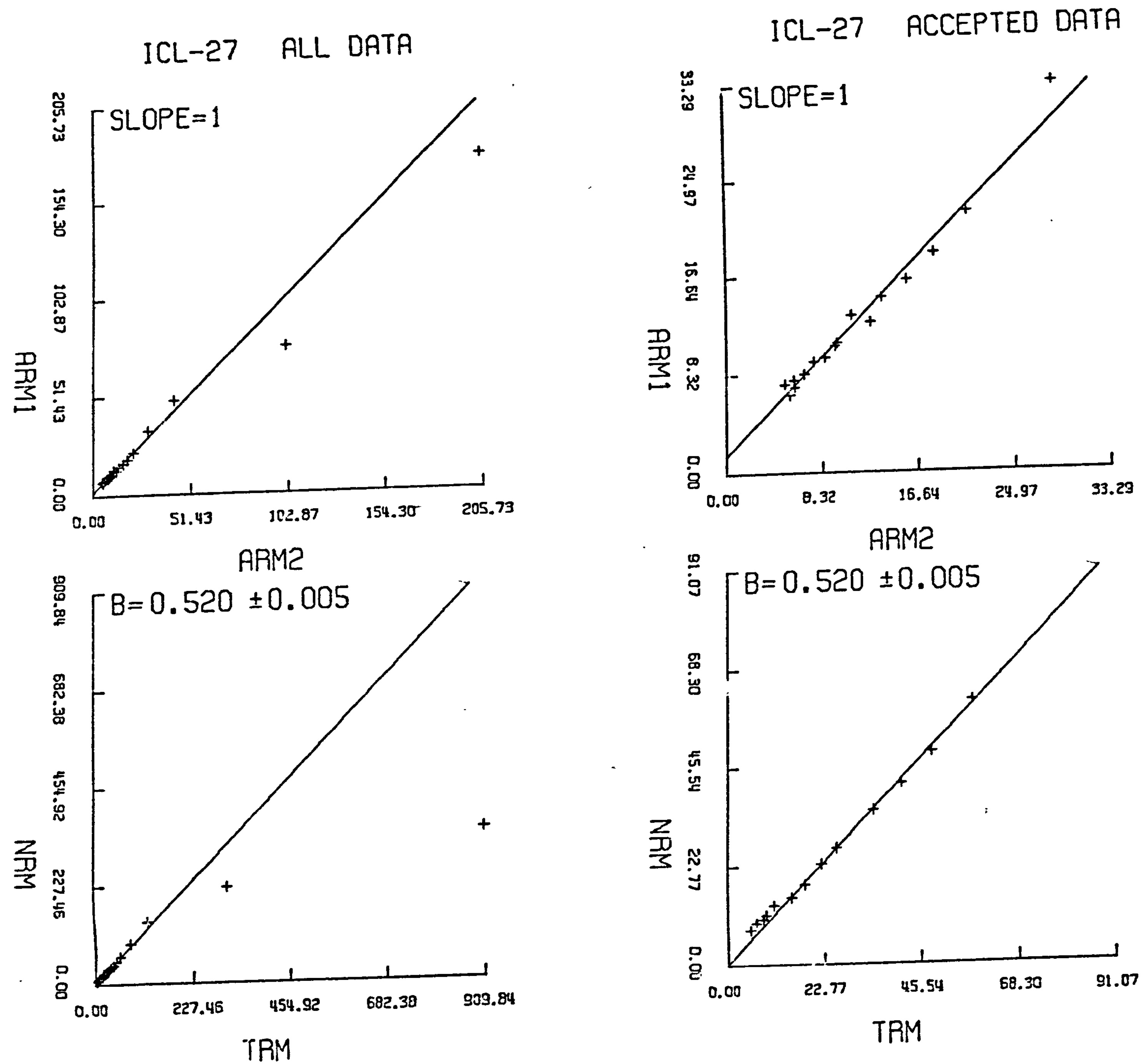

ICL-27 ALL DATA
SLOPE=1
ARM1
ARM2
0.00
51.43
102.87
154.30
205.73
B=0.520 ±0.005
NRM
TRM
0.00
227.46
454.92
682.38
909.84
ICL-27 ACCEPTED DATA
SLOPE=1
ARM1
ARM2
0.00
8.32
16.64
24.97
33.29
B=0.520 ±0.005
NRM
TRM
0.00
22.77
45.54
68.30
91.07

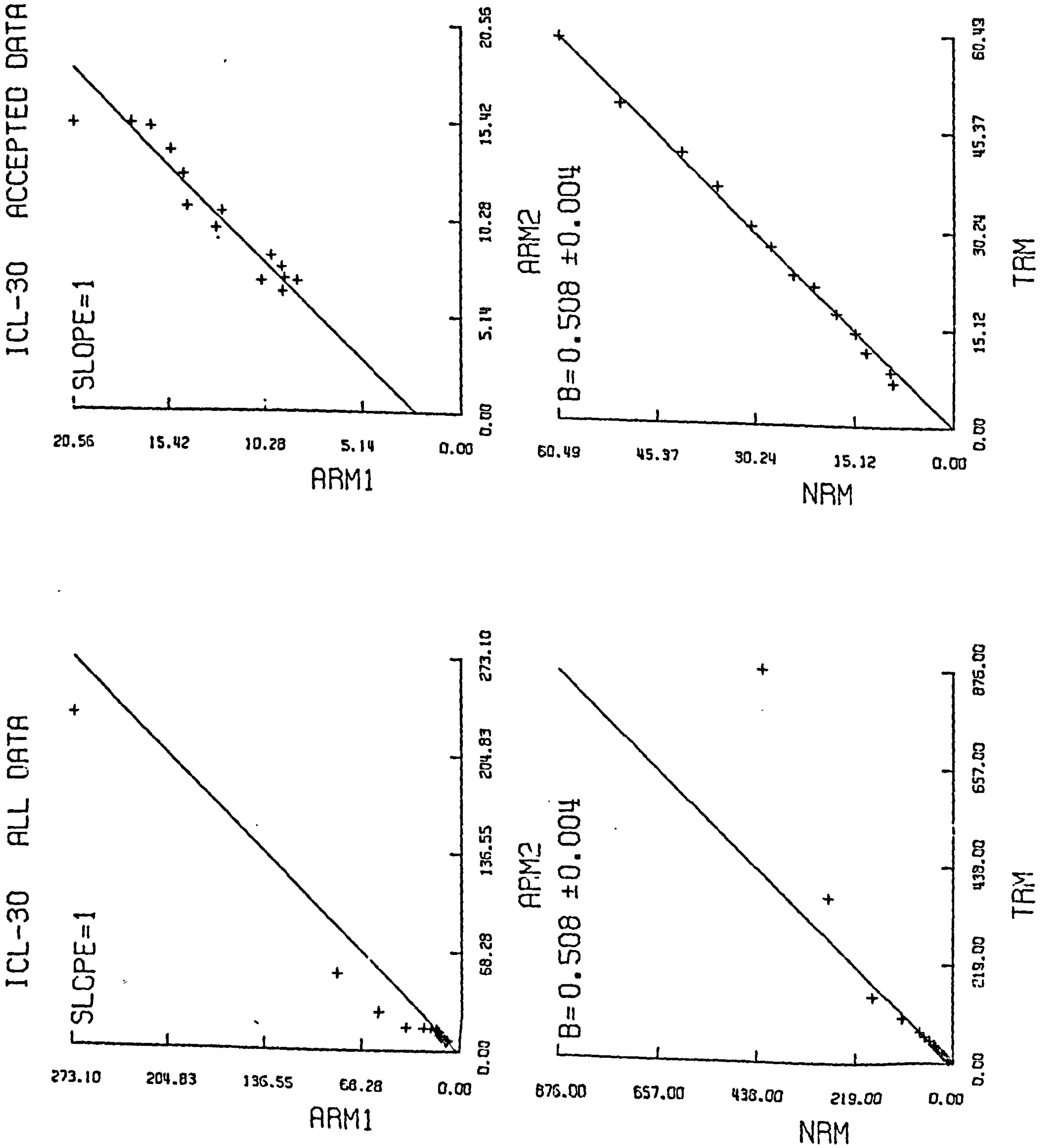

ICL-30 ACCEPTED DATA
SLOPE=1
ARM1
ARM2
B=0.508 ±0.004
NRM
TRM
ICL-30 ALL DATA
SLOPE=1
ARM1
ARM2
B=0.508 ±0.004
NRM
TRM

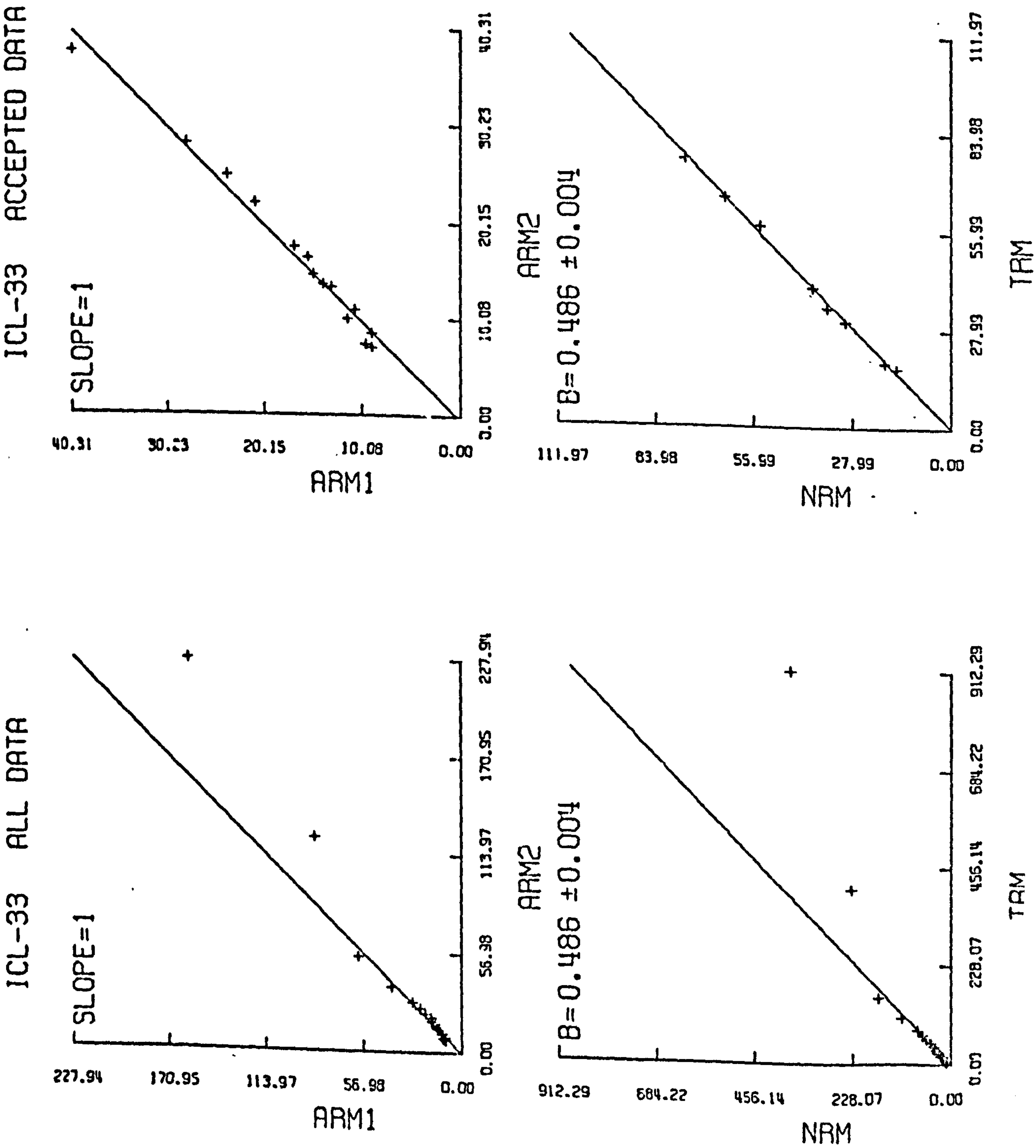
ICL-33 ACCEPTED DATA
SLOPE=1
ARM1
ARM2
B=0.486 ±0.004
NRM
TRM
ICL-33 ALL DATA
SLOPE=1
ARM1
ARM2
B=0.486 ±0.004
NRM
TRM

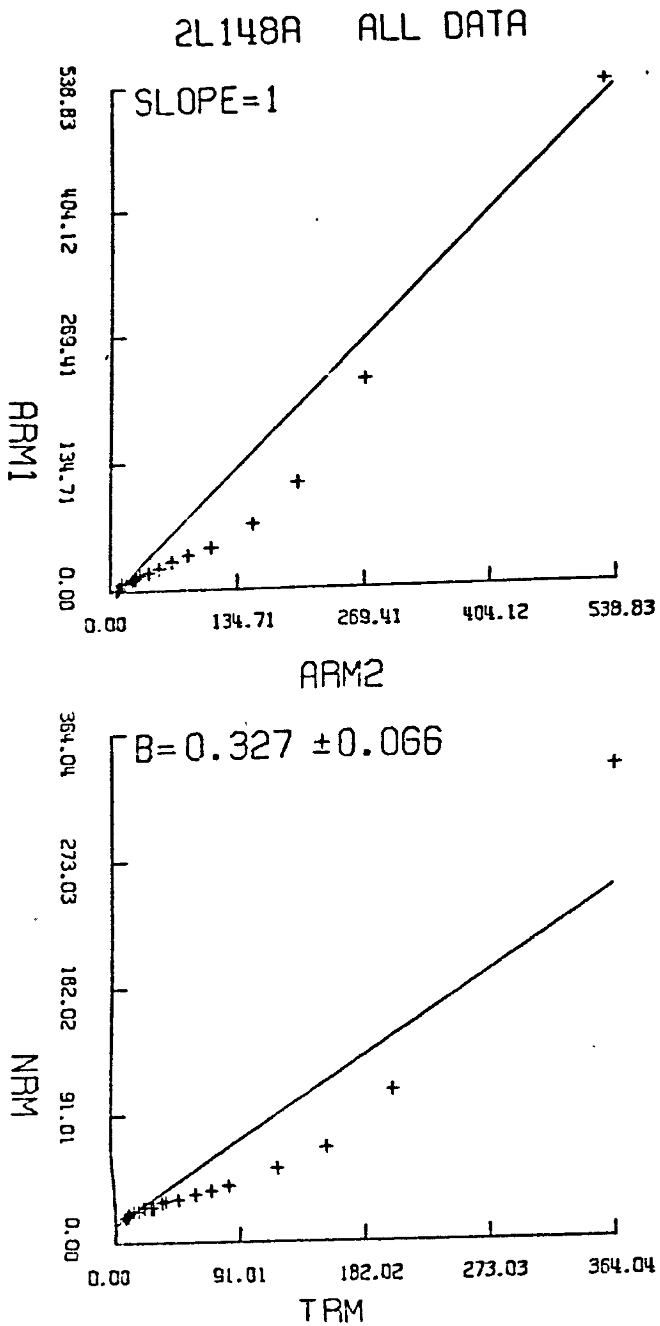

2L148A ALL DATA
SLOPE=1
ARM1
ARM2
0.00
134.71
269.41
404.12
538.83
B=0.327 ±0.066
NRM
TRM
0.00
91.01
182.02
273.03
364.04

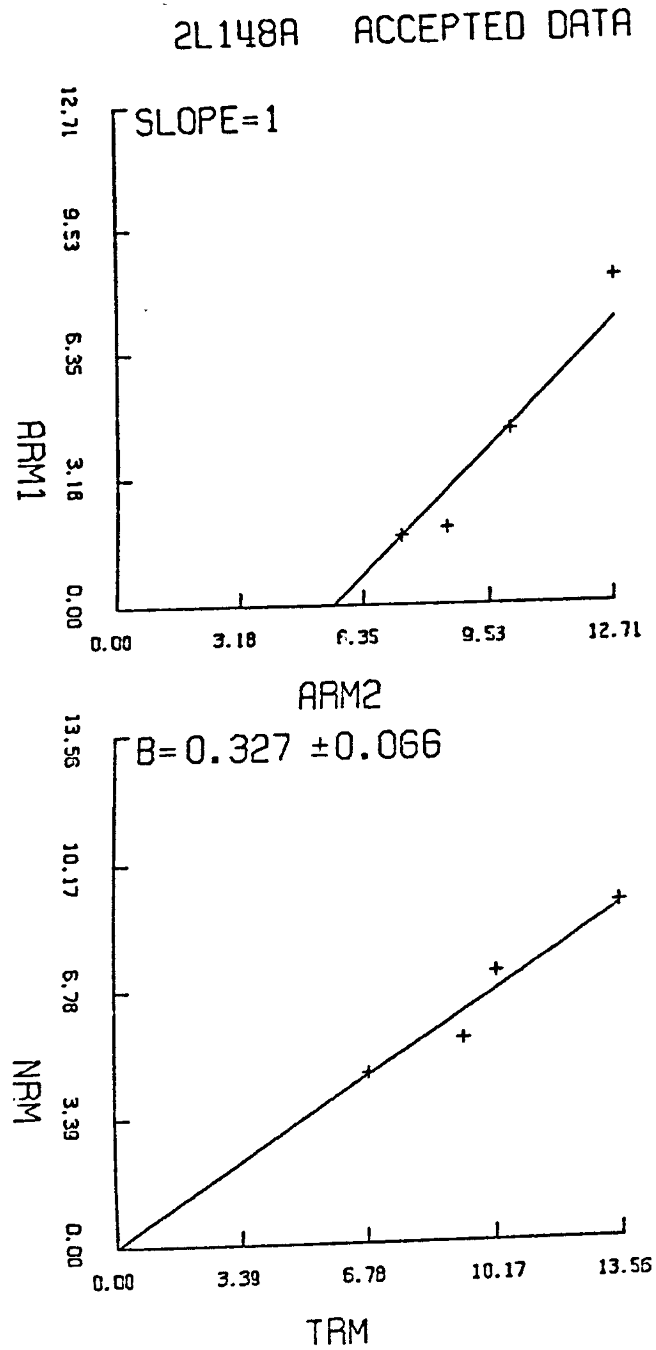

2L148A ACCEPTED DATA
SLOPE=1
ARM1
ARM2
0.00
3.18
6.35
9.53
12.71
B=0.327 ±0.066
NRM
TRM
0.00
3.39
6.78
10.17
13.56

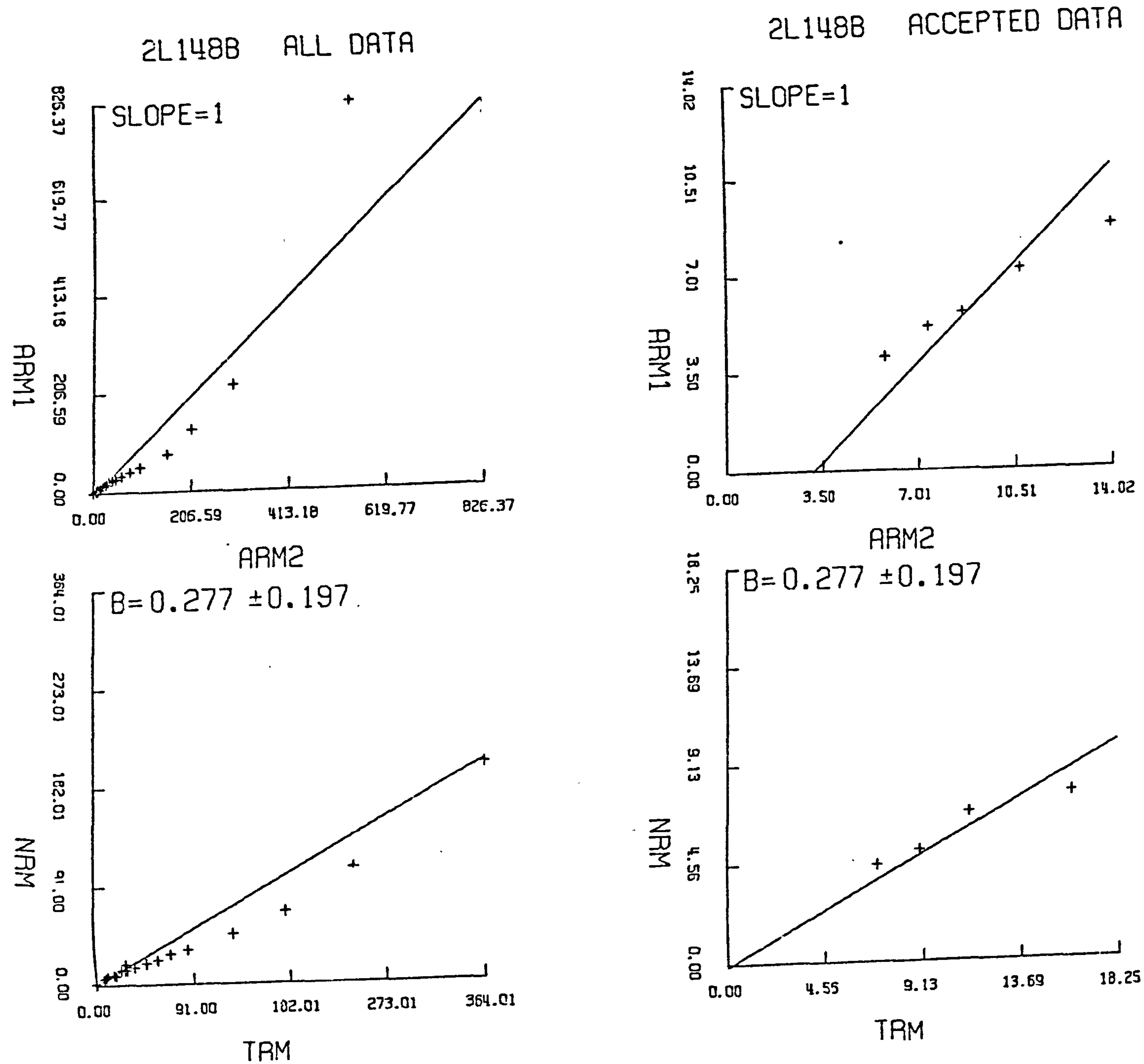
2L148B ALL DATA
2L148B ACCEPTED DATA
SLOPE=1
ARM1
ARM2
0.00
206.59
413.18
619.77
826.37
3.50
7.01
10.51
14.02
B=0.277 ±0.197
NRM
TRM
91.00
182.01
273.01
364.01
4.55
4.56
9.13
13.69
18.25

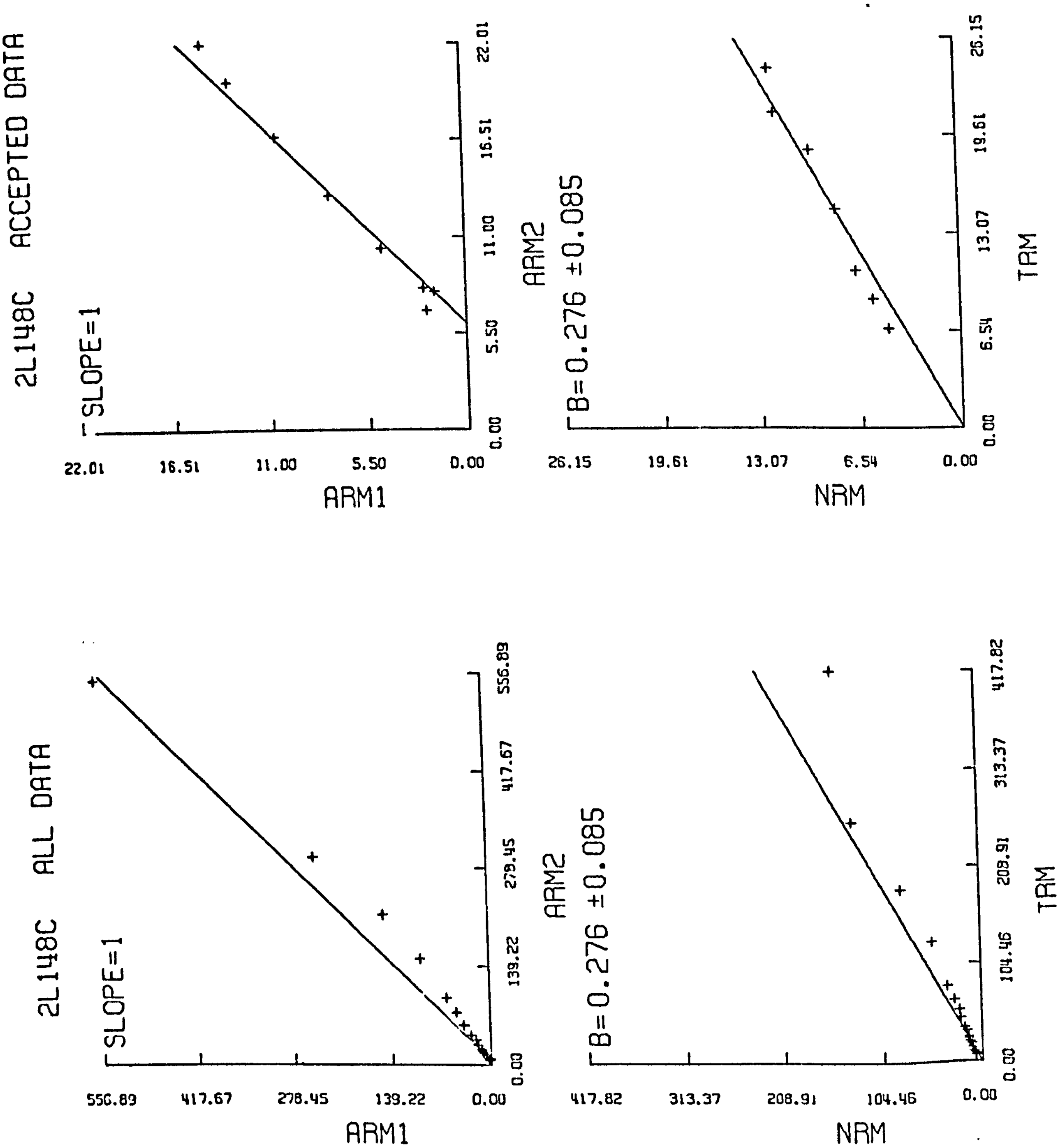
2L148C ACCEPTED DATA
SLOPE=1
ARM2
ARM1
22.01 16.51 11.00 5.50 0.00
B= 0.276 ±0.085
TRM
NRM
26.15 19.61 13.07 6.54 0.00
2L148C ALL DATA
SLOPE=1
ARM2
ARM1
556.89 417.67 278.45 139.22 0.00
B= 0.276 ±0.085
TRM
NRM
417.82 313.37 208.91 104.46 0.00

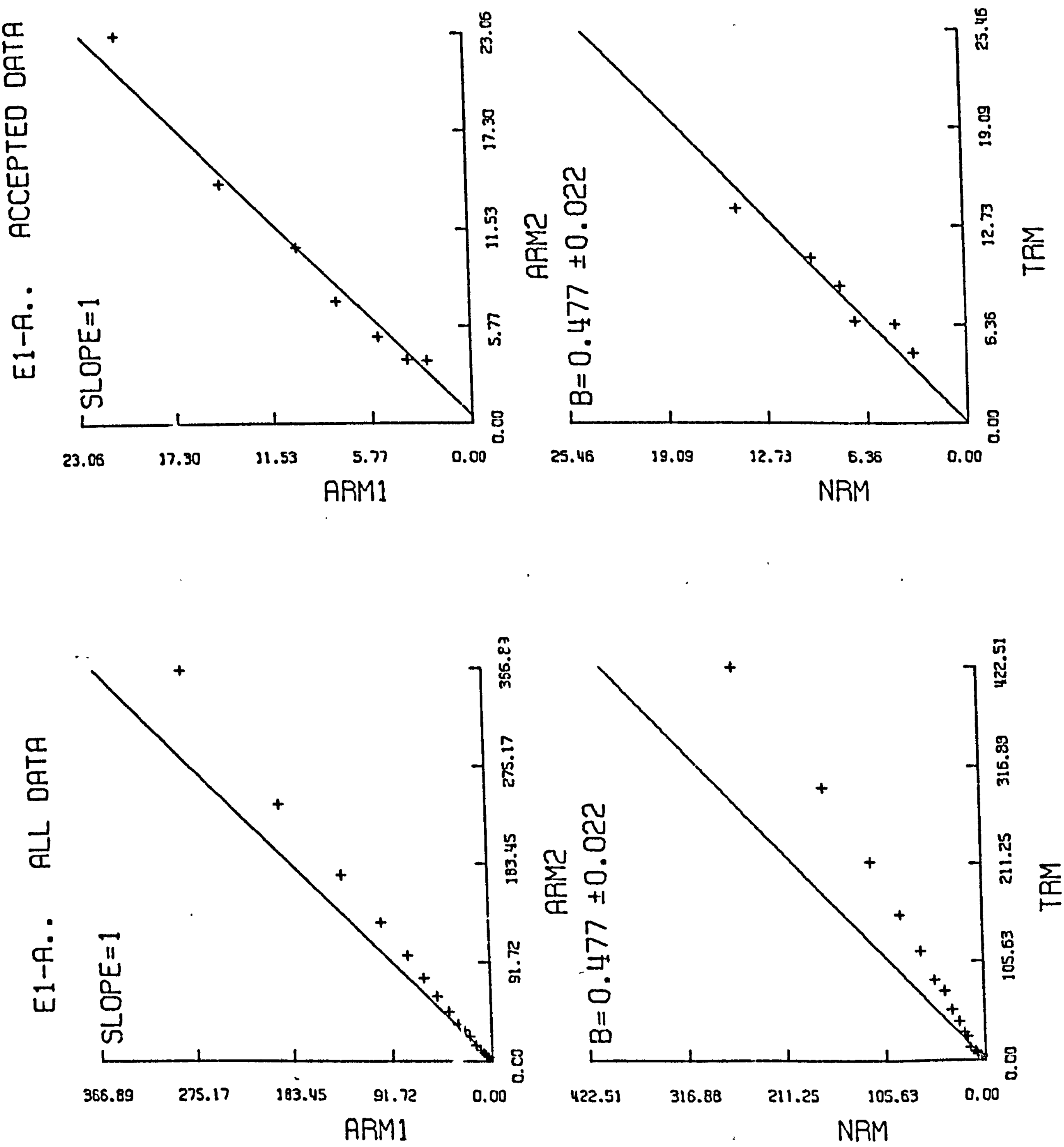
E1-A.. ACCEPTED DATA
SLOPE=1
ARM2
B=0.477 ±0.022
ARM1
NRM
TRM
E1-A.. ALL DATA
SLOPE=1
ARM2
B=0.477 ±0.022
ARM1
NRM
TRM

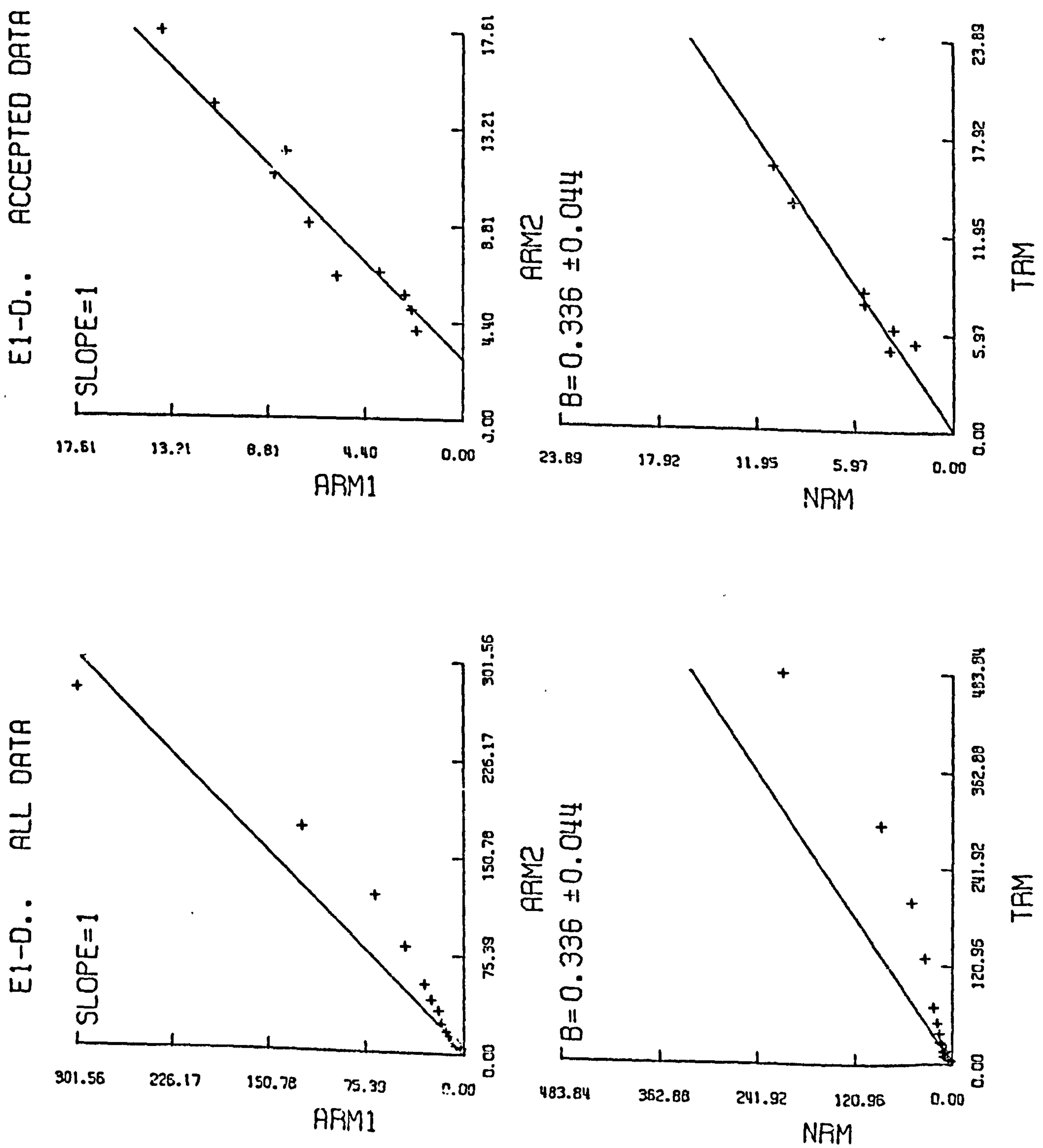
E1-D.. ACCEPTED DATA
SLOPE=1
ARM1
ARM2
B=0.336 ±0.044
NRM
TRM
E1-D.. ALL DATA
SLOPE=1
ARM1
ARM2
B=0.336 ±0.044
NRM
TRM

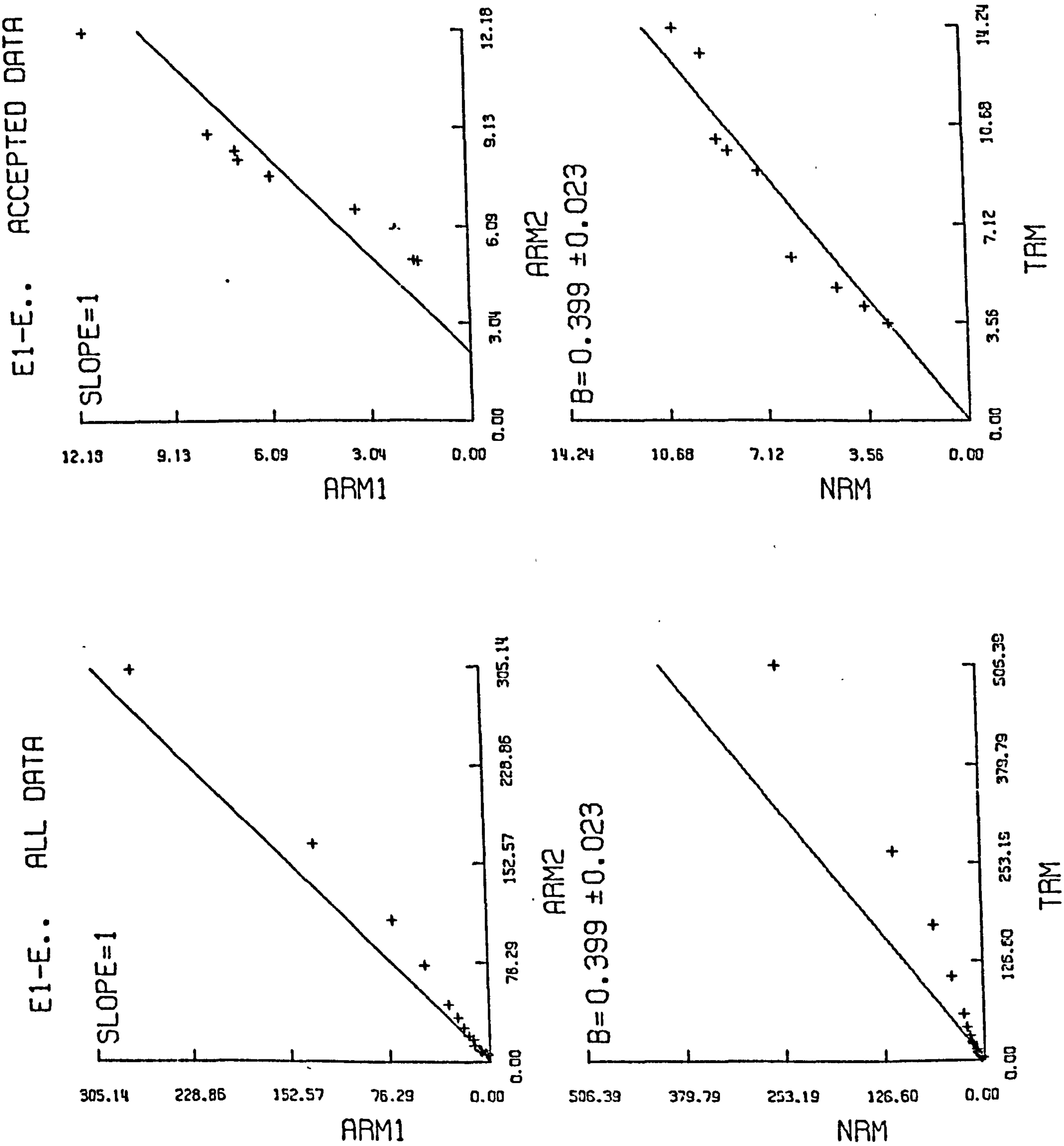
E1-E.. ACCEPTED DATA
SLOPE=1
ARM1
ARM2
B=0.399 ±0.023
NRM
TRM
E1-E.. ALL DATA
SLOPE=1
ARM1
ARM2
B=0.399 ±0.023
NRM
TRM

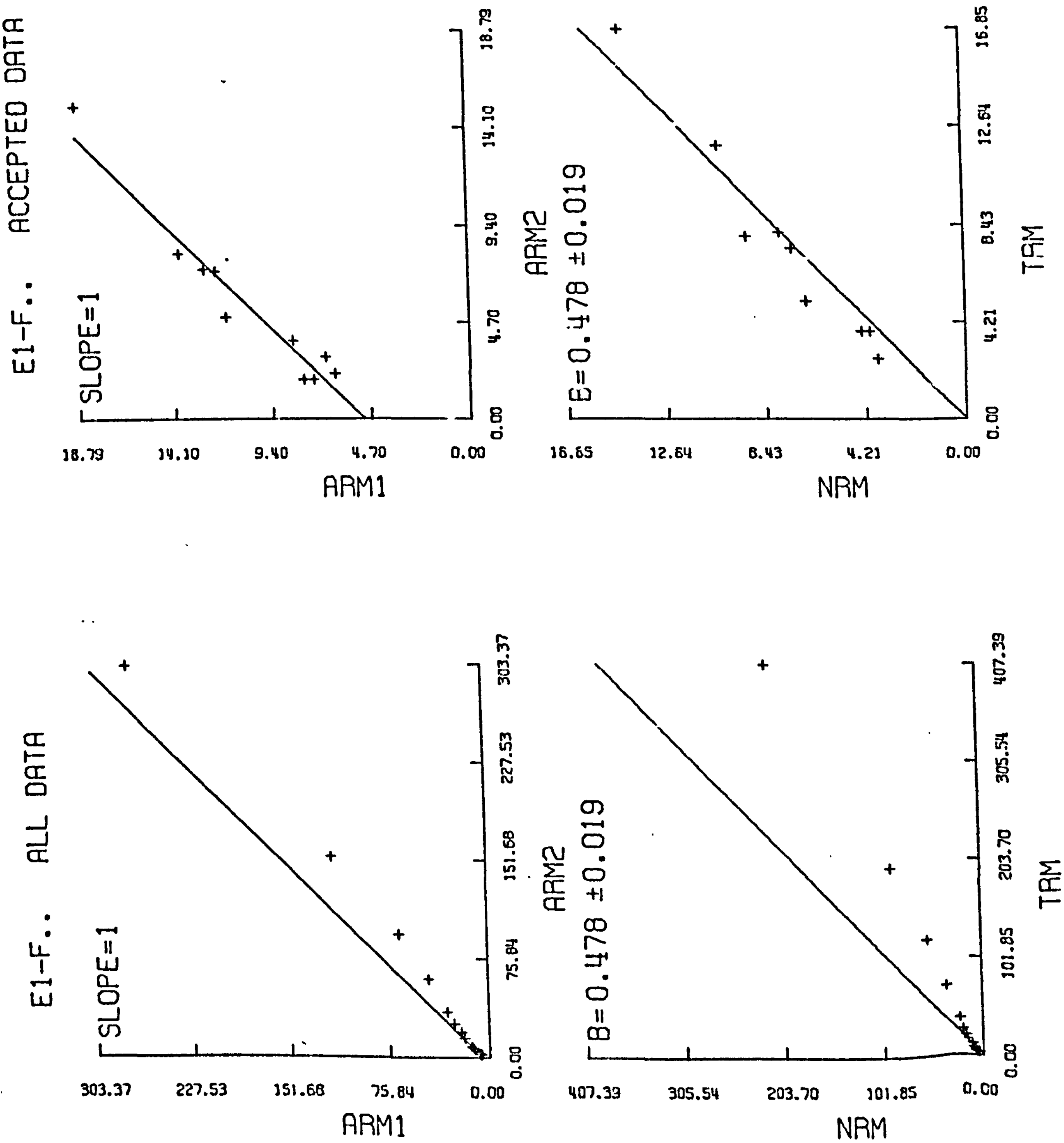
E1-F.. ACCEPTED DATA
SLOPE=1
18.79 14.10 9.40 4.70 0.00
ARM1
ARM2
B=0.478 ±0.019
16.65 12.64 8.43 4.21 0.00
NRM
16.85 12.64 8.43 4.21 0.00
TRM
E1-F.. ALL DATA
SLOPE=1
303.37 227.53 151.68 75.84 0.00
ARM1
ARM2
B=0.478 ±0.019
407.39 305.54 203.70 101.85 0.00
NRM
TRM

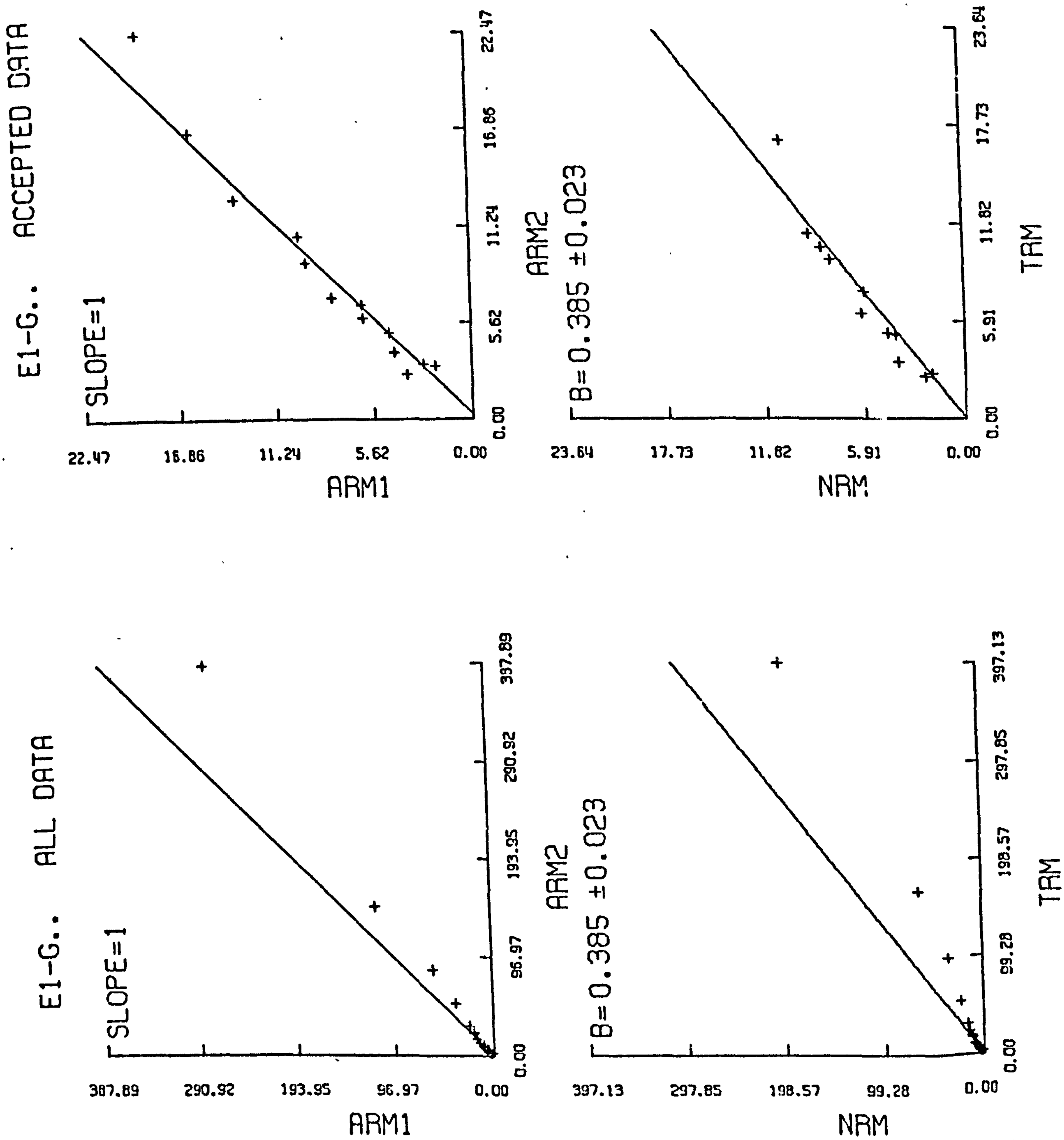
E1-G.. ALL DATA
SLOPE=1
ARM1
ARM2
387.89
290.92
193.95
96.97
0.00
B= 0.385 ±0.023
NRM
TRM
397.13
297.85
198.57
99.28
0.00
E1-G.. ACCEPTED DATA
SLOPE=1
ARM1
ARM2
22.47
16.86
11.24
5.62
0.00
B= 0.385 ±0.023
NRM
TRM
23.64
17.73
11.82
5.91
0.00

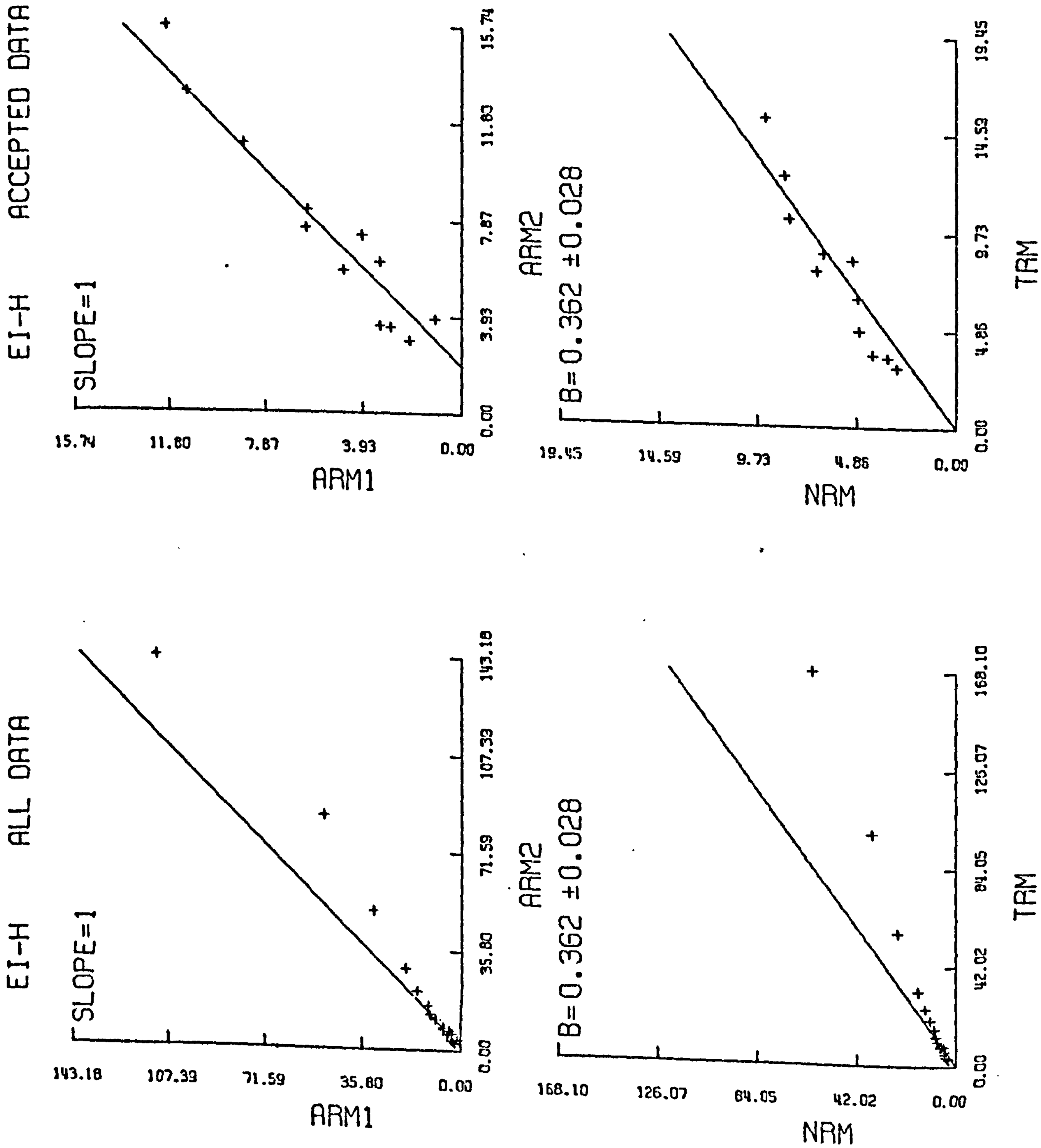
EI-H ACCEPTED DATA
SLOPE=1
ARM1
ARM2
B=0.362 ±0.028
NRM
TRM
EI-H ALL DATA
SLOPE=1
ARM1
ARM2
B=0.362 ±0.028
NRM
TRM

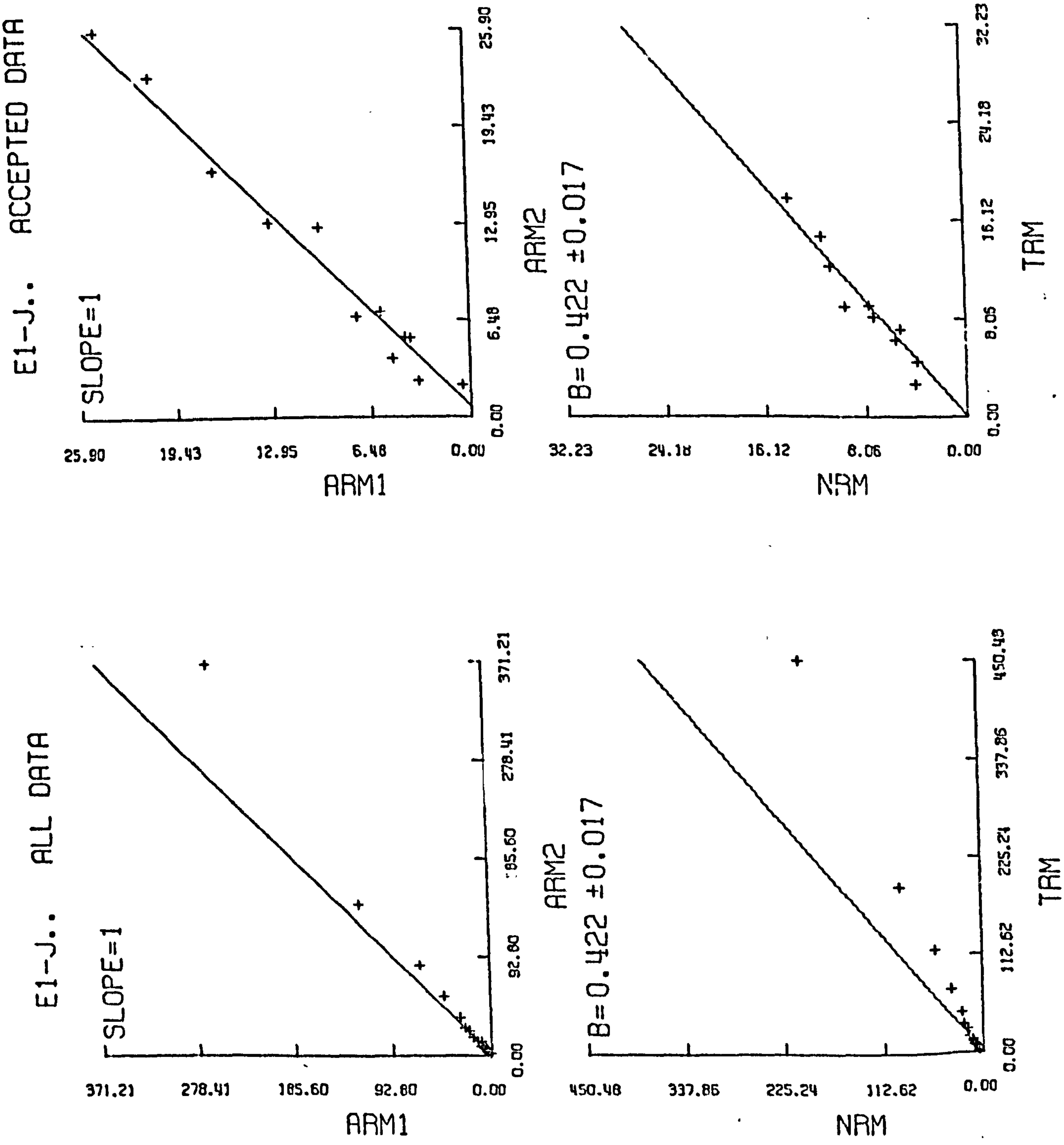
E1-J.. ACCEPTED DATA
SLOPE=1
ARM1
ARM2
25.90 19.43 12.95 6.48 0.00
B=0.422 ±0.017
NRM
TRM
32.23 24.18 16.12 8.06 0.00
E1-J.. ALL DATA
SLOPE=1
ARM1
ARM2
371.21 278.41 185.60 92.80 0.00
B=0.422 ±0.017
NRM
TRM
450.48 337.86 225.24 112.62 0.00

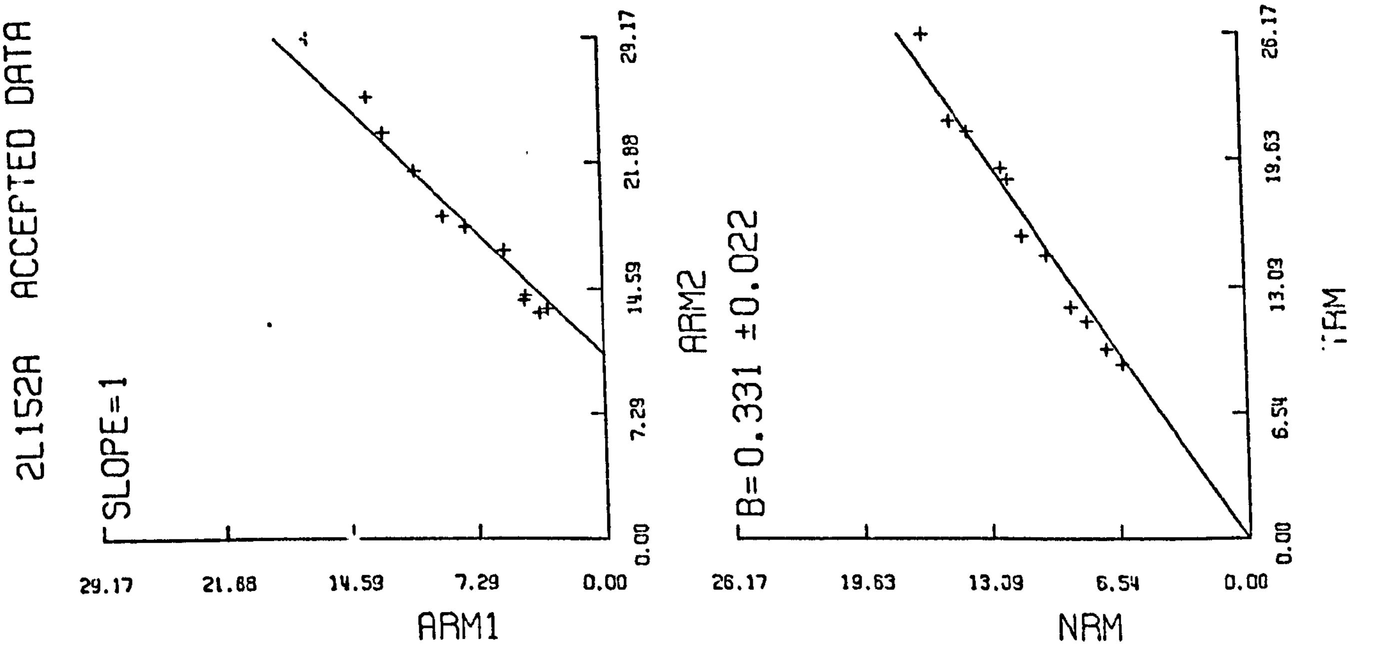
2L152A ACCEPTED DATA
SLOPE=1
ARM1
ARM2
B=0.331 ±0.022
NRM
TRM
29.17
21.88
14.59
7.29
0.00
26.17
19.63
13.09
6.54

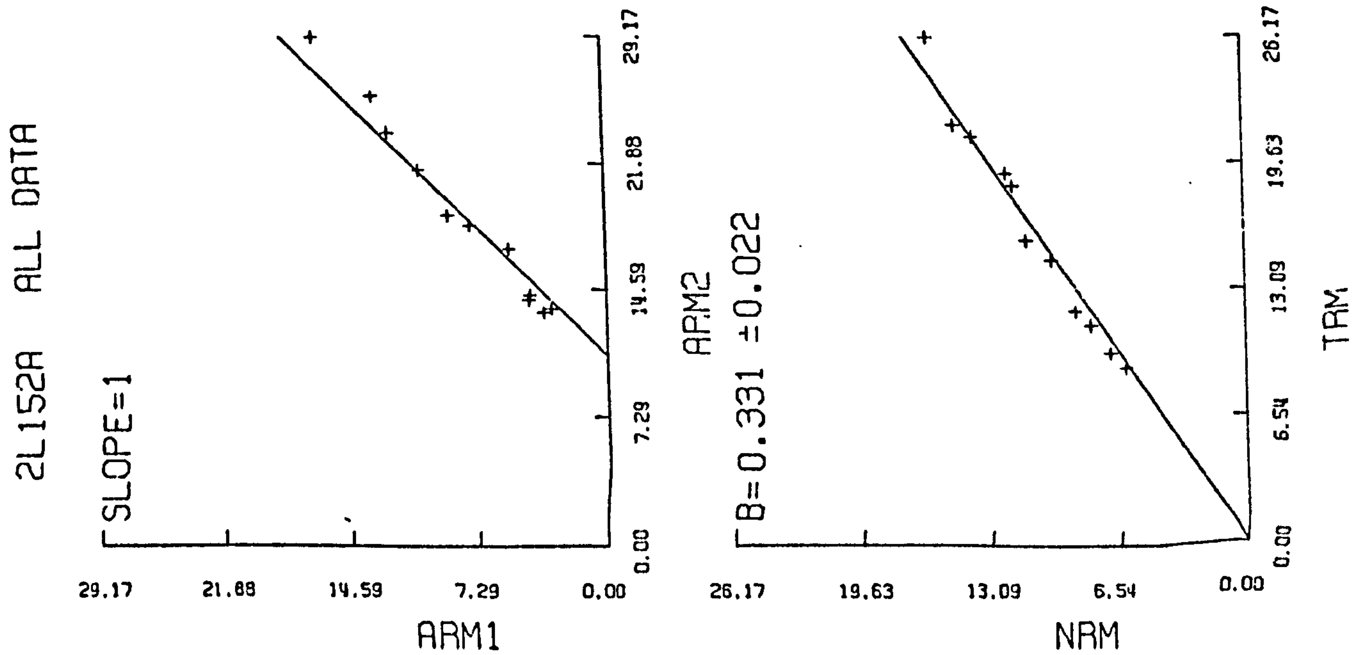
2L152A ALL DATA
SLOPE=1
ARM1
ARM2
B=0.331 ±0.022
NRM
TRM
29.17
21.88
14.59
7.29
0.00
26.17
19.63
13.09
6.54

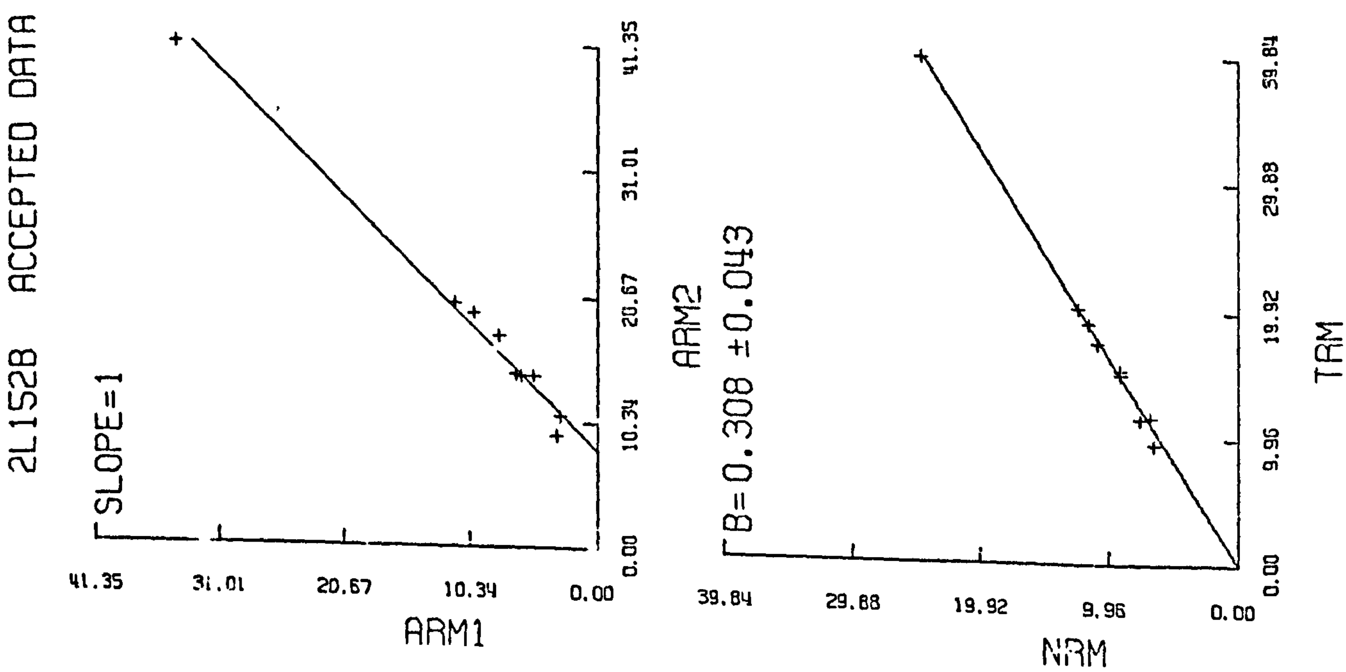
2L152B ACCEPTED DATA
SLOPE=1
ARM1
ARM2
41.35
31.01
20.67
10.34
0.00
B= 0.308 ±0.043
NRM
TRM
39.84
29.88
19.92
9.96
0.00

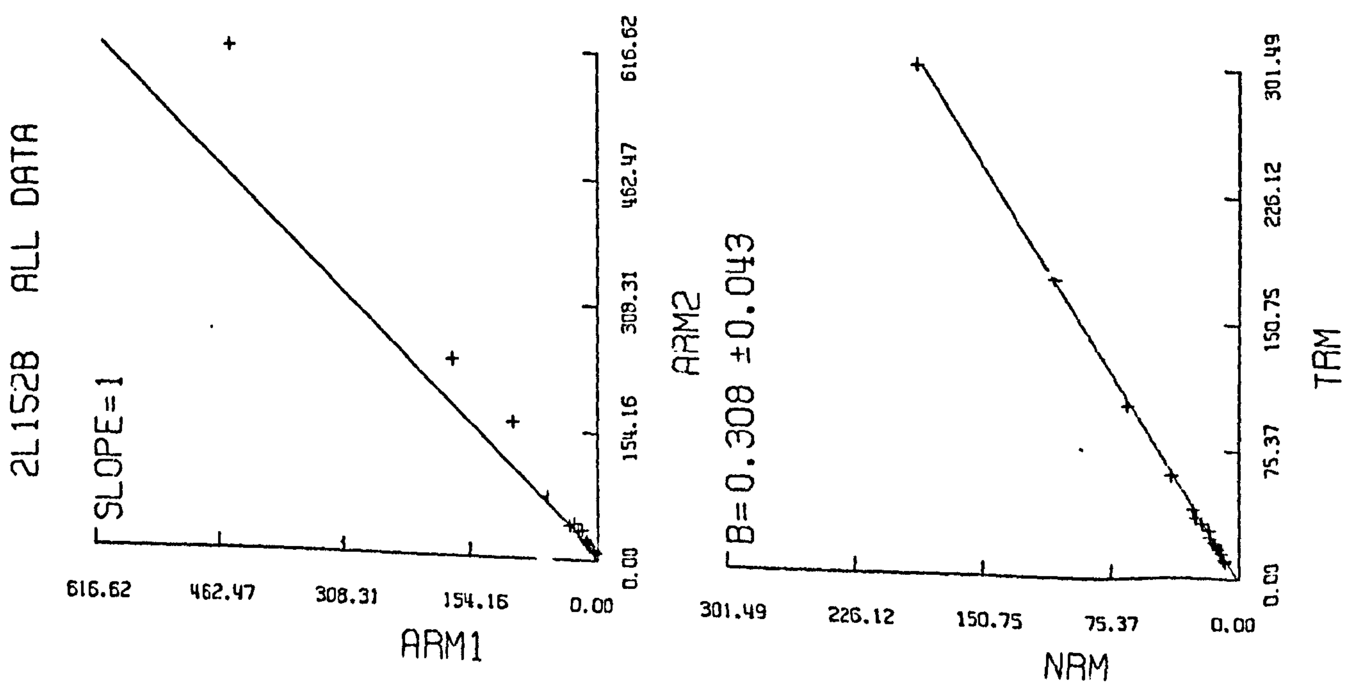
2L152B ALL DATA
SLOPE=1
ARM1
ARM2
616.62
462.47
308.31
154.16
0.00
B= 0.308 ±0.043
NRM
TRM
301.49
226.12
150.75
75.37
0.00

2L152C ALL DATA

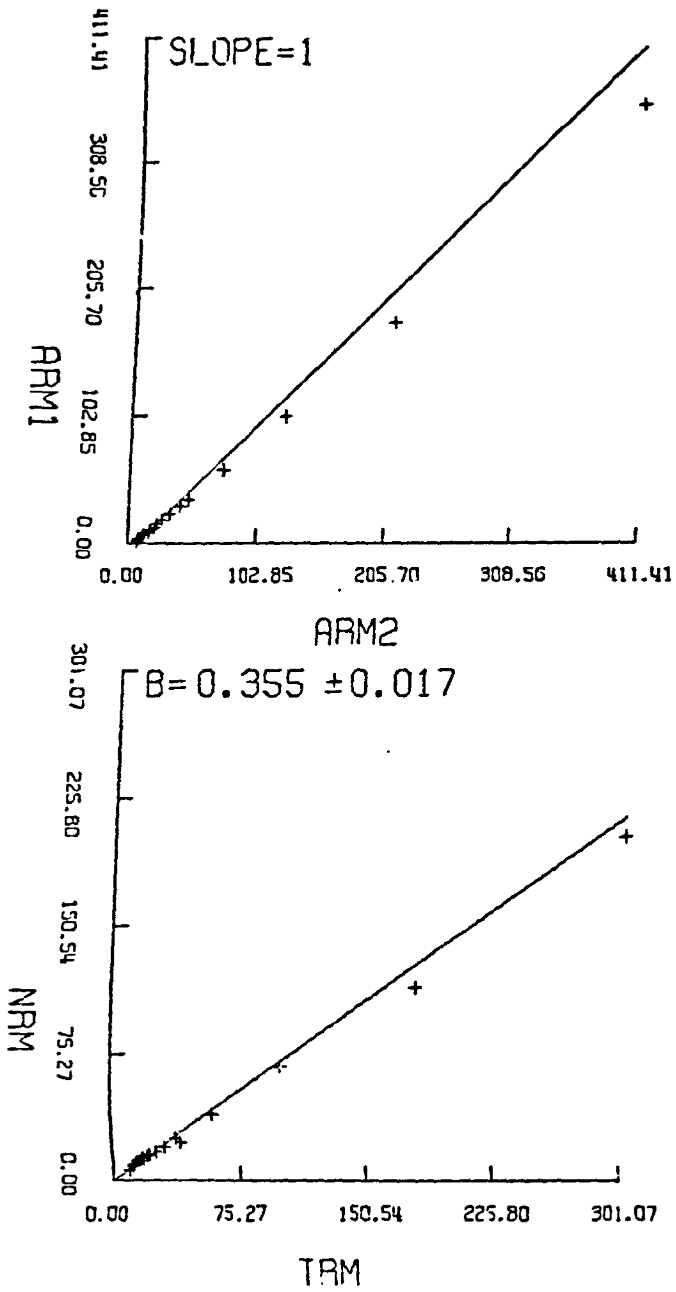

2L152C ACCEPTED DATA

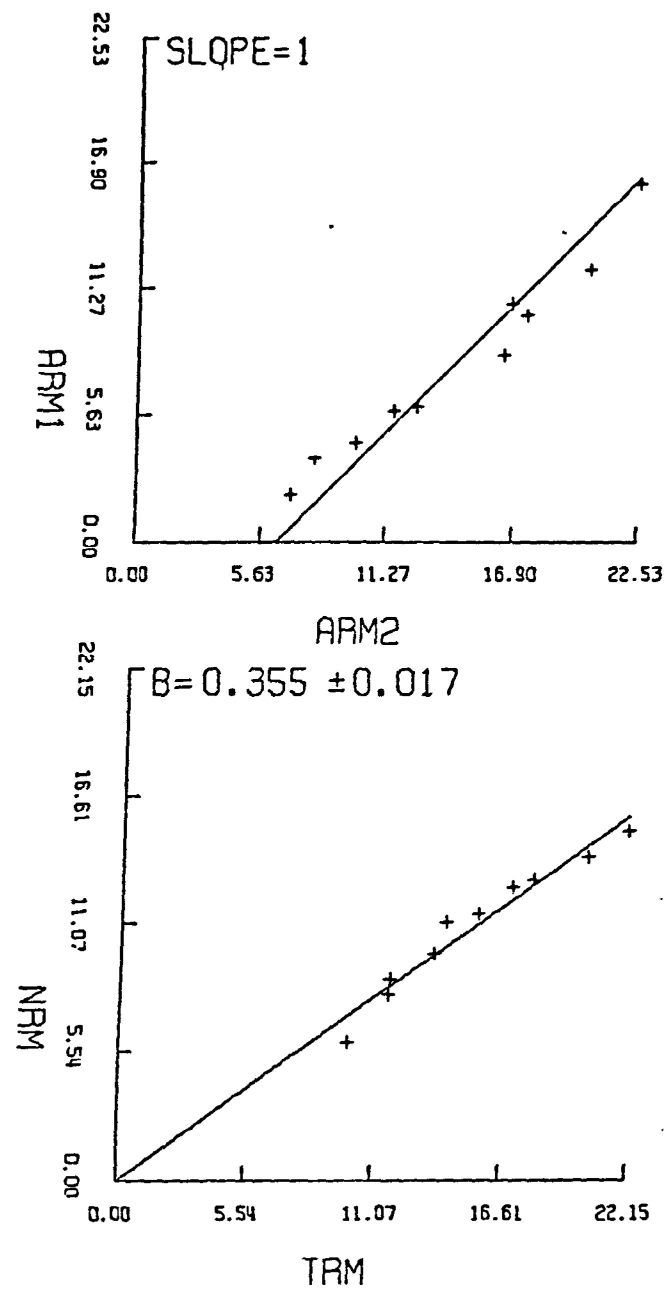

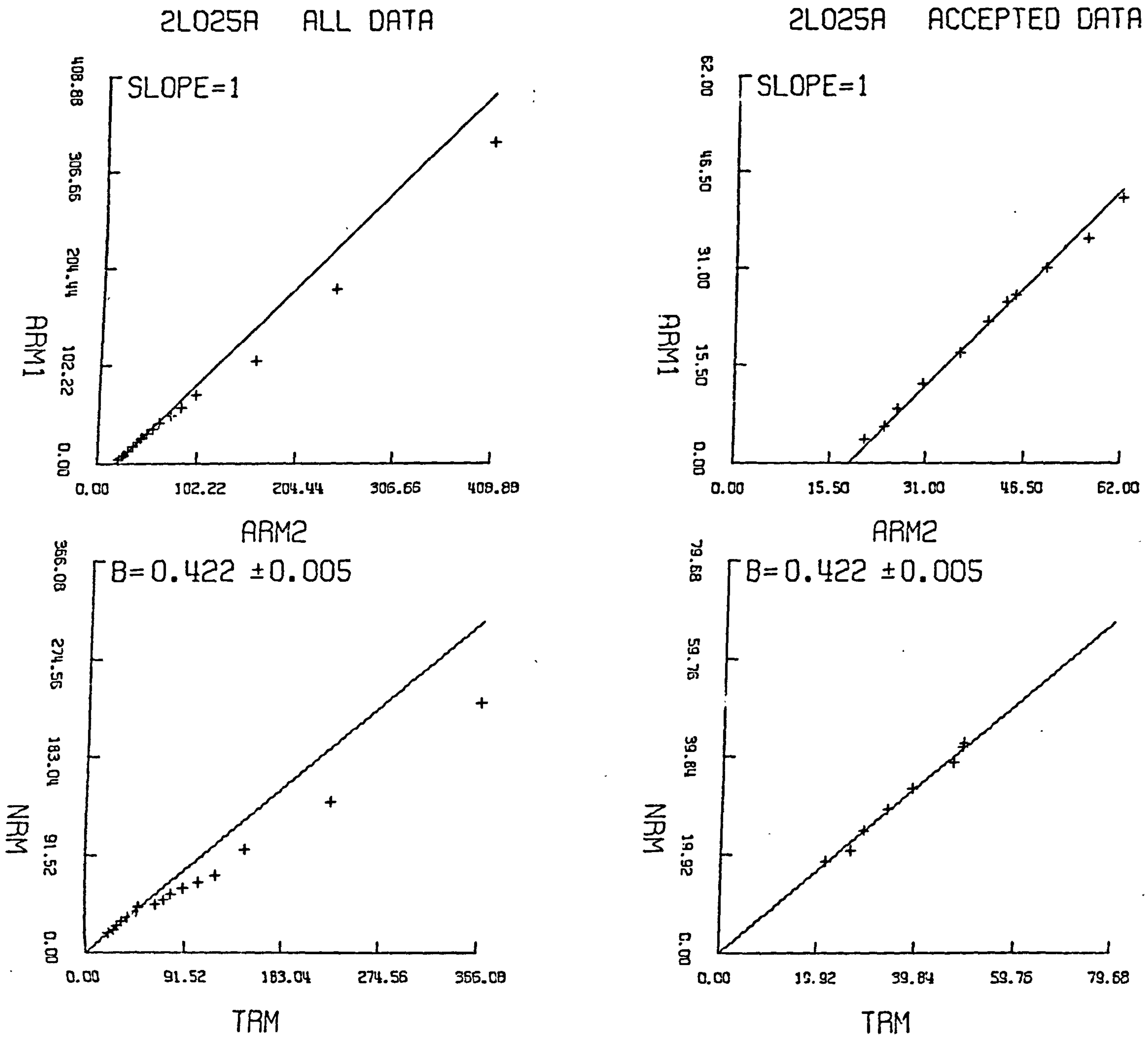
2LO25A ALL DATA
SLOPE=1
ARM1
0.00
102.22
204.44
306.66
408.88
ARM2
2LO25A ACCEPTED DATA
SLOPE=1
ARM1
0.00
15.50
31.00
46.50
62.00
ARM2
B=0.422 ±0.005
NRM
0.00
91.52
183.04
274.56
366.08
TRM
B=0.422 ±0.005
NRM
0.00
19.92
39.84
59.76
79.68
TRM

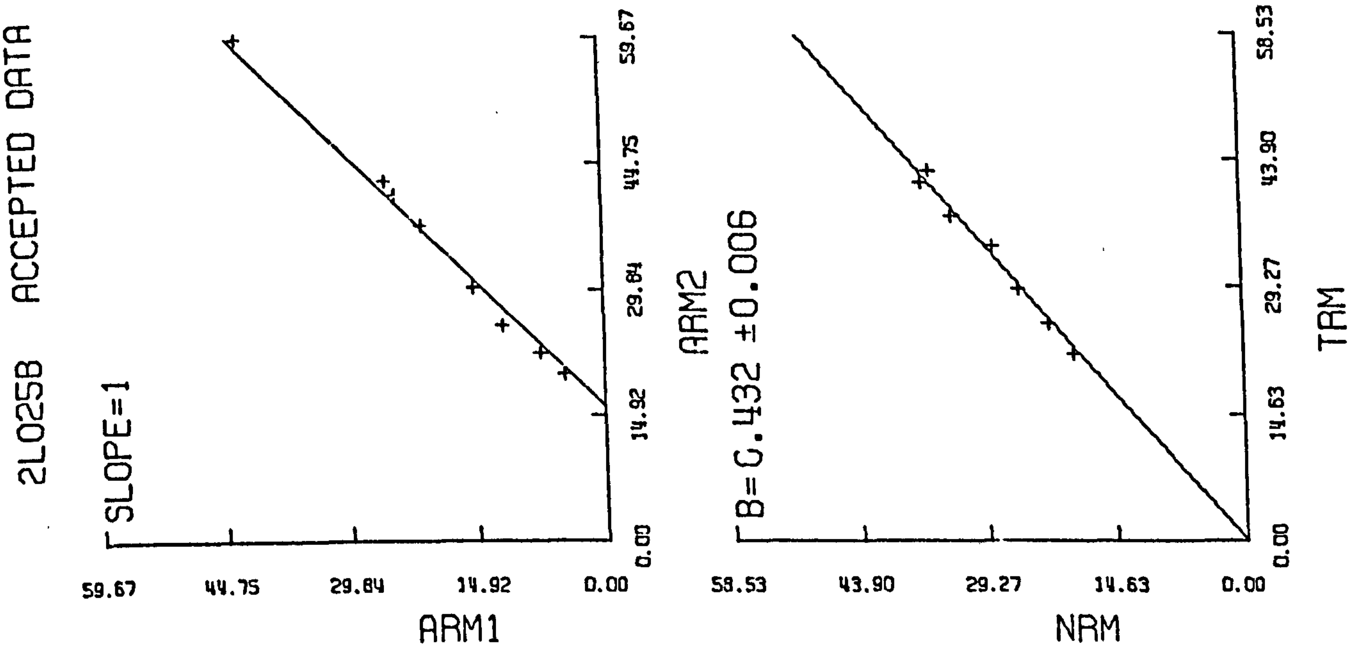
2L025B ACCEPTED DATA
SLOPE=1
ARM2
ARM1
59.67
44.75
29.84
14.92
0.00
B=0.432 ±0.006
NRM
TRM
58.53
43.90
29.27
14.63
0.00

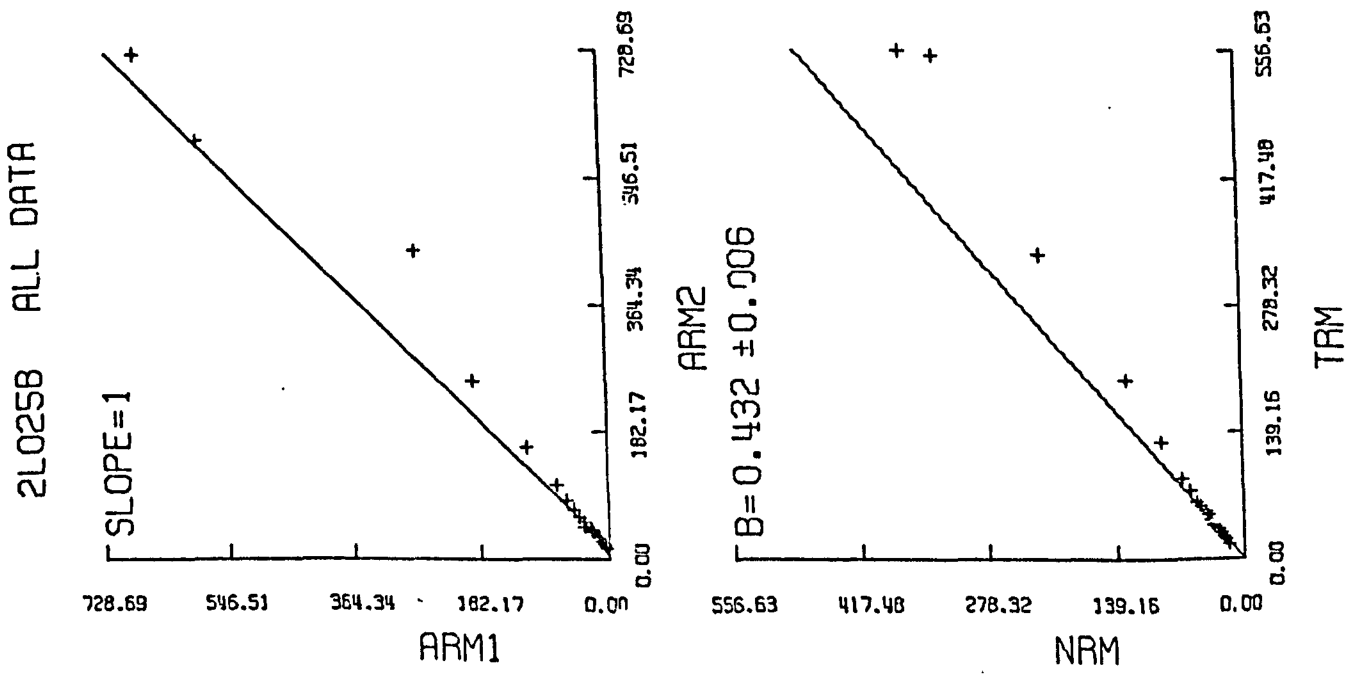
2L025B ALL DATA
SLOPE=1
ARM2
ARM1
728.69
546.51
364.34
182.17
0.00
B=0.432 ±0.006
NRM
TRM
556.63
417.48
278.32
139.16
0.00

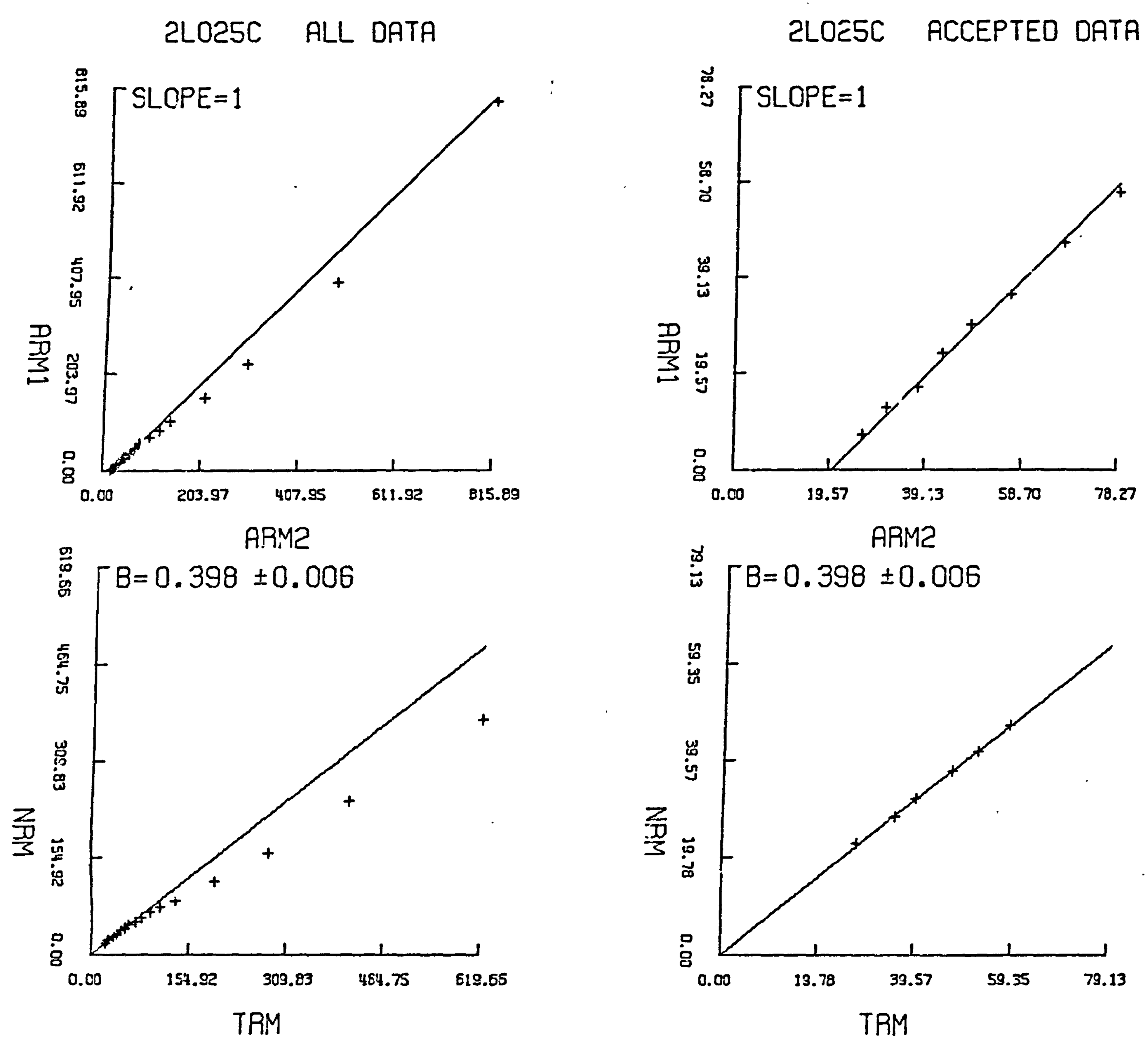
2L025C ALL DATA
SLOPE=1
ARM1
ARM2
0.00
203.97
407.95
611.92
815.89
B=0.398 ±0.006
NRM
TRM
0.00
154.92
309.83
464.75
619.65
619.66
2L025C ACCEPTED DATA
SLOPE=1
ARM1
ARM2
0.00
19.57
39.13
58.70
78.27
B=0.398 ±0.006
NRM
TRM
0.00
19.78
39.57
59.35
79.13

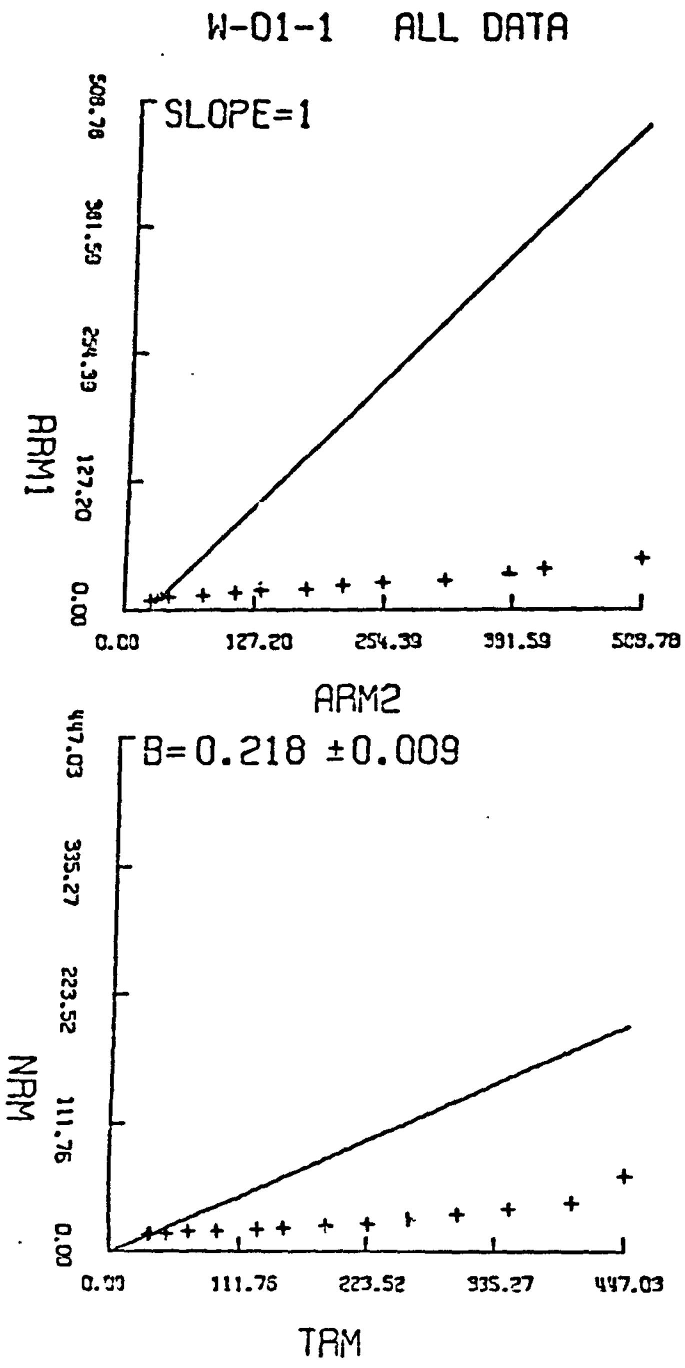
W-01-1 ALL DATA
SLOPE=1
ARM1
ARM2
0.00
127.20
254.39
381.59
508.78
B=0.218 ±0.009
NRM
TRM
0.00
111.76
223.52
335.27
447.03

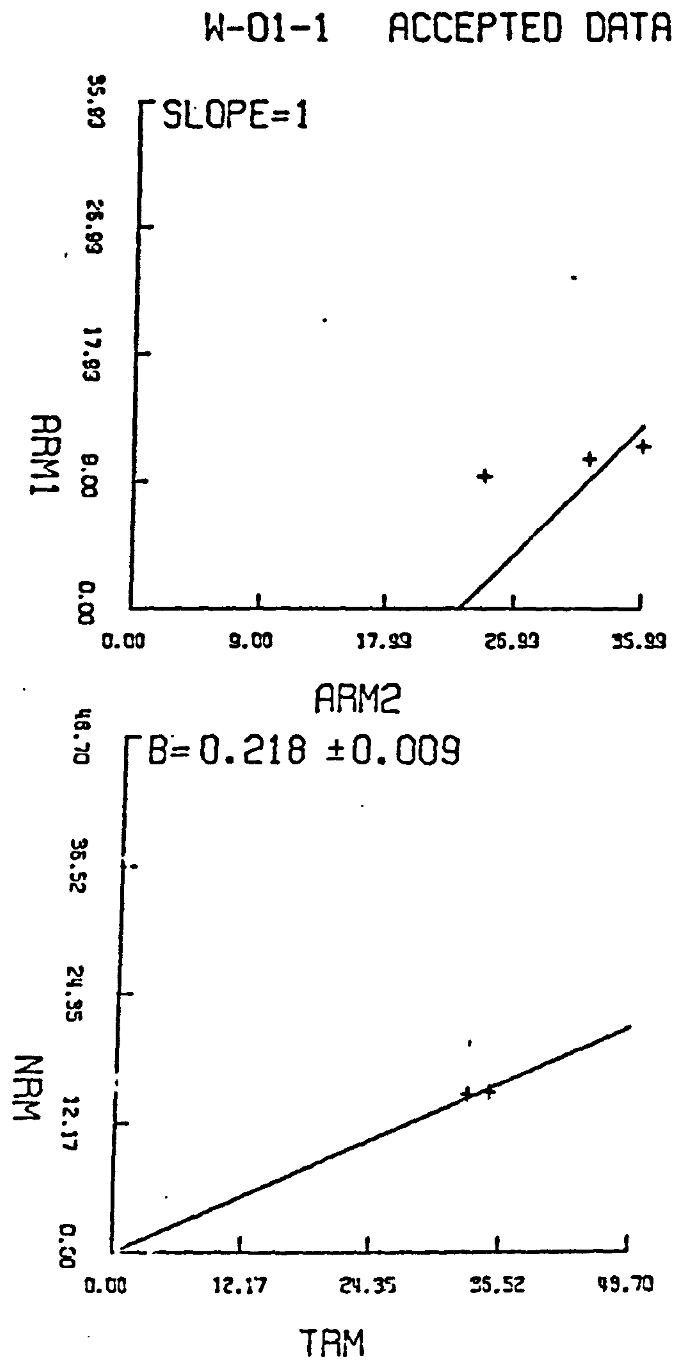
W-01-1 ACCEPTED DATA
SLOPE=1
ARM1
ARM2
0.00
9.00
17.93
26.93
35.93
B=0.218 ±0.009
NRM
TRM
0.00
12.17
24.35
36.52
48.70

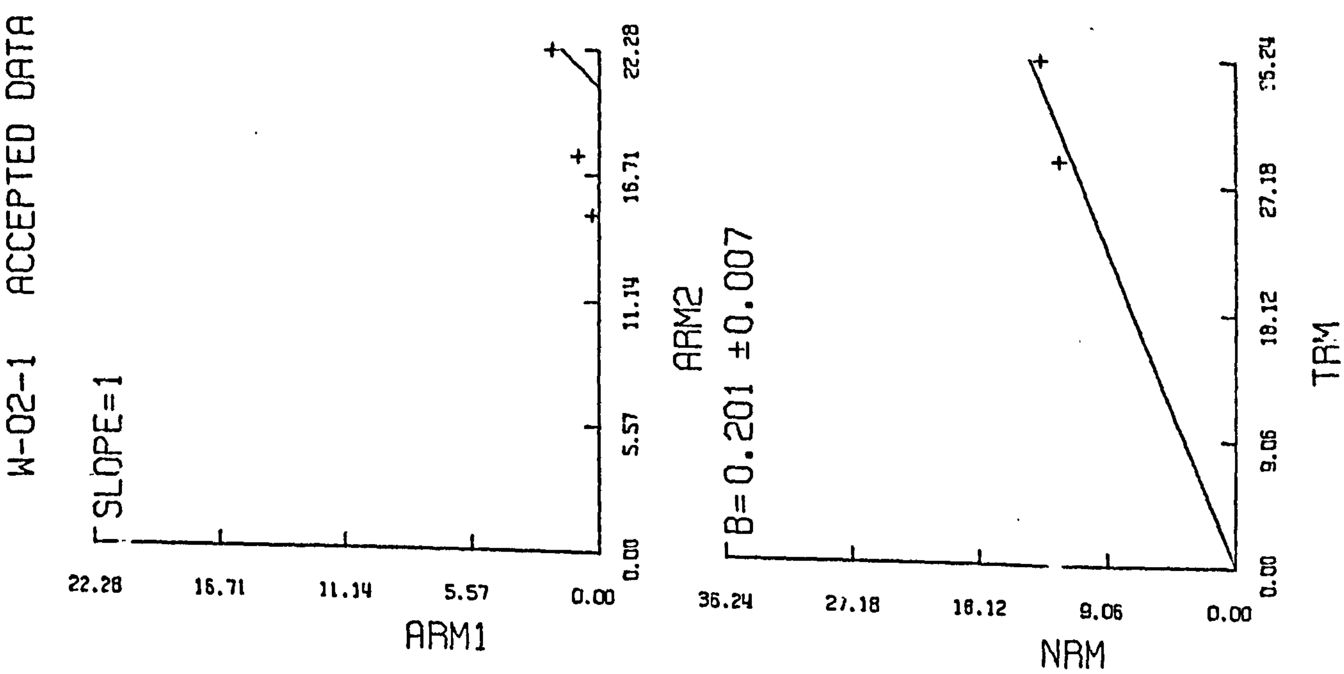
W-02-1 ACCEPTED DATA
SLOPE=1
22.28
16.71
11.14
5.57
0.00
ARM1
ARM2
B=0.201 ±0.007
36.24
27.18
18.12
9.06
0.00
NRM
TRM

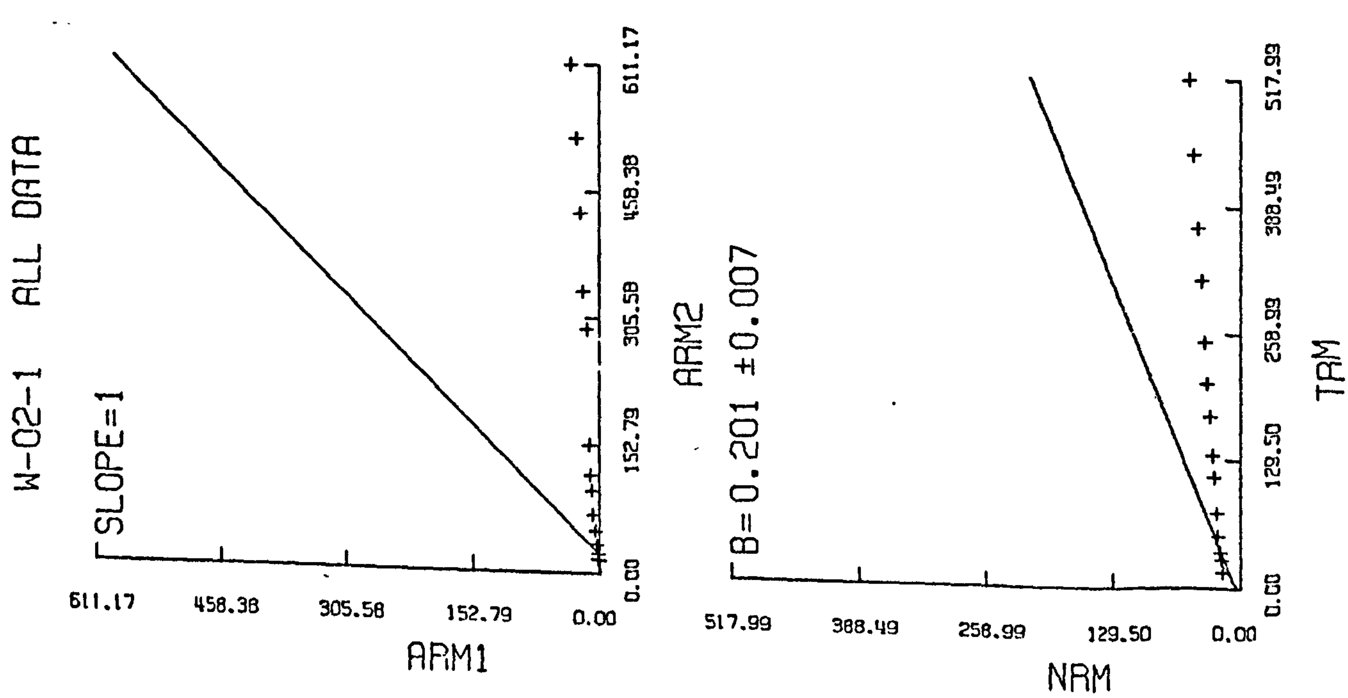
W-02-1 ALL DATA
SLOPE=1
611.17
458.38
305.58
152.79
0.00
ARM1
ARM2
B=0.201 ±0.007
517.99
388.49
258.99
129.50
0.00
NRM
TRM

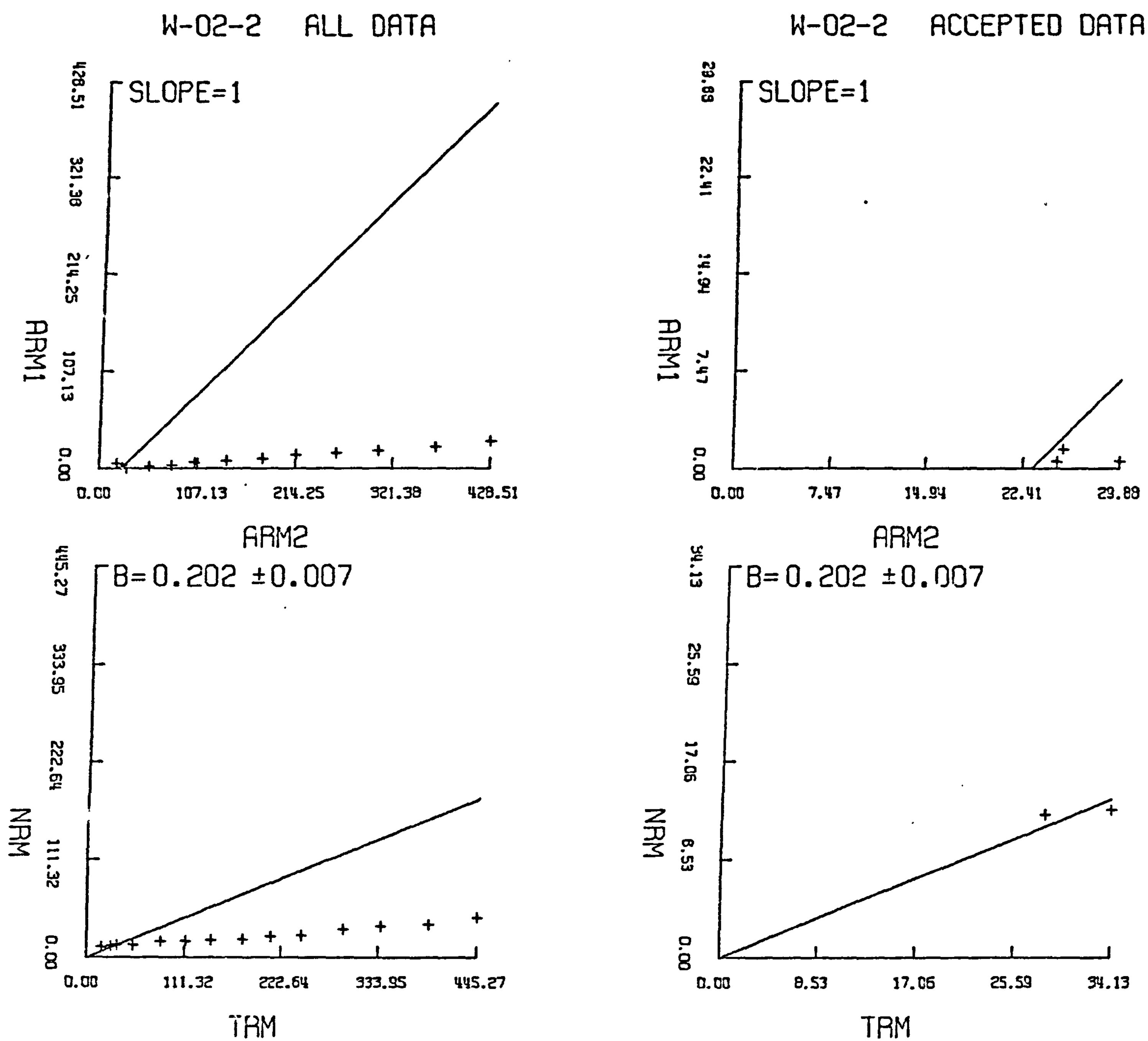
W-02-2 ALL DATA
SLOPE=1
ARM1
ARM2
0.00
107.13
214.25
321.38
428.51
B=0.202 ±0.007
NRM
TRM
0.00
111.32
222.64
333.95
445.27
W-02-2 ACCEPTED DATA
SLOPE=1
ARM1
ARM2
0.00
7.47
14.94
22.41
29.88
B=0.202 ±0.007
NRM
TRM
0.00
8.53
17.06
25.59
34.13

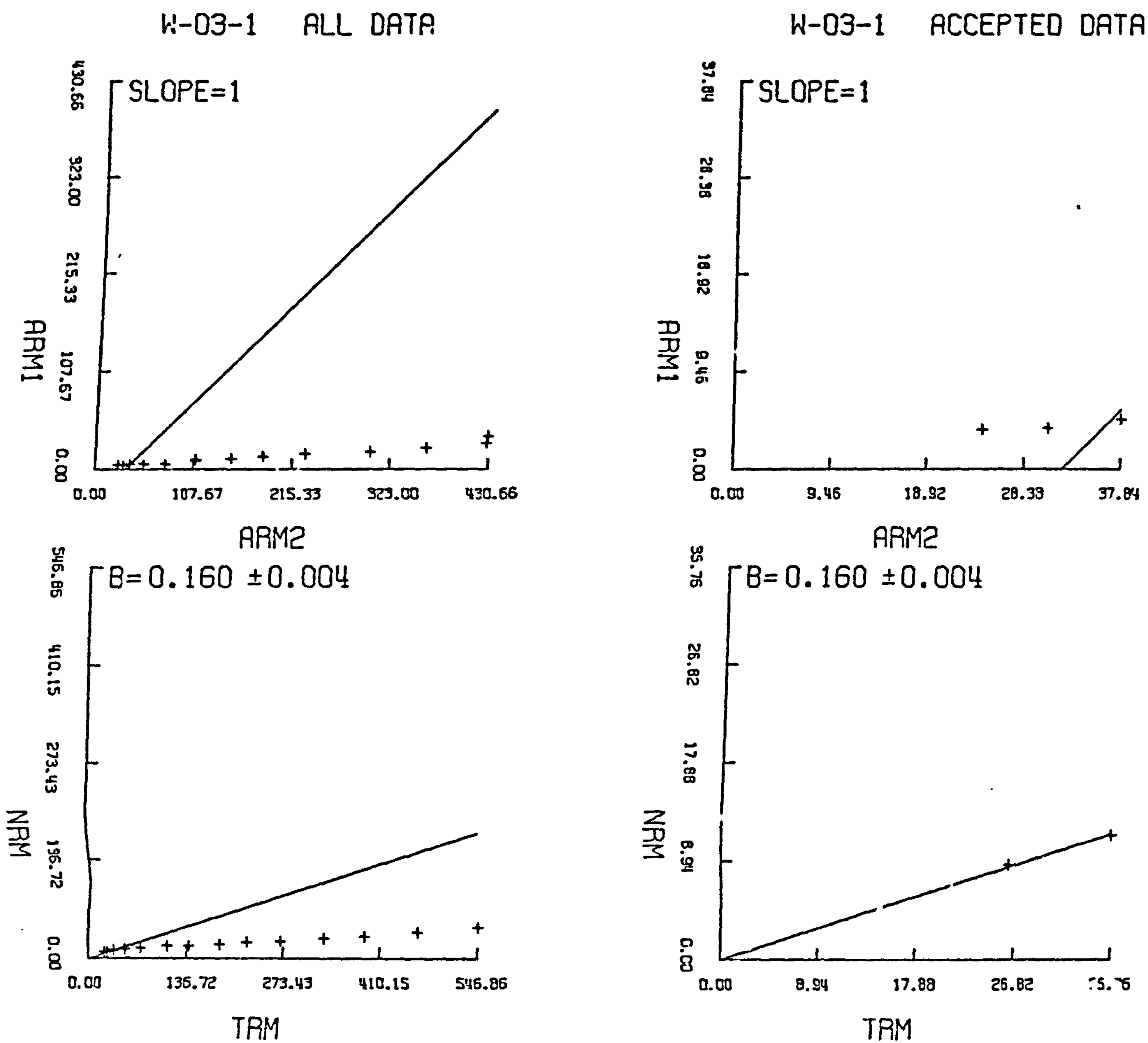
W-03-1 ALL DATA
SLOPE=1
ARM1
ARM2
0.00 107.67 215.33 323.00 430.66
B=0.160 ±0.004
NRM
TRM
0.00 136.72 273.43 410.15 546.86
W-03-1 ACCEPTED DATA
SLOPE=1
ARM1
ARM2
0.00 9.46 18.92 28.38 37.84
B=0.160 ±0.004
NRM
TRM
0.00 8.94 17.88 26.82 35.76

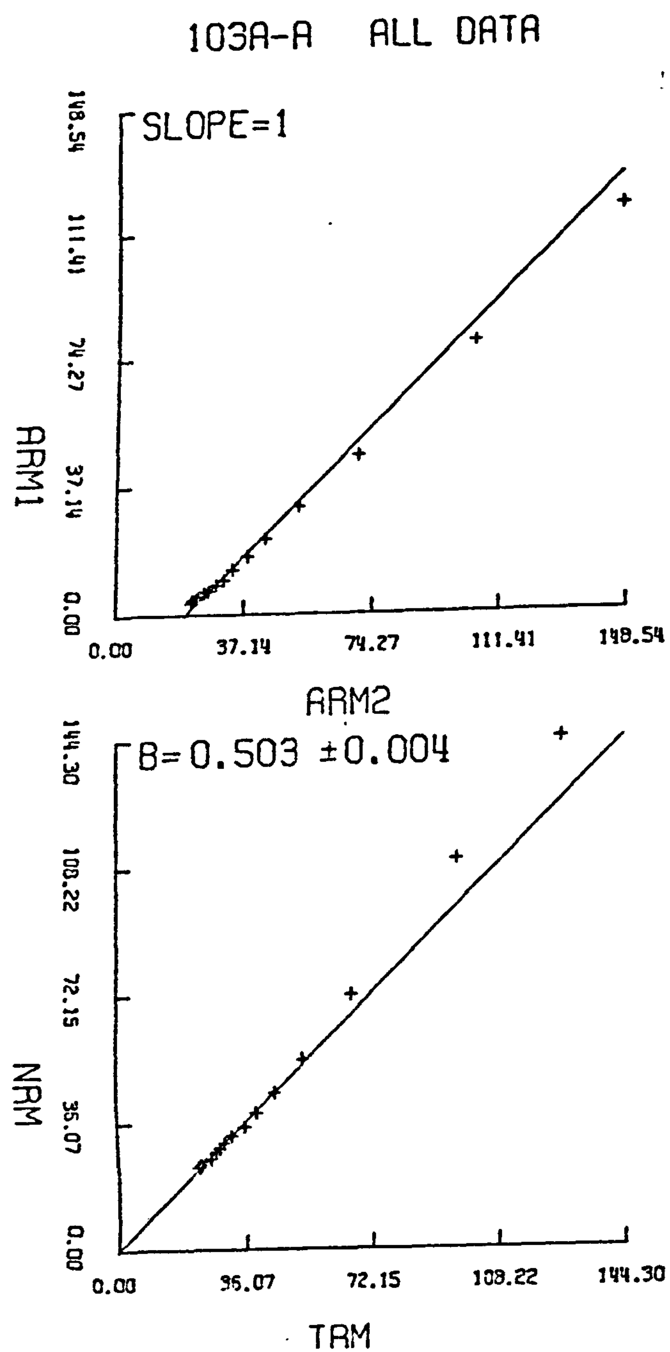
103A-A ALL DATA
SLOPE=1
ARM1
ARM2
0.00
37.14
74.27
111.41
148.54
B=0.503 ±0.004
NRM
TRM
0.00
36.07
72.15
108.22
144.30

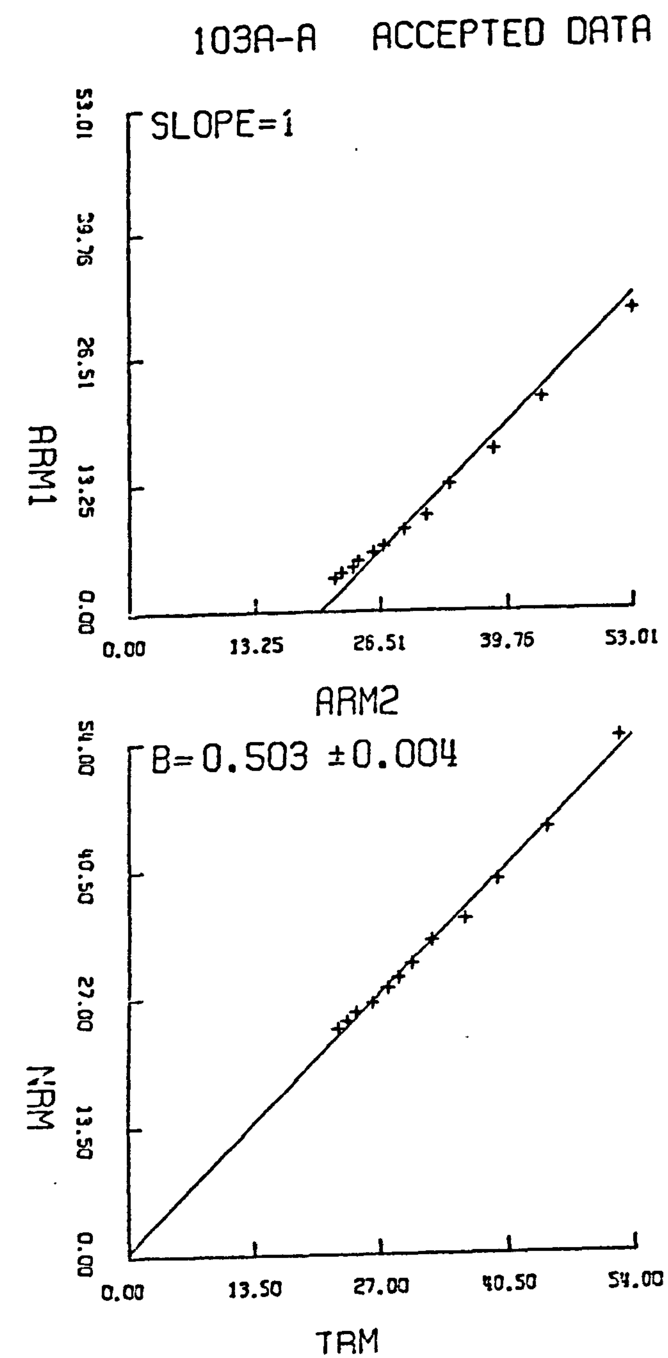
103A-A ACCEPTED DATA
SLOPE=1
ARM1
ARM2
0.00
13.25
26.51
39.76
53.01
B=0.503 ±0.004
NRM
TRM
0.00
13.50
27.00
40.50
54.00

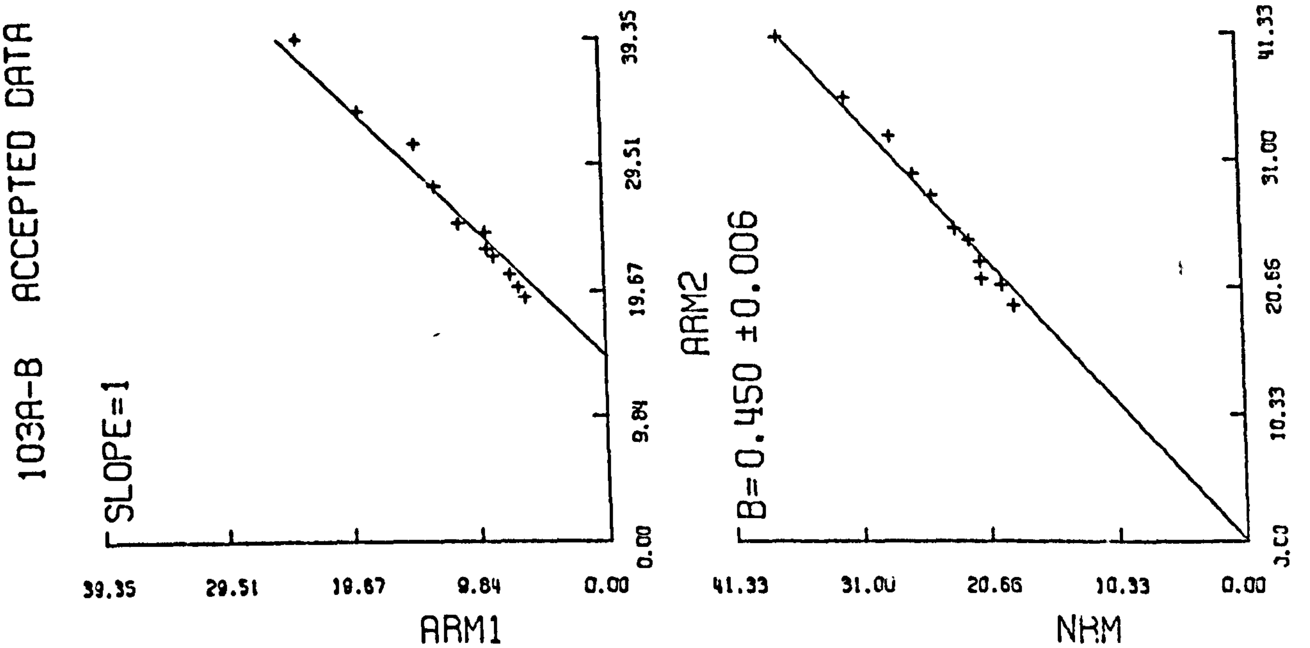
103A-B ACCEPTED DATA
SLOPE=1
ARM1
ARM2
39.35 29.51 19.67 9.84 0.00
0.00 9.84 19.67 29.51 39.35
B=0.450 ±0.006
NRM
TRM
41.33 31.00 20.66 10.33 0.00
0.00 10.33 20.66 31.00 41.33

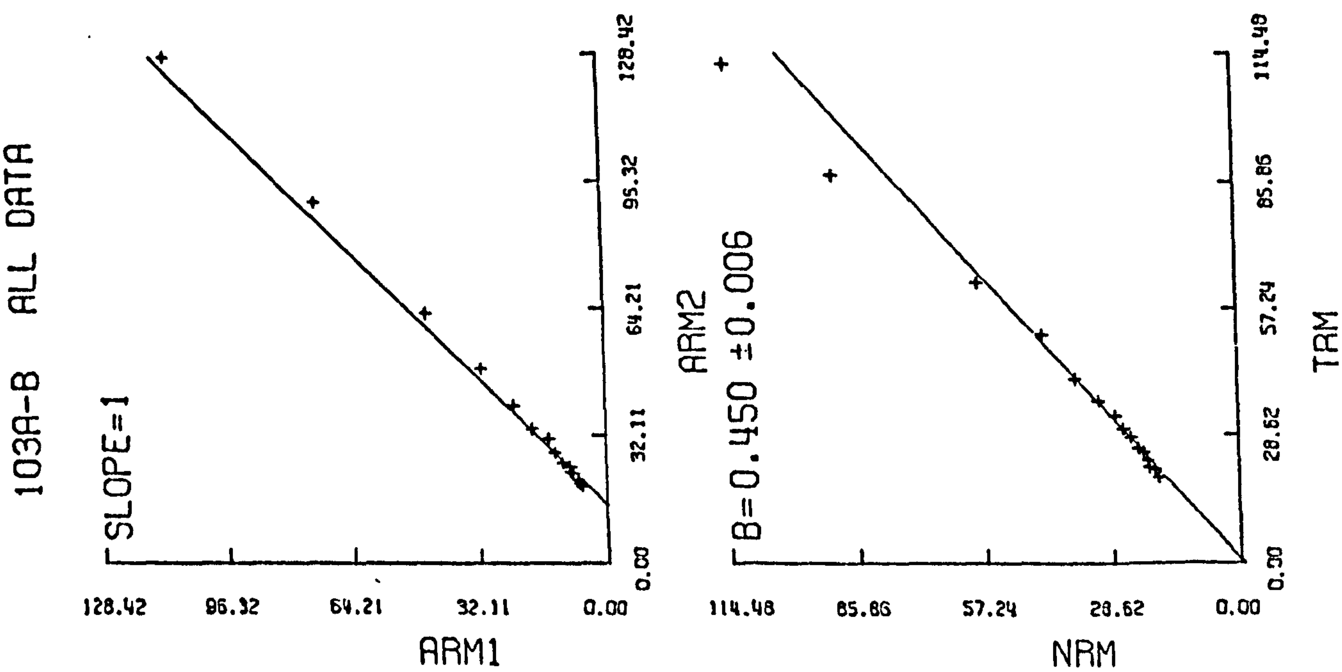
103A-B ALL DATA
SLOPE=1
ARM1
ARM2
128.42 96.32 64.21 32.11 0.00
0.00 32.11 64.21 95.32 128.42
B=0.450 ±0.006
NRM
TRM
114.48 85.86 57.24 28.62 0.00
0.00 28.62 57.24 85.86 114.48

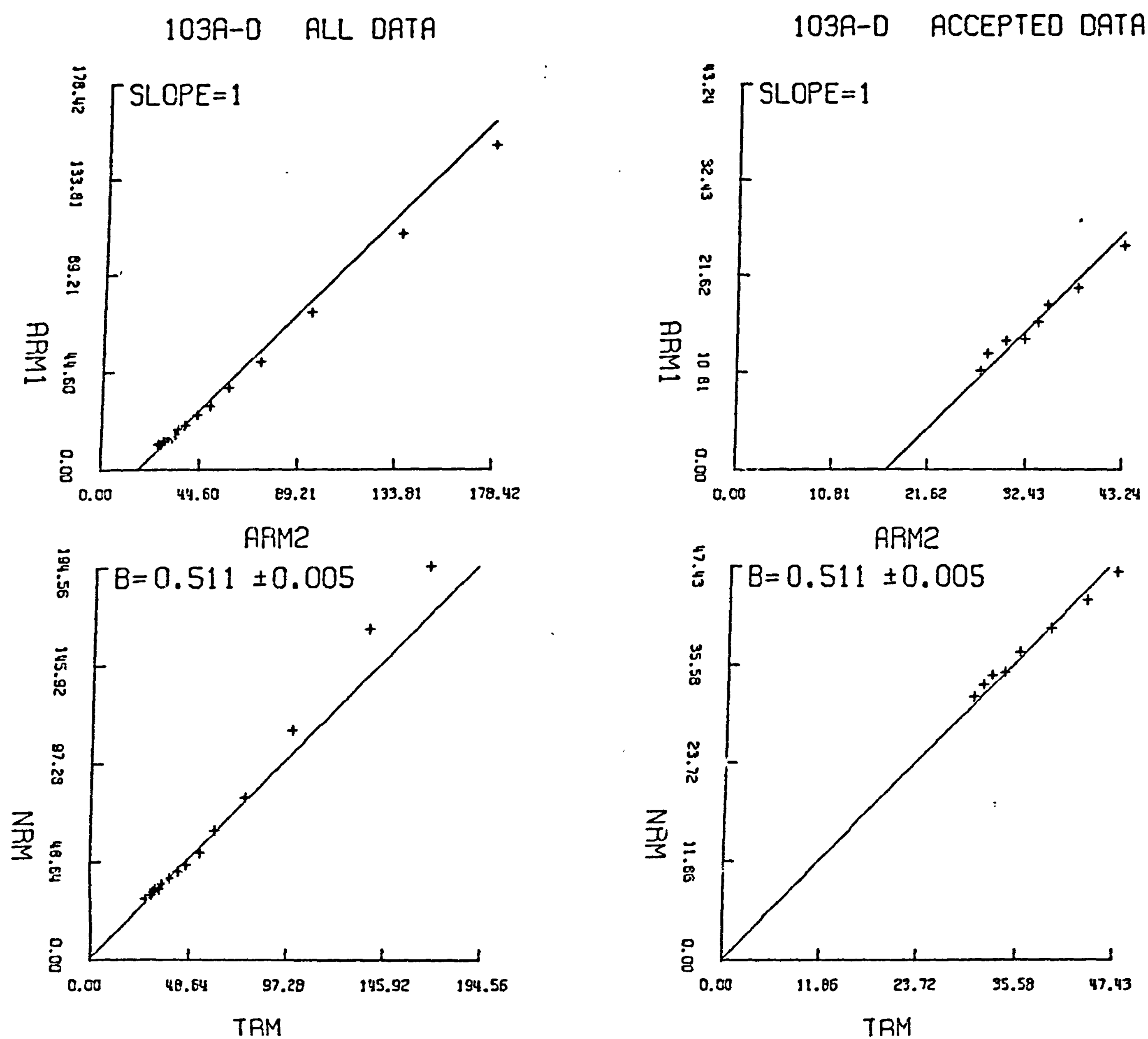
103A-D ALL DATA
SLOPE=1
ARM1
ARM2
0.00 44.60 89.21 133.81 178.42
B=0.511 ±0.005
NRM
TRM
0.00 48.64 97.28 145.92 194.56
103A-D ACCEPTED DATA
SLOPE=1
ARM1
ARM2
0.00 10.81 21.62 32.43 43.24
B=0.511 ±0.005
NRM
TRM
0.00 11.86 23.72 35.58 47.43

S2-1A. ALL DATA

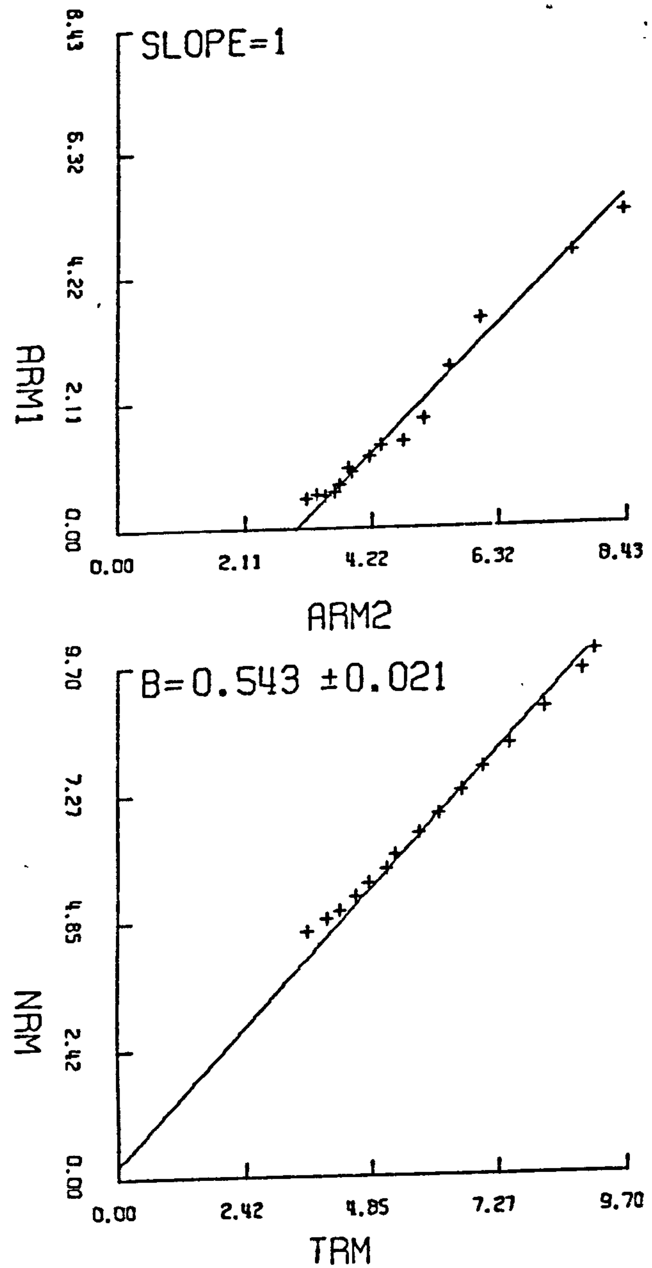

S2-1A. ACCEPTED DATA

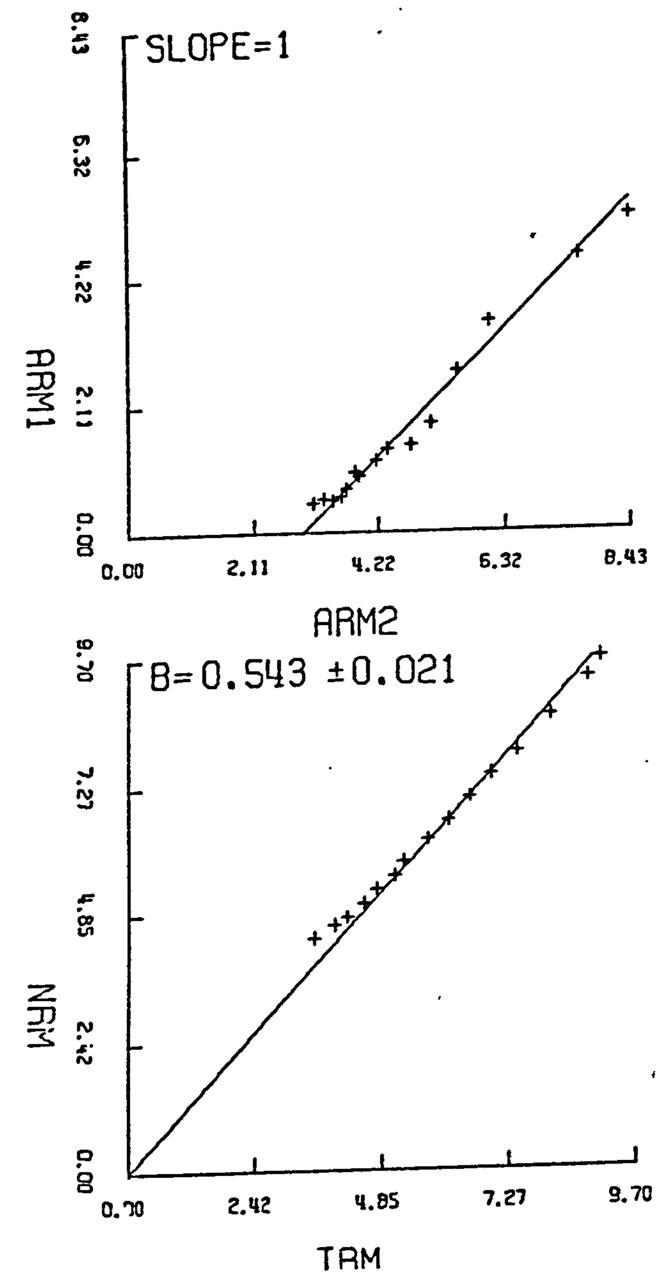

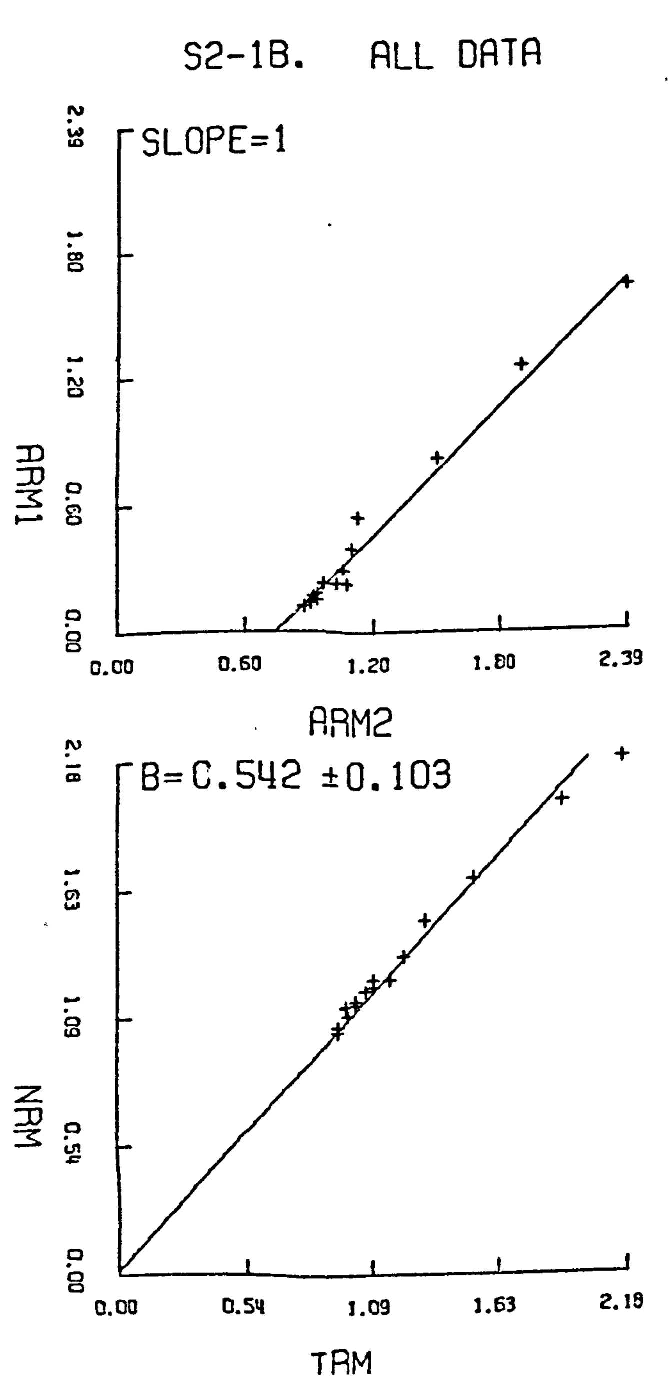
S2-1B. ALL DATA
SLOPE=1
ARM1
ARM2
0.00
0.60
1.20
1.80
2.39
B=C.542 ±0.103
NRM
TRM
0.00
0.54
1.09
1.63
2.18

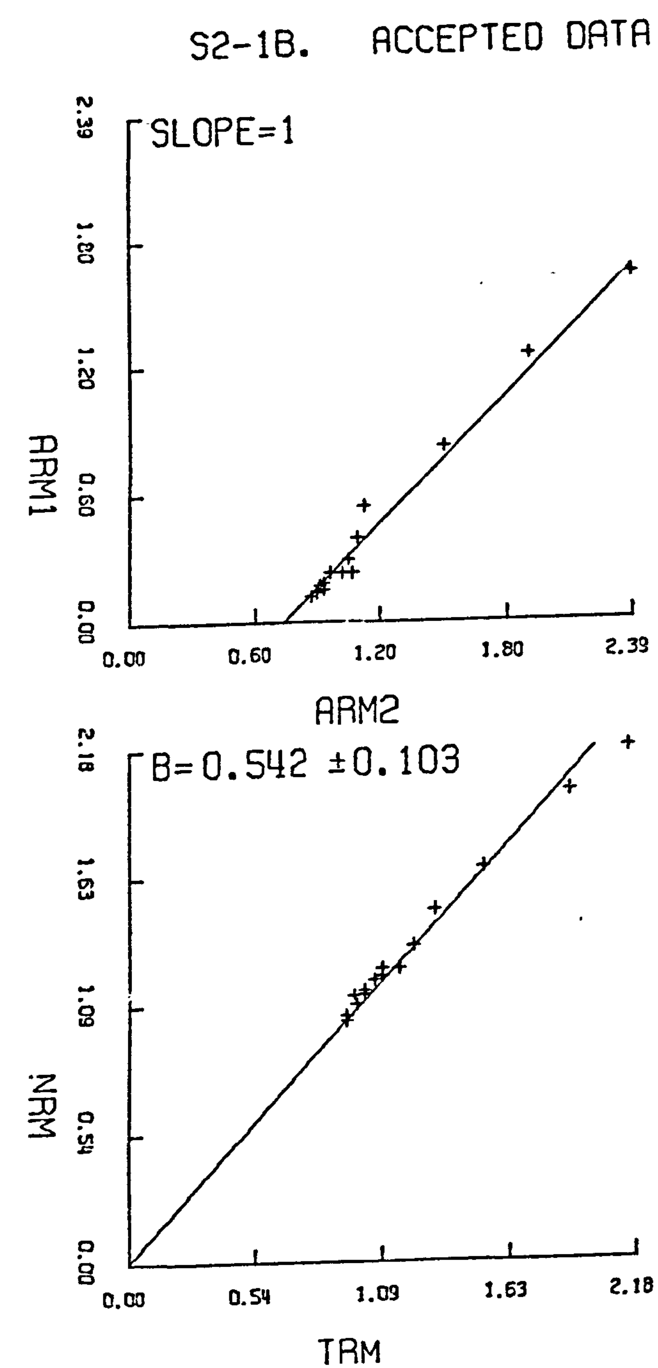
S2-1B. ACCEPTED DATA
SLOPE=1
ARM1
ARM2
0.00
0.60
1.20
1.80
2.39
B=0.542 ±0.103
NRM
TRM
0.00
0.54
1.09
1.63
2.18

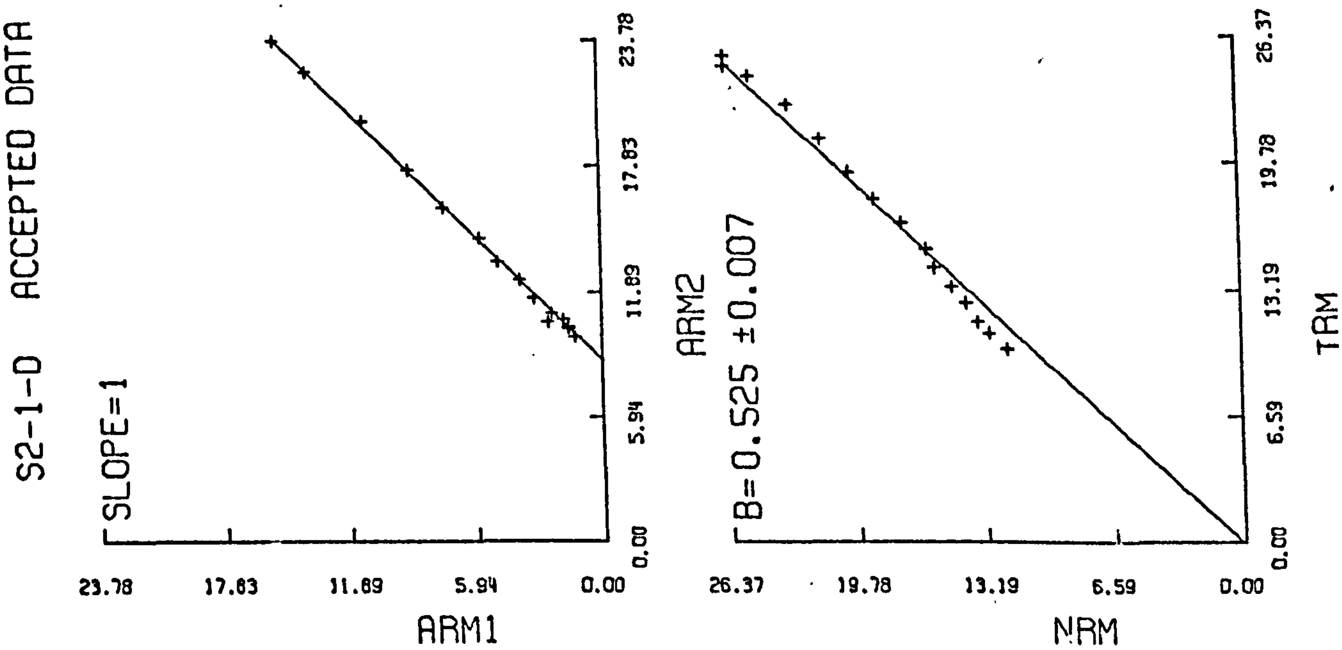

S2-1-D ACCEPTED DATA
SLOPE=1
ARM1
ARM2
23.78
17.83
11.89
5.94
0.00
B=0.525 ±0.007
NRM
TRM
26.37
19.78
13.19
6.59
0.00

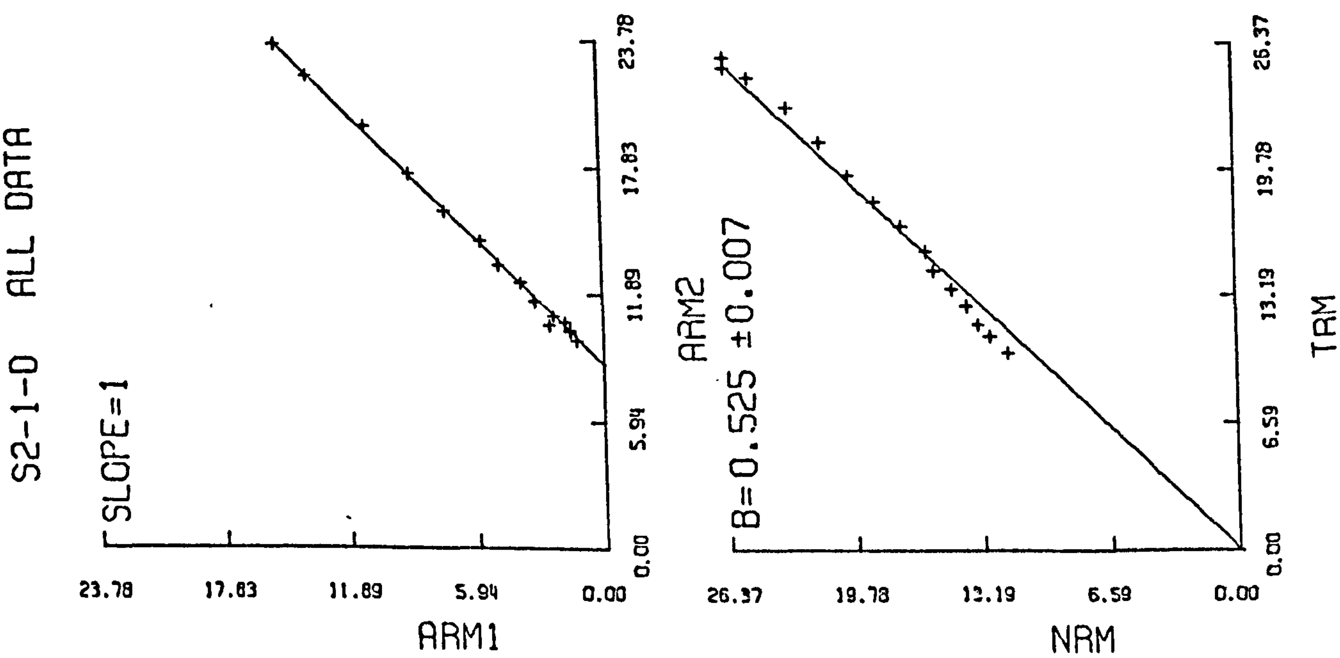

S2-1-D ALL DATA
SLOPE=1
ARM1
ARM2
23.78
17.83
11.89
5.94
0.00
B=0.525 ±0.007
NRM
TRM
26.37
19.78
13.19
6.59
0.00

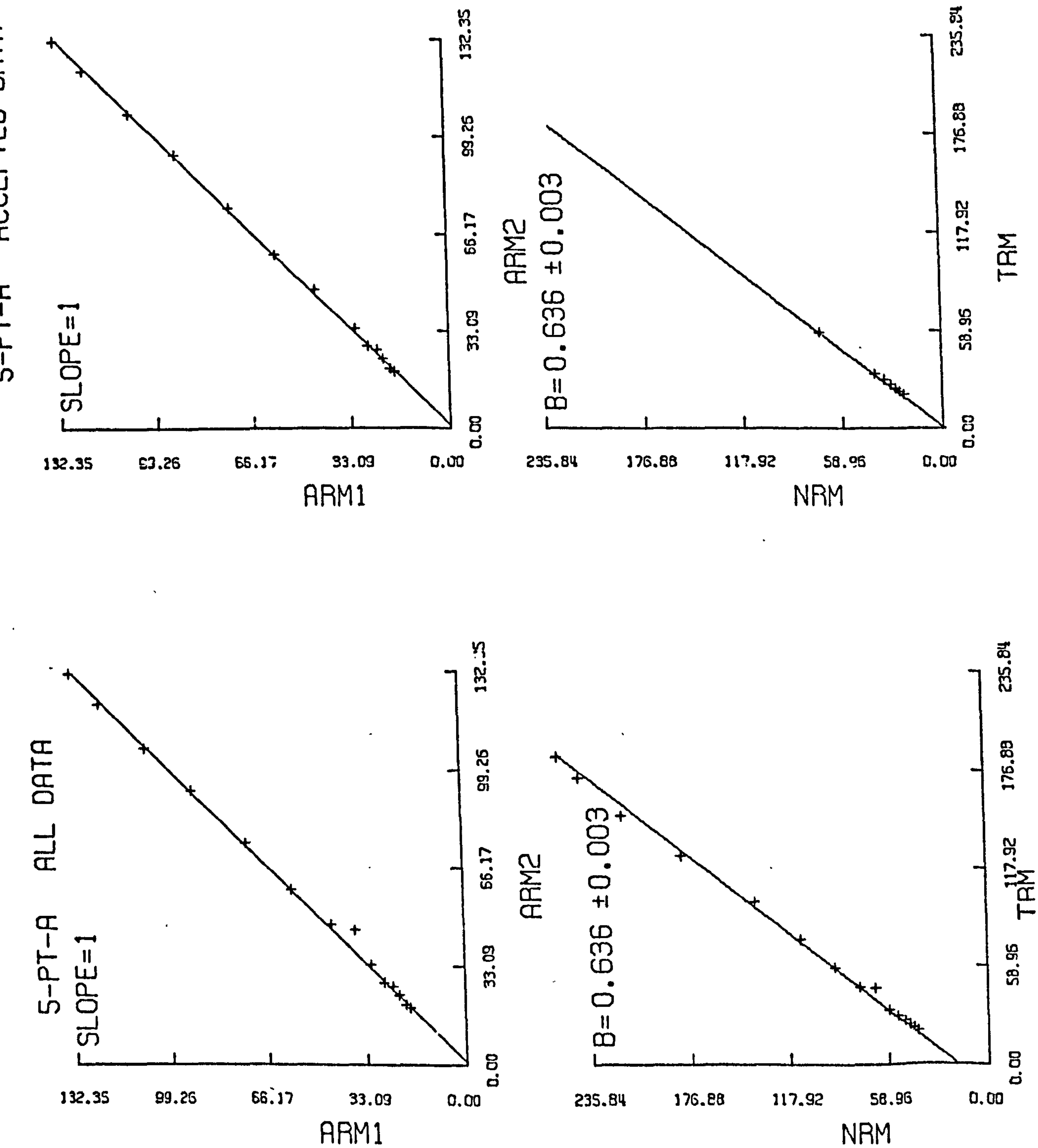

5-PT-A ACCEPTED DATA
SLOPE=1
ARM1
ARM2
B=0.636 ±0.003
NRM
TRM
5-PT-A ALL DATA
SLOPE=1
ARM1
ARM2
B=0.636 ±0.003
NRM
TRM

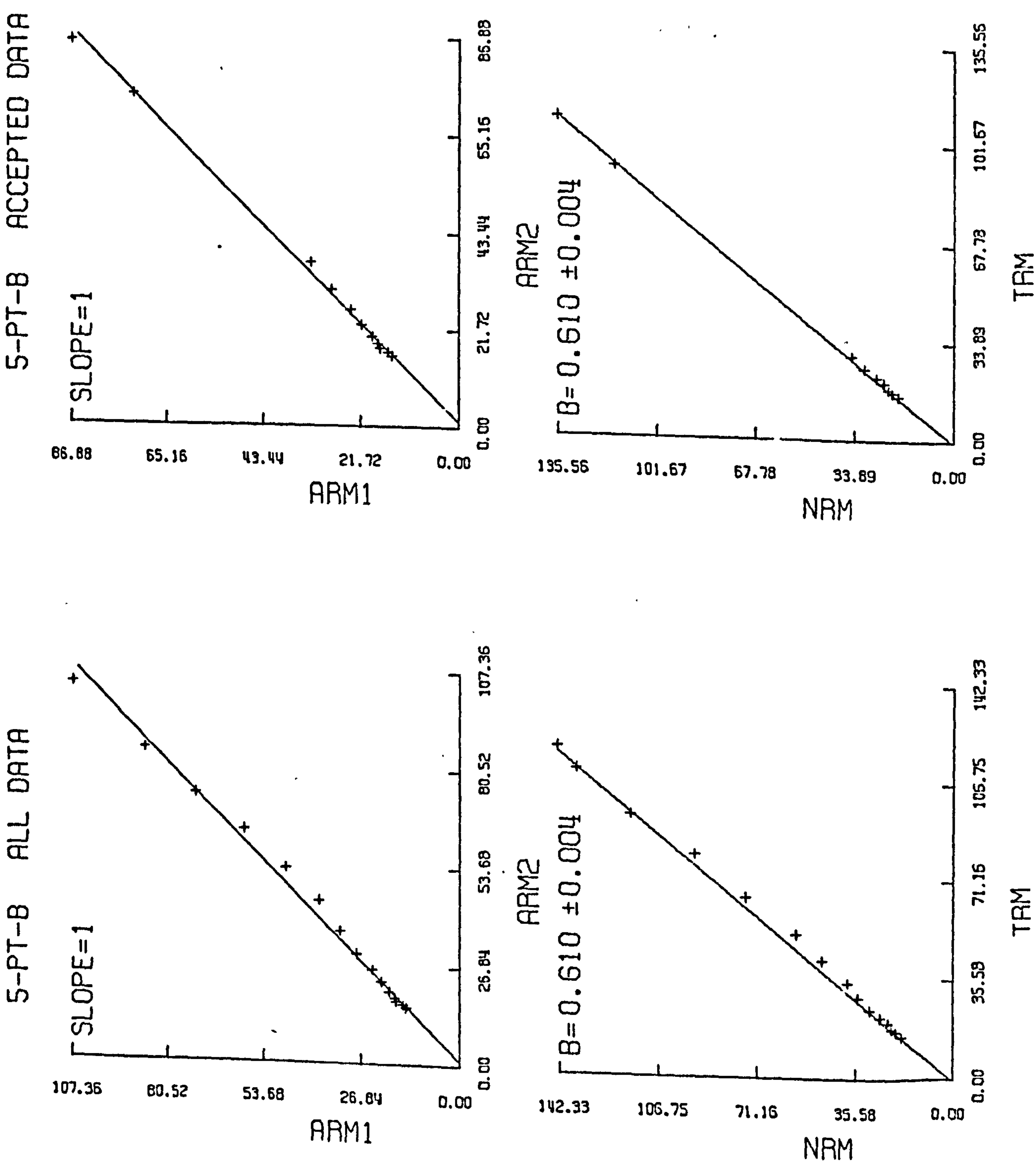
5-PT-B ACCEPTED DATA
SLOPE=1
ARM1
86.88
65.16
43.44
21.72
0.00
ARM2
B= 0.610 ±0.004
NRM
TRM
135.56
101.67
67.78
33.89
0.00
5-PT-B ALL DATA
SLOPE=1
ARM1
107.36
80.52
53.68
26.84
0.00
ARM2
B= 0.610 ±0.004
NRM
TRM
142.33
106.75
71.16
35.58
0.00

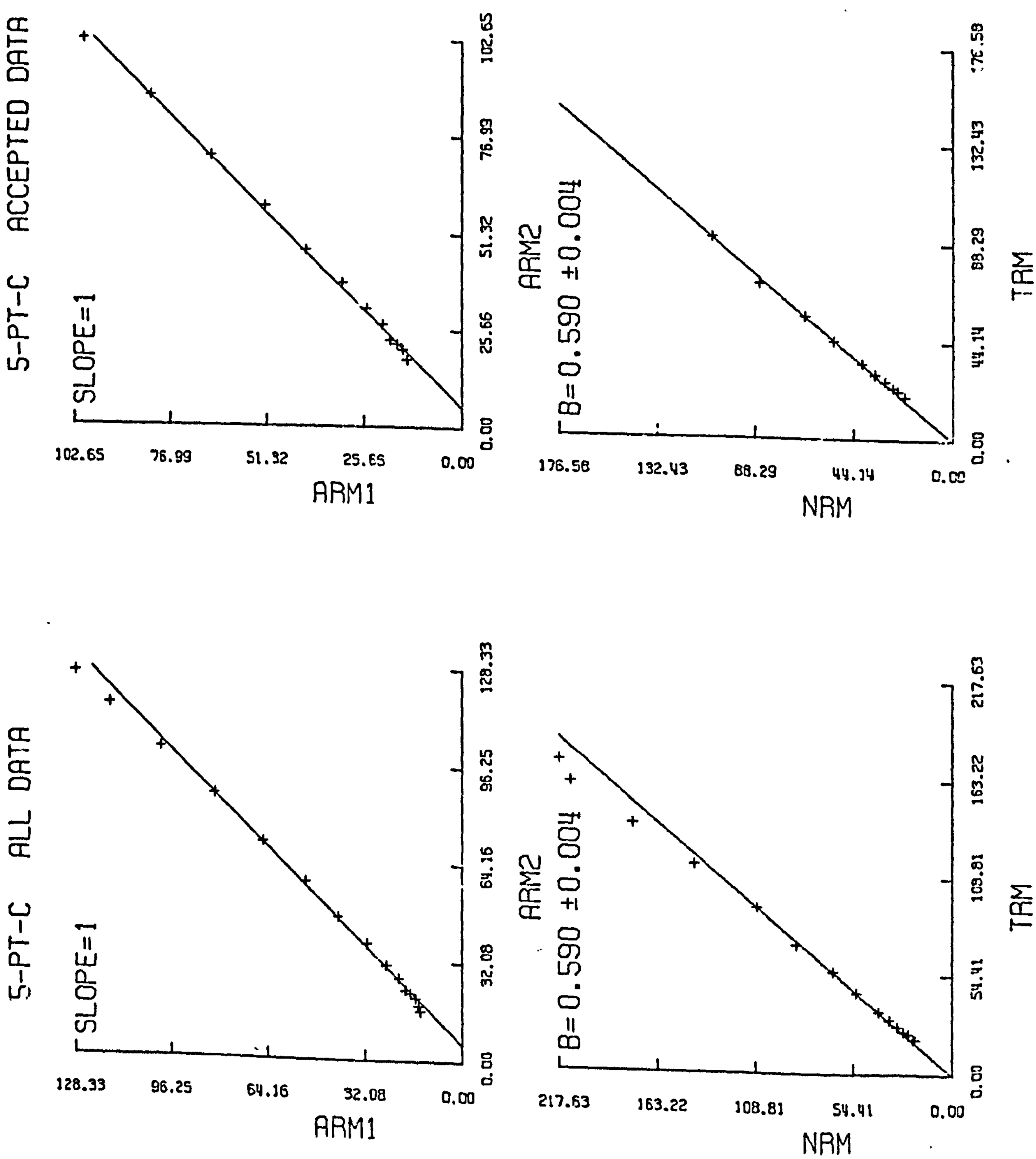

5-PT-C ACCEPTED DATA
SLOPE=1
ARM1
ARM2
B=0.590 ±0.004
NRM
TRM
5-PT-C ALL DATA
SLOPE=1
ARM1
ARM2
B=0.590 ±0.004
NRM
TRM

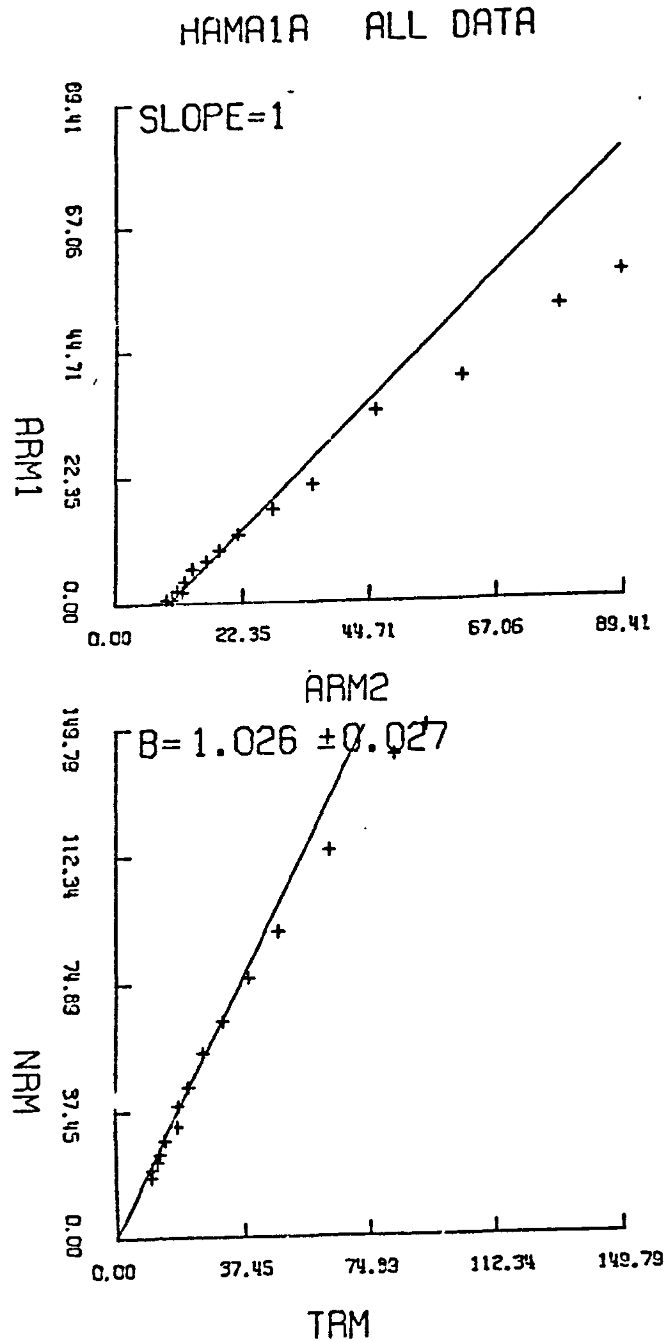
HAMA1A ALL DATA
SLOPE=1
ARM1
ARM2
0.00
22.35
44.71
67.06
89.41
B= 1.026 ±0.027
NRM
TRM
37.45
74.89
112.34
149.79
74.93

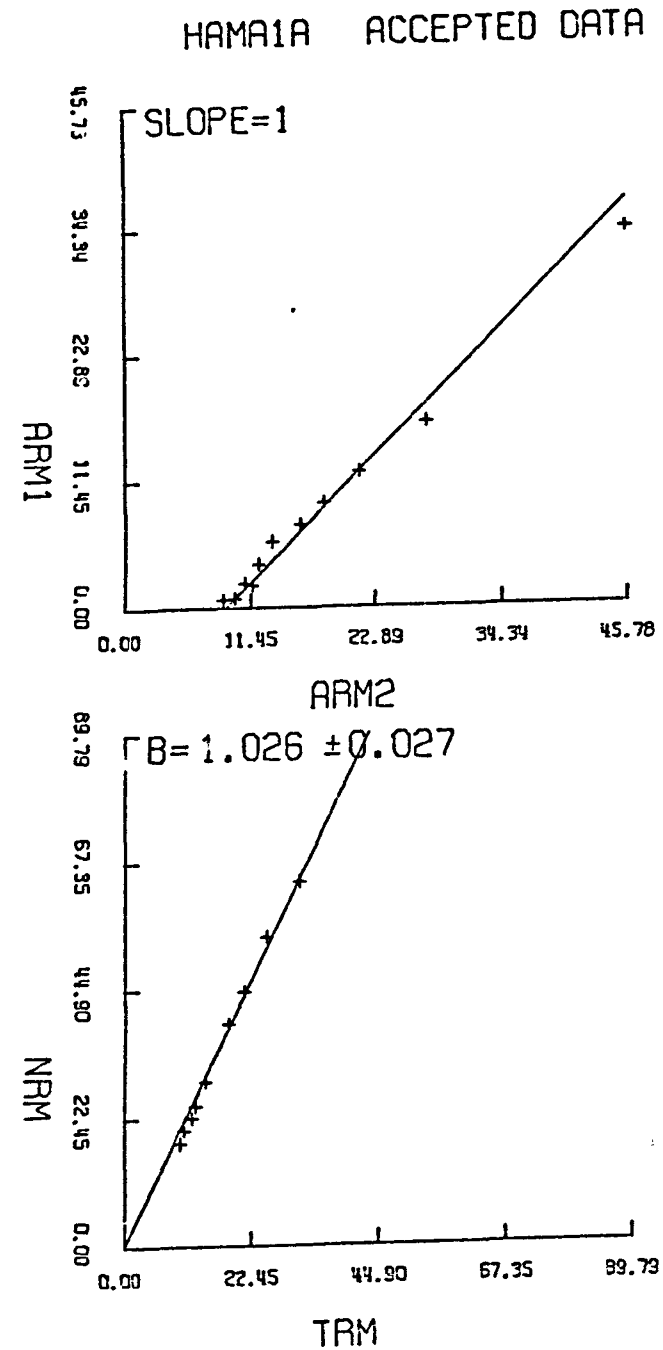
HAMA1A ACCEPTED DATA
SLOPE=1
ARM1
ARM2
0.00
11.45
22.89
34.34
45.78
45.73
22.83
B= 1.026 ±0.027
NRM
TRM
22.45
44.90
67.35
89.73
89.79

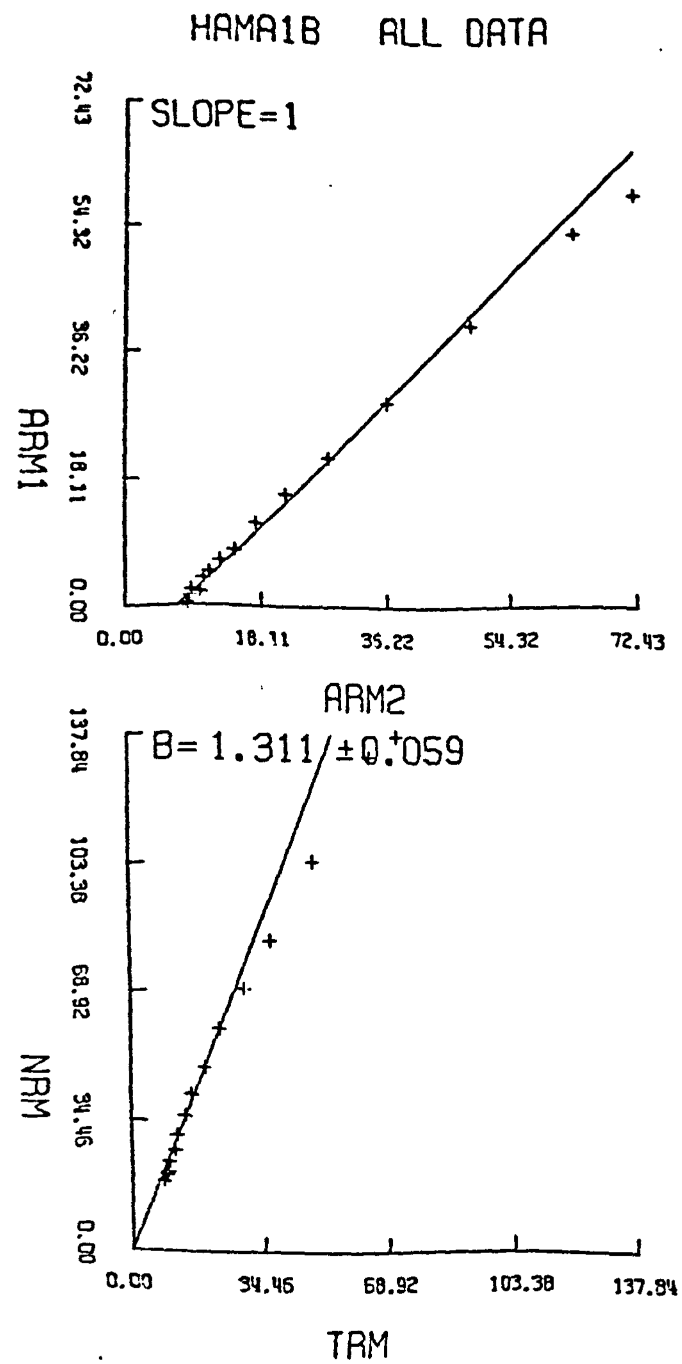
HAMA1B ALL DATA
SLOPE=1
ARM1
ARM2
0.00
18.11
36.22
54.32
72.43
B= 1.311/±0.059
NRM
TRM
0.00
34.46
68.92
103.38
137.84

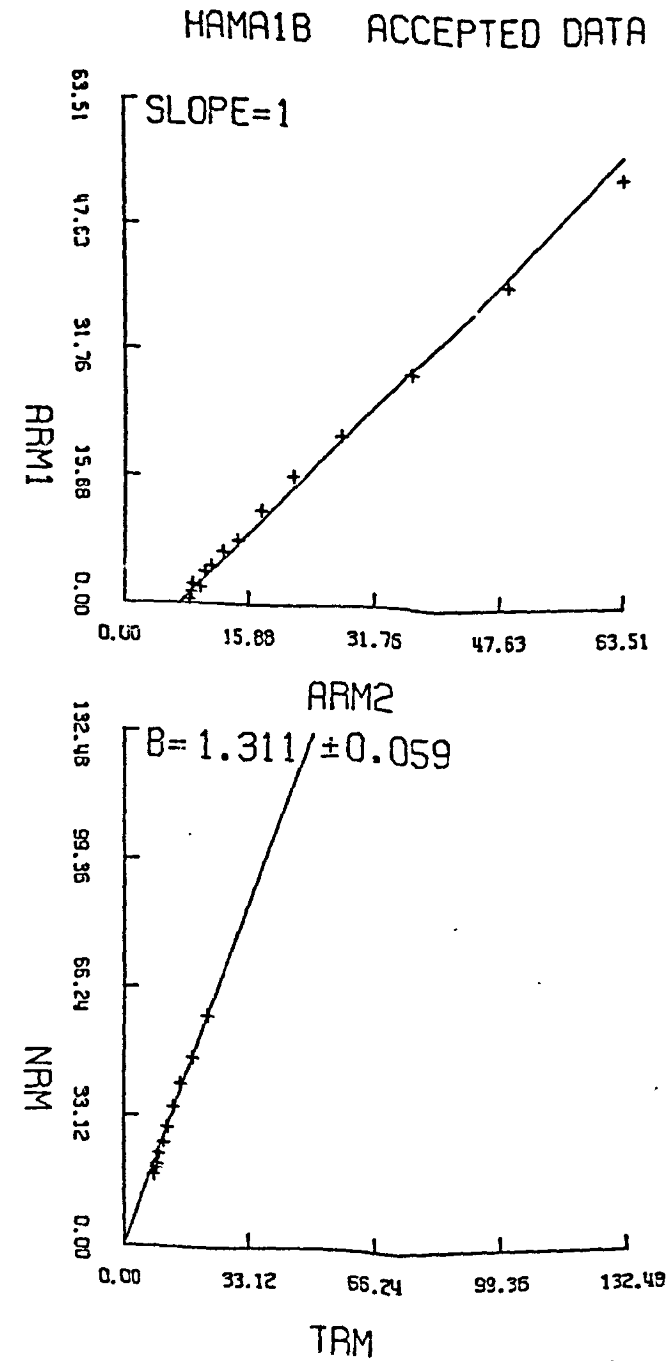
HAMA1B ACCEPTED DATA
SLOPE=1
ARM1
ARM2
0.00
15.88
31.76
47.63
63.51
B= 1.311/±0.059
NRM
TRM
0.00
33.12
66.24
99.36
132.48

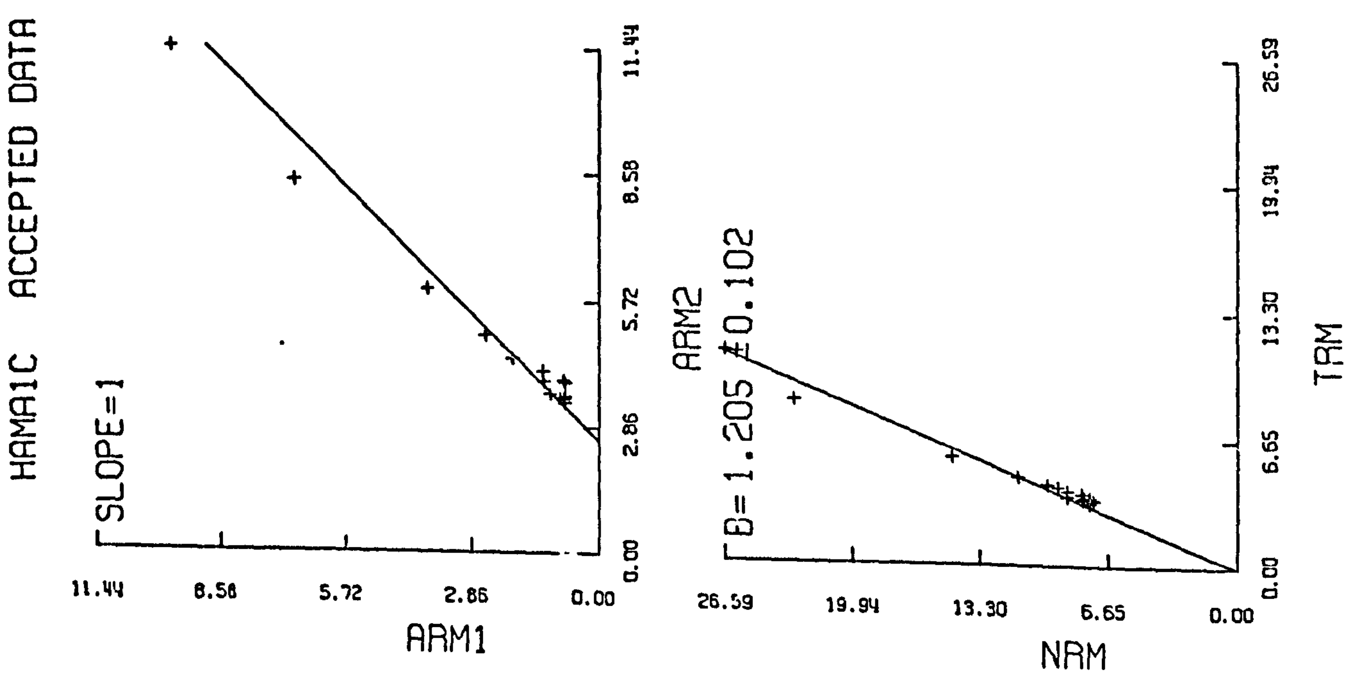
HAMA1C ACCEPTED DATA
SLOPE=1
ARM1
ARM2
B= 1.205 ±0.102
NRM
TRM
11.44
8.58
5.72
2.86
0.00
26.59
19.94
13.30
6.65

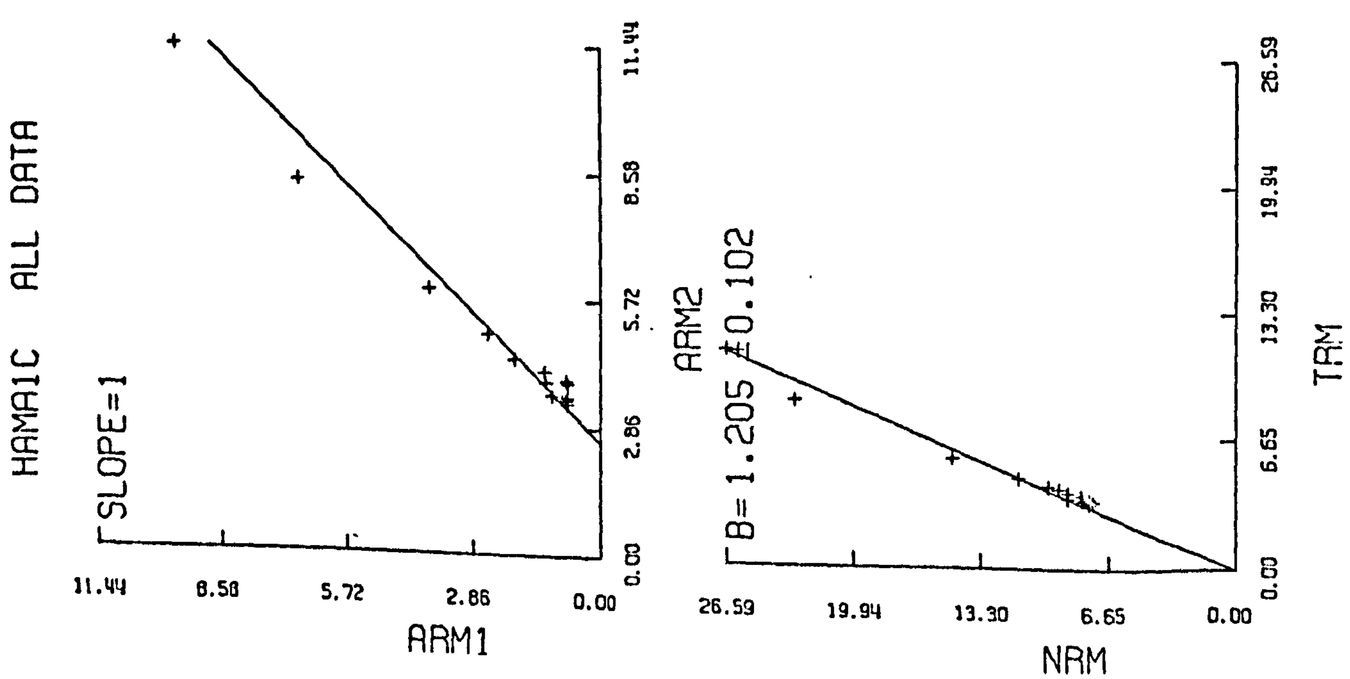
HAMA1C ALL DATA
SLOPE=1
ARM1
ARM2
B= 1.205 ±0.102
NRM
TRM
11.44
8.58
5.72
2.86
0.00
26.59
19.94
13.30
6.65

HAMA1D ALL DATA

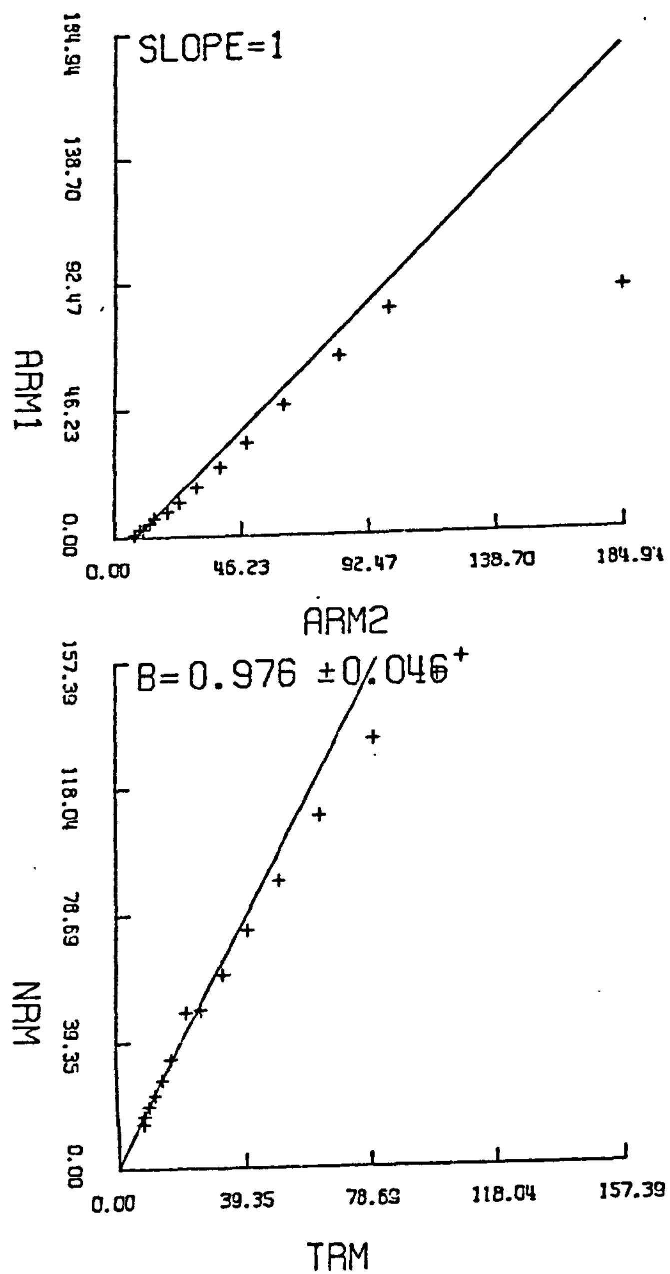

HAMA1D ACCEPTED DATA

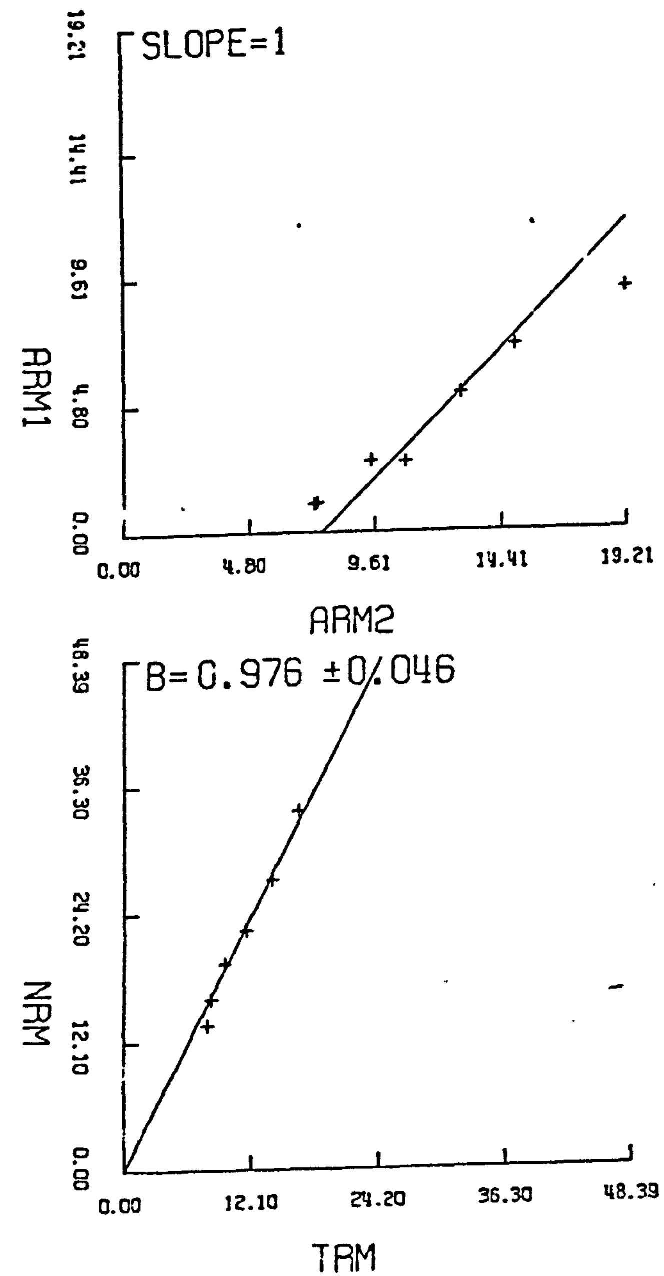

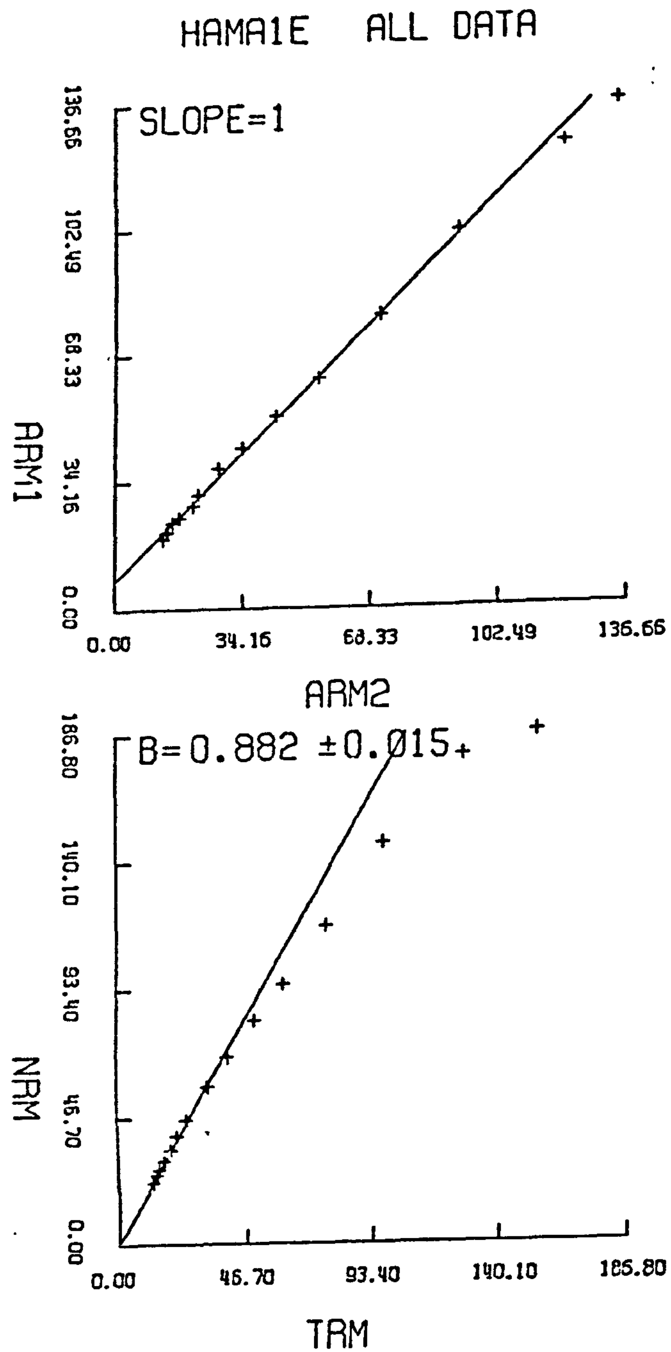
HAMA1E ALL DATA
SLOPE=1
ARM1
ARM2
0.00
34.16
68.33
102.49
136.66
B=0.882 ±0.015
NRM
TRM
0.00
46.70
93.40
140.10
186.80

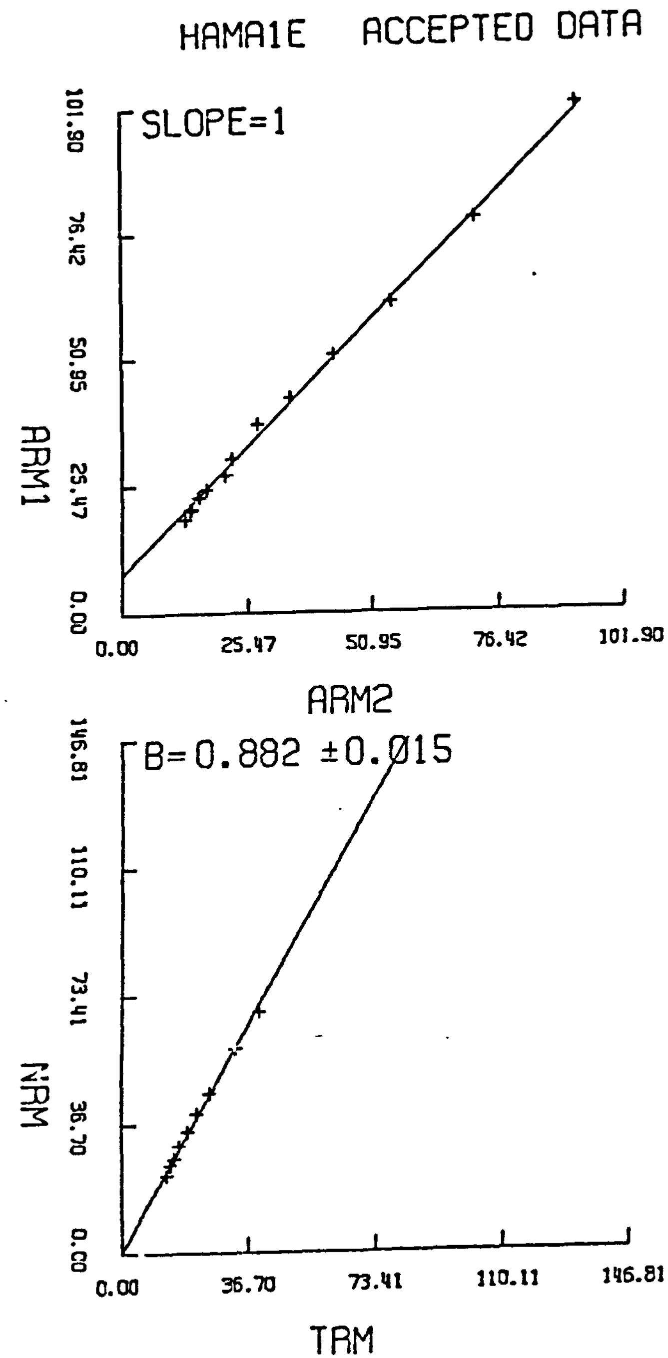
HAMA1E ACCEPTED DATA
SLOPE=1
ARM1
ARM2
0.00
25.47
50.95
76.42
101.90
B=0.882 ±0.015
NRM
TRM
0.00
36.70
73.41
110.11
146.81

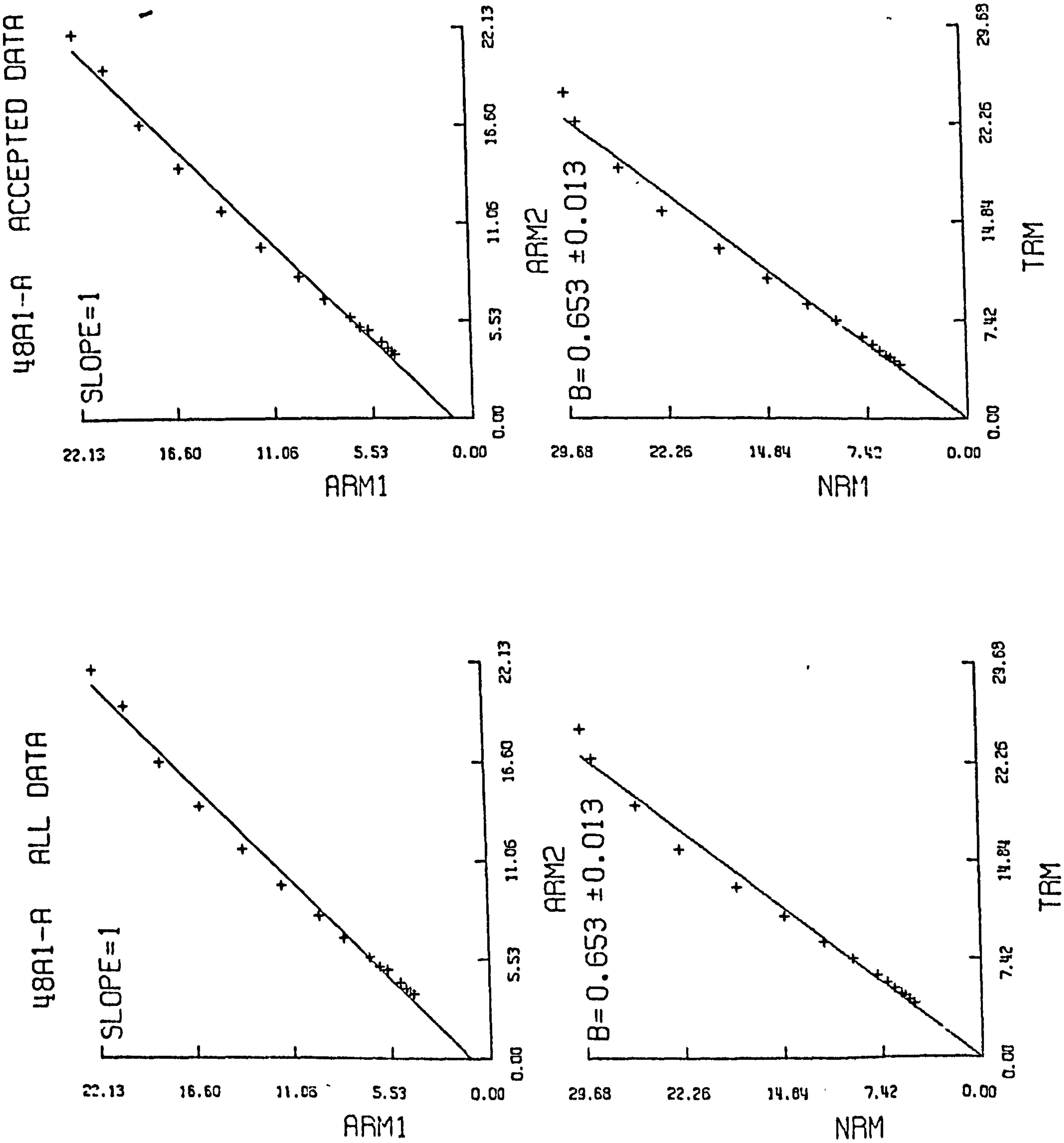
48A1-A ACCEPTED DATA
SLOPE=1
ARM1
ARM2
B=0.653 ±0.013
NRM
TRM
48A1-A ALL DATA
SLOPE=1
ARM1
ARM2
B=0.653 ±0.013
NRM
TRM

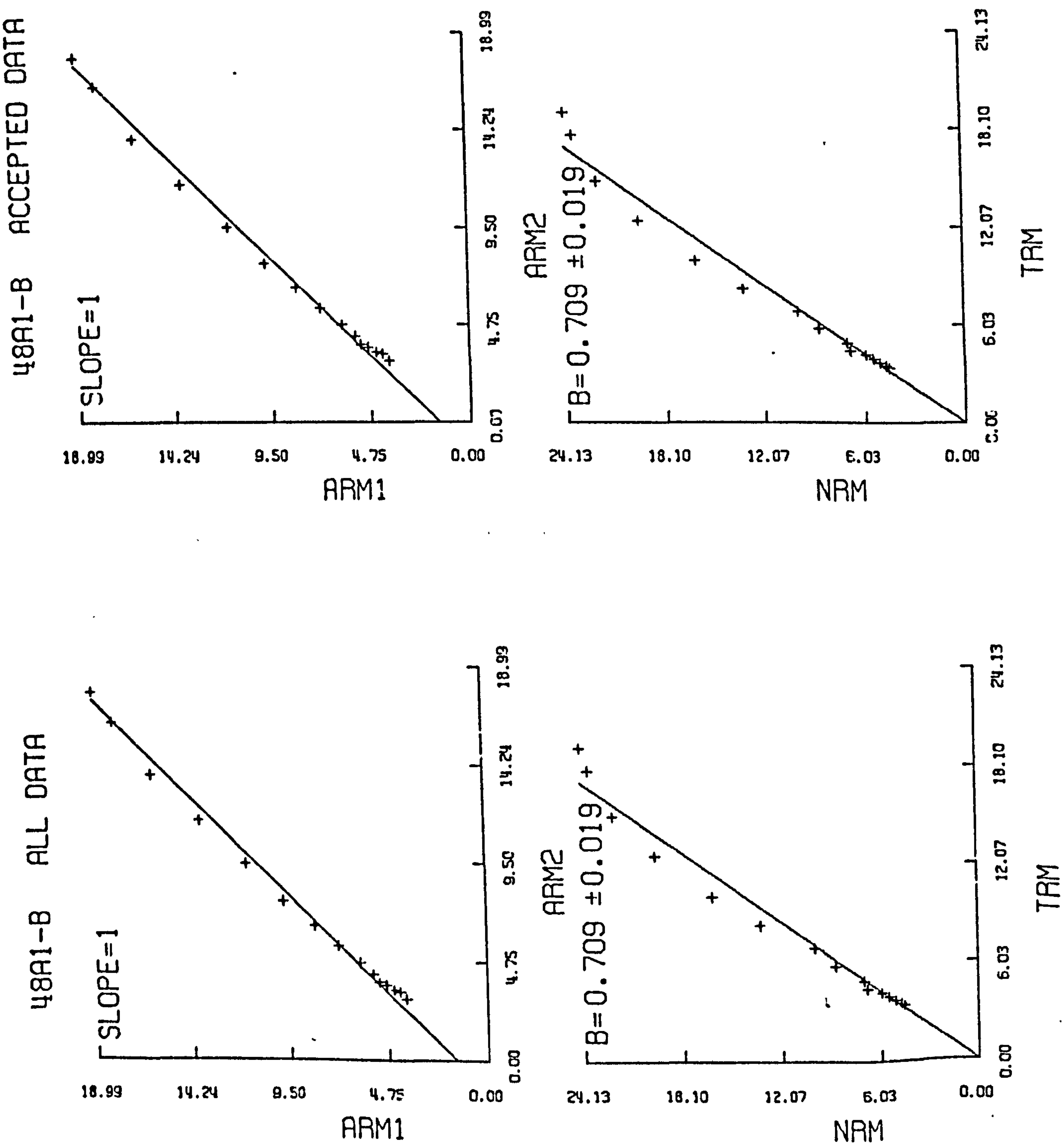
48A1-B ACCEPTED DATA
SLOPE=1
ARM1
ARM2
B=0.709 ±0.019
NRM
TRM
48A1-B ALL DATA
SLOPE=1
ARM1
ARM2
B=0.709 ±0.019
NRM
TRM

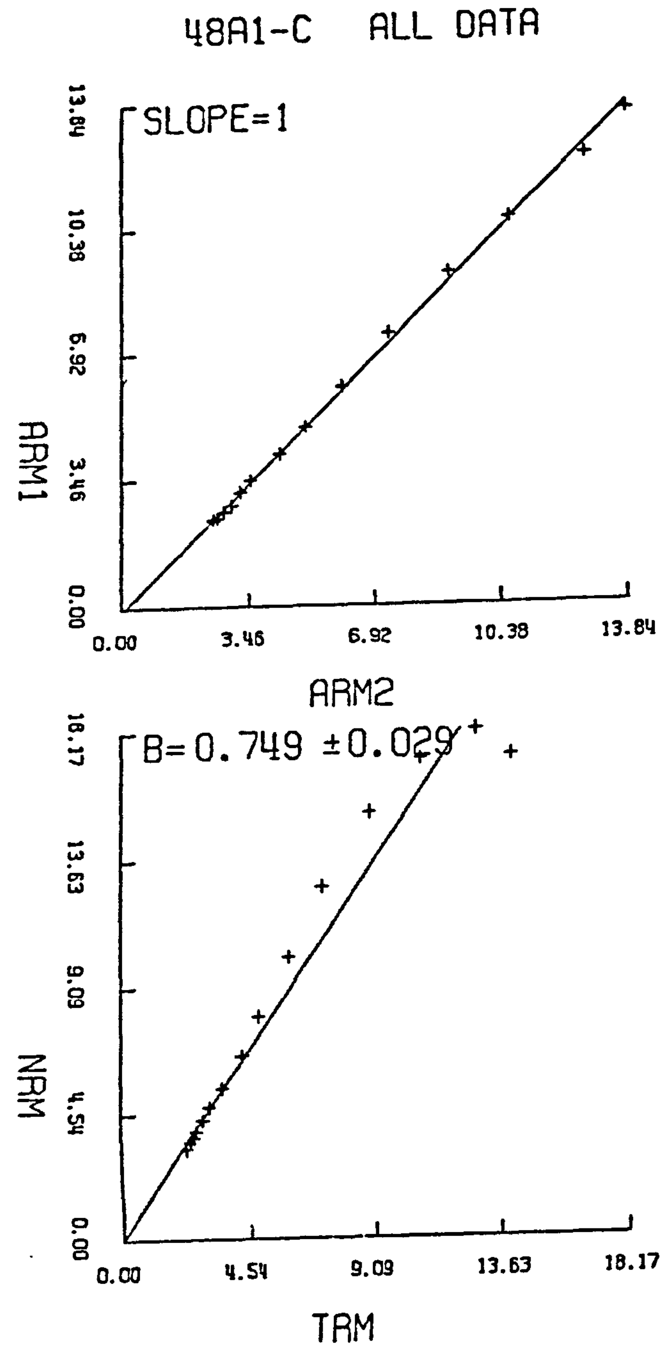
48A1-C ALL DATA
SLOPE=1
ARM1
ARM2
0.00
3.46
6.92
10.38
13.84
B=0.749 ±0.029
NRM
TRM
4.54
9.09
13.63
18.17

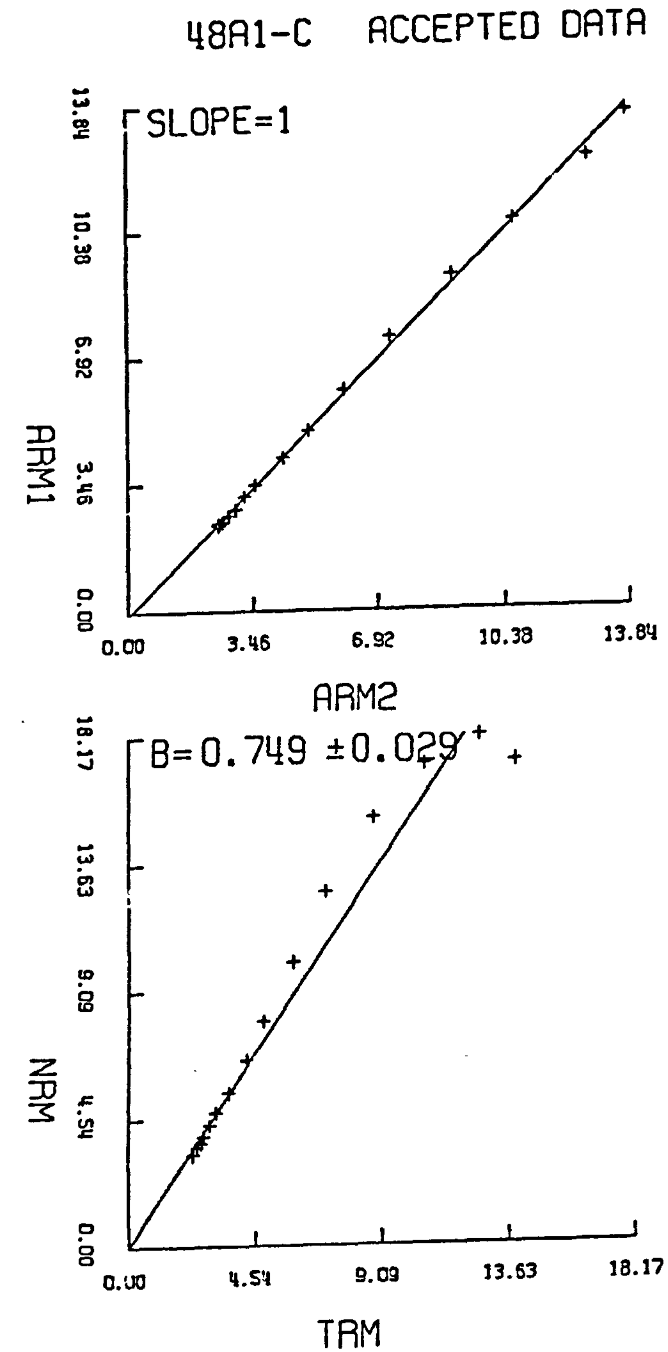
48A1-C ACCEPTED DATA
SLOPE=1
ARM1
ARM2
0.00
3.46
6.92
10.38
13.84
B=0.749 ±0.029
NRM
TRM
4.54
9.09
13.63
18.17

APPENDIX 3 CALCULATION OF 'VIRTUAL DIPOLE MOMENTS'.

If we assume that the earth's magnetic field can be represented by a centred magnetic dipole, measurements of the direction and magnitude of the magnetic field at the surface of the earth define both the magnitude on the orientation of the assumed magnetic dipole. The magnitude of the assumed dipole is referred to as the 'virtual dipole moment' (V.D.M., Smith 1967) and the orientation of the dipole is often defined by the co-ordinates of the south magnetic pole at the surface of the earth, called the 'virtual geomagnetic pole' (V.G.P., Cox and Doell 1960).

If r is the radius of the earth and B the magnitude of the magnetic field at latitude L, the dipole moment, M, is given by

$$M = \frac{B\,r^3}{\mu_o}\;(1 + 3\sin^2 L)^{-\frac{1}{2}} \quad Am^2$$

where $\mu_o = 10^{-7}$, B = magnetic field in Tesla and r = 63710 km.

So for any value of B and L, M is uniquely defined. For very recent samples, like ours, we may take L as the present latitude relative to the geographic pole. For geologically older samples, L may have to be taken as the "palaeomagnetic" latitude of the site relative either to the mean palaeomagnetic pole, or to the V.G.P. for that single lava. These are not always the same poles and some confusion about latitude can result.

REFERENCES

Abranson, C.E., 1970. A Discussion of the Alternating Field Method and New Palaeointensity Measurements of the Miocene Geomagnetic Field in Oregon, Pure Appl. Geo., 82, 189-221.

Angenheister, G., Petersen, N., Schweitzer, Chr., 1971. Bestimmung der Intensität des erdmagnetischen Feldes aus Messungen der thermoremanenten Magnetisierung von rezenten Laven des Atna (Sizilien), Bayer, Akad, Wiss, Sitz, Ber, Math, Naturwiss, Kl, 51-76.

Barbetti, M., McElhinny, M., 1972. Evidence of a Geomagnetic Excursion 30,000 yr. BP., Nature, 239, 327-330.

Brynjolfsson, A., 1957. Studies of Remanent Magnetism and Viscous Magnetism in the Basalts of Iceland, Adv. Physics, 6, 247-254.

Bullard, E., Gellman, H., 1954. Homogeneous Dynamos and Terrestrial Magnetism, Phil. Trans. Roy. Soc. London, Ser.A., 247, 213-278.

Carmichael, C.M., 1968. An Outline of the Intensity of the Palaeomagnetic Field of the Earth, Earth Plan. Sci. Lett., 3, 351-354.

Coe, R.S., 1967. Palaeointensities of the Earth's Magnetic Field Determined from Tertiary and Quaternary Rocks, J. Geophys., Res., 72, 3247-3262.

Collinson, D.W., 1965. Origin of Remanent Magnetisation and Initial Susceptibility of Certain Red Sandstones, Geophys., J.R. astr. Soc., 9, 203-217.

Cox, A., 1957. Remanent Magnetisation of Lower to Middle Eocene Basalt Flows from Oregon, Nature, 179, 685-686.

Cox, A., Doell, R.R., 1960. Review of Palaeomagnetism, Bull. Geol. Soc. America, 71, 645-768.

Domen, H., 1962. Piezo-Remanent Magnetism in Rock and its Field Evidence, J. Geomag. Geoel., 13, 66-72.

Einarsson, Tr., 1957. Magneto - Geological Mapping in Iceland with the use of a Compass, Phil. Mag. Sup., 6, 232-239.

Goldstein, M.A., Larson, E.E., Strangway, D.W., 1969. Palaeomagnetism of a Miocene transition zone in South East Oregon, Earth Planet. Sci. Lett. 7, 231-239.

Heinrichs, D., 1967. Palaeomagnetism of Plio-Pleistocene Lousetown Formation, Virginia City, Nevada, J. Geophys. Res., 72, 3277-3294.

Heller, F., Markert, H., 1973. The age of Viscous Remanent Magnetisation of Hadrians Wall (Northern England), Geophys. J.R. astr. Soc., 31, 395-406.

Kawai, N., Harvaki, I., Katsumi, Y., Shoichi, K, 1959. Chemical - pressure Remanent Magnetism in Sedimentary and Metamorphic Rocks Mem. Coll. Sci., University Kyoto, 26, 235-239.

Koenigsberger, J.G., 1938. Natural Residual Magnetism of Eruptive Rocks (pts. 1 and 2), Terr. Ma n. Atmos. Elec. 43, 119-127, 299-330.

Kono, M., 1974. Intensites of the Earth's Magnetic Field About 60 m.y. Ago Determined from the Deccan Trap Basalts, India, J. Geophys. Res., 79, 1135-1141.

Lawley, E.A., 1970. The Intensity of the Geomagnetic Field in Iceland During Neogene Polarity Transitions and Systematic Deviations, Earth Planet, Sci. Lett., 10, 145-149.

McElhinny, M.W., Briden, J.C., Jones, D.L., Brock, A., 1968. Geological and Geophysical Implications of Palaeomagnetic Results from Africa, Rev. Geophys, 6, 201-238.

Momose, K., 1963. Studies on the Variations of the Earths Magnetic Field during Pliocene Time, Bull. Earthq. Res. Inst.,41, 487-534.

Nagata, T., 1943. The Natural Remanent Magnetism of Voleanic Rocks and its Relation to Geomagnetic Phenomena, Bull. Earthq. Res. Inst., 21, 1-196.

Ozima, M., Ozima, M., Nagata, T., 1964. Low Temperature Treatment as an Effective Means of "Magnetic Cleaning" of Natural Remanent Magnetisation, J. Geomag. Geoelect. 16, 37-40.

Prevot, M., Watkins, N.D., 1969. Essai de Determination de L'intensite du Champ Magnetique Terrestre au cours dun Renversement de polarite, Ann. Geophys., 25, 351-369.

Rubens, S.M., 1945. Cube-Surface Coil for producing a Uniform Magnetic Field, Rev. Sci. Inst., 16, 243-245.

Shaw, J., 1974(a). A New Method of Determining the Magnitude of the Palaeomagnetic Field. Application to Five Historic Lavas and Five Archaeological Samples, Geophys. J.R. astr. Soc., 39, 133-146.

Shaw, J., 1974(b). Strong Geomagnetic fields during a single Icelandic polarity transition, Geophys. J.R. astr. Soc., in press.

Sigurgeirsson, Th, 1957. Direction of Magnetisation in Icelandic Basalts, Phil. Mag. Sup., 6, 240-246.

Smith, P.J., 1967(a). On the Suitability of Igneous Rocks for Ancient Geomagnetic Field Intensity Determination, Earth, Plant. Sci. Lett., 2, 99-105.

Smith, P.J., 1967(b). The Intensity of The Tertiary Geomagnetic Field, Geophys. J.R. astr. Soc, 12, 239-258.

Thellier, E., Thellier, O., 1959. Sur L'intensite Du Champ Magnetique Terrestre Dans le Passe Historique et Geologique, Ann. Geophys., 15, 285-376.

Van Zijl, J.S.V., 1961. A Palaeomagnetic Investigation on Karroo Lavas, Thesis presented to the University of Witwatersrand.

Watkins, N.D., 1965(a). Palaeomagnetism of the Columbia Plateaus, J. Geophys. Res. 70, 1379-1406.

Watkins, N.D., 1965(b). Frequency of Extrusion of some Miocene Lavas in Oregon during an apparent Transition of the Polarity of the Geomagnetic Field, Nature., 206, 801-803.

Watkins, N.D., 1969. Non-dipole behaviour during an Upper Miocene Geomagnetic Polarity transition, Geophys, J.R. astr. Soc., 17, 121-149.

Weaver, G.H., 1966. Measurement of the Past Intensity of the Earth's Magnetic Field. Archaeometry., 9, 174-186.

Wilson, R.L., 1961. Palaeomagnetism in Northern Ireland (pts. 1 and 2), Geophys. J.R. astr. Soc., 5, 45-69.

Wilson, R.L., Watkins, N.D., Einarsson, Tr., Sigurgeirsson, Th., Haggerty, S.E., Smith, P.J., Dagley, P., McCormack, A.G., 1972(a). Palaeomagnetism of Tin Lava Sequences from South-Western Iceland, Geophs. J.R. astr. Soc., 29, 459-471.

Wilson, R.L., Dagley, P., McCormack, A.G., 1971(b). Palaeomagnetic Evidence about the source of the Geomagnetic Field, Geophys. J.R. astr. Soc. 28, 213-224.

(a)

Geophys. J. R. astr. Soc. (1974) 39, 133-141.

A New Method of Determining the Magnitude of the Palaeomagnetic Field

Application to five historic lavas and five archaeological samples

J. Shaw

(Received 1974 April 9)

Summary

A new method for determining the magnitude of the palaeomagnetic field (palaeofield), *B*, has been developed and applied to five historic lavas and five archaeological samples.

The palaeofield was determined for four lavas. The fifth gave no result.

The palaeofield was determined for all five archaeological samples. The Thellier method had previously been applied to three of these samples and the results are compared.

1. Introduction

A new method for determining the palaeofield, B*, has been developed. The method has been tested on five recent lavas, that had been extruded in the known geomagnetic field, and on five archaeomagnetic samples of known age. The palaeofield is usually determined by comparing the natural remanent magnetization (NRM) with a laboratory thermoremanent magnetization (TRM) (Thellier & Thellier 1959), produced in a known field (B_{lab}). The palaeofield (B_{anc}), is given by equation (1), which is valid for small constant magnetic fields of up to 10^{-4} T (Nagata 1943).

$$\frac{\text{TRM}}{\text{NRM}} = \frac{B_{lab}}{B_{anc}}. \tag{1}$$

Usually the TRM does not have the same coercive force spectrum as the NRM, because of changes that occur during the laboratory heating of the sample when producing the TRM. Therefore the direct comparison of the NRM and the TRM (equation (1)) can produce very large errors.

In the new method described in this paper only that part of the coercive force spectrum which has not been altered by the (TRM) heating, is used to determine the palaeofield. Empirically, this always lies in the high coercive force region and is therefore not likely to be affected by viscous components of magnetization.

2. The method

The method involves comparing two ARM's created before and after heating. The comparison permits selection of a coercive force region within which the heating

* The IAGA (Kyoto 1973) recommended that values of the geomagnetic field be expressed in terms of B. $1T = 10^4$ G.

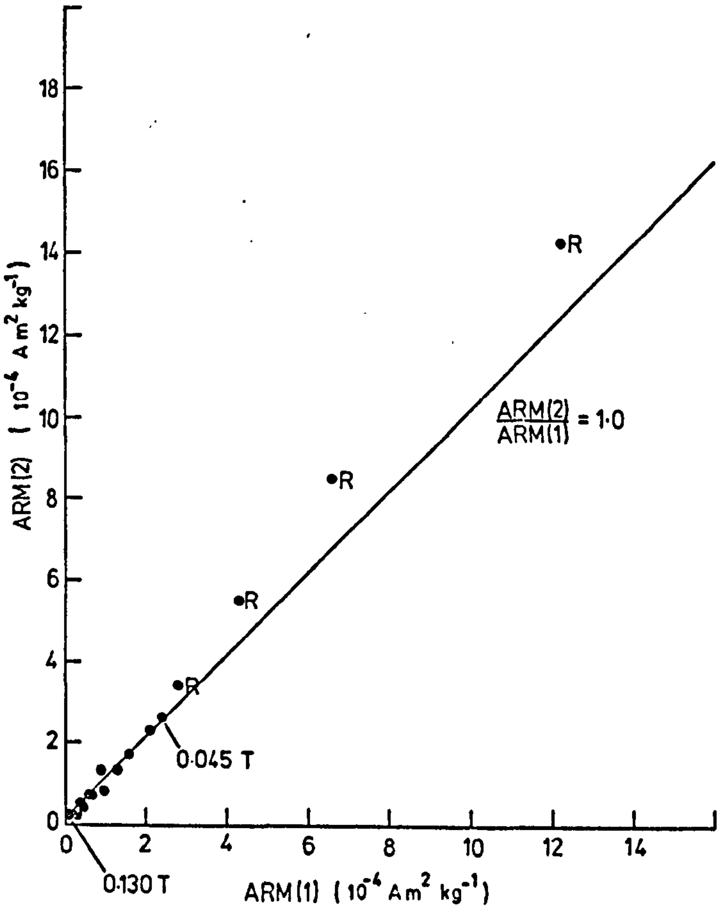

FIG. 1. A graph of ARM(2) (given after heating) against ARM(1) (given before heating) for a typical case (ETNA, E–1J). The line has gradient = 1·0. The points marked R (rejected) do not fall on the line because they represent the altered region of the coercive force spectrum.

has not changed the magnetic properties. The NRM and TRM are compared only within that selected coercive force region, to deduce the palaeofield, *B*.

The TRM is produced by heating the sample above its Curie temperature and then cooling it in a known constant magnetic field. The ARM's are produced by placing the sample inside a small set of Rubens coils (Rubens 1945) which produce a very uniform magnetic field throughout the sample. The coil and sample are then tumbled together in an alternating magnetic field which is taken to some high value and then reduced to zero. The tumbling of the Rubens coils ensures that the ARM process is the precise inverse of the af demagnetization process. The current through the coils is supplied by a constant current source which is isolated from induced currents by a filter circuit.

The ARM and TRM are generally not equal for the same applied constant magnetic field and the ratio of TRM to ARM varies between samples of the same

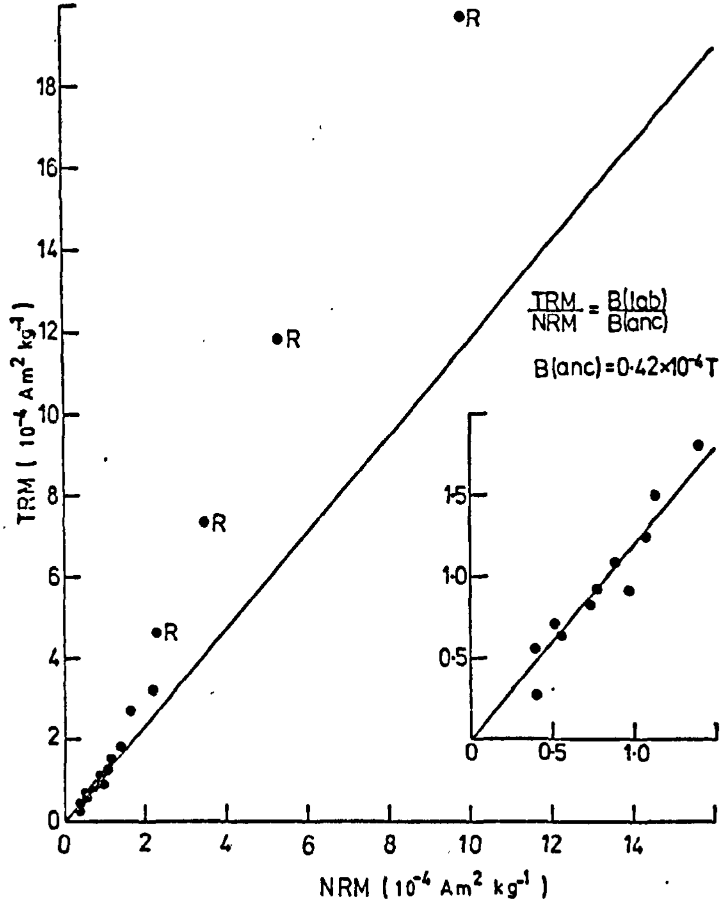

FIG. 2. A graph of TRM against NRM. The points marked R correspond to those marked R in Fig. 1 and are therefore not used to determine B_{anc}. A further two points were rejected at this stage leaving the data in the inset for a palaeofield calculation, quoted in column A, Table 1.

rock type. The coercive force spectra of TRMs and ARMs are also not necessarily equivalent. Nevertheless, any magnetic alteration (for example due to heating) will change the af demagnetization curves of both TRMs and ARMs. However, there may be a continuous coercive force range in which no change has occurred. This range can be determined by comparing ARM demagnetization curves before and after heating (Fig. 1). Equality of the two ARM coercive force spectra implies a straight line relationship at 45° (as in Fig. 1 between 0·045 and 0·130 *T* demagnetization field). This coercive force range may then be used for comparison of the af demagnetization curves of NRM and TRM, to deduce the palaeofield (Fig. 2), on the reasonable assumption that the same coercive force range remains unaltered in the TRM. The NRM and the TRM remaining after af demagnetization in 0·130 *T* are still present when the ARMs are af demagnetized in 0·130 *T* and so the slope of Fig. 1 is not constrained to pass through the origin.

3. Experimental procedure

The magnitude and direction of the palaeofield are determined in the following way.

1. The NRM is af demagnetized with increasing values of the peak alternating magnetic field. The remaining NRM is measured after each successive demagnetization up to the maximum demagnetizing field ($0 \cdot 13\ T$). The same demagnetizing intervals are used in all later demagnetizations of the same specimen.

2. The sample is then given an ARM (called ARM(1)) in the maximum peak alternating field used in 1. The ARM(1) is progressively af demagnetized and measured as in 1.

3. The sample is then given a TRM, by heating it above its Curie temperature and then allowing it to cool to room temperature, in a constant magnetic field of $0 \cdot 50 \times 10^{-4}\ T$. This TRM is af demagnetized and measured as in 1.

4. The sample is then given an ARM(2) as in 2. This ARM(2) is af demagnetized and measured as in 1.

We then have four tables of af demagnetizations, for NRM, ARM(1), TRM, ARM(2).

5. A plot of ARM(2) against ARM(1) (Fig. 1), using the af demagnetizing field as a parameter, will give a straight line with gradient $= 1 \cdot 0$ if the rock is unaltered after heating, since both ARM(1) and ARM(2) were given in the same constant magnetic field ($0 \cdot 50 \times 10^{-4}\ T$).

A line of gradient $= 1 \cdot 0$ is fitted to the points by the method of least squares. If the points do not fit the line within the 95 per cent confidence level of the chi-squared distribution then the point with the largest deviation is rejected and the line re-fitted to the remaining points. This process is repeated until the remaining points fit the line within the 95 per cent confidence level of a chi-squared distribution. Empirically, only those data at the low end of the coercive force spectrum were rejected by this test, for any specimen so far investigated.

Within the remaining high coercive force range the ARM(1) and ARM(2) coercive force spectra are identical and we assume that therefore the sample has not been altered as far as this coercive force range is concerned.

6. The TRM is plotted against the NRM (Fig. 2) using the af demagnetizing field as a parameter, the best straight line is fitted only to those points corresponding to the unaltered coercive force region determined in 5. The line is constrained to pass through the origin, which is the point corresponding to an infinite demagnetizing field, and is fitted to the points by the method of least squares. If the points do not fit the line within the 95 per cent confidence level of a chi-squared distribution, then the point with the largest deviation is rejected and the line re-fitted to the remaining points. This process is repeated until the remaining points fit the line within the 95 per cent confidence level of a chi-squared distribution (inset of Fig. 2).

Equation (1) is valid for each remaining point since this particular region of the coercive force spectrum has not been altered. The gradient of the line is the best average value of the ratio TRM/NRM and this value is substituted in equation (1) to determine the palaeofield.

This procedure was followed for several specimens from each sample. The mean value for each sample was calculated by weighting each specimen by the inverse variance of the data accepted for the final straight line.

Generally less than three points are rejected at stage 6. The mean results determined by rejecting points at this stage (Table 1, column A) can be compared with results determined by not rejecting points at this stage (Table 1, column B). When

Table 1

The Hawaiian 'known field' is the field measured at Honolulu (300 km away) as no measurements were taken on Hawaii Island. Column A is the mean deduced field with points rejected at stage 6. Column B is the mean deduced field with no points rejected at stage 6.

Lava	No. of specimens	Known field	Mean deduced field A	Mean deduced field B
1907 Hawaii	3	$0{\cdot}38\times10^{-4}\,T$	$0{\cdot}31\pm0{\cdot}03\times10^{-4}\,T$	$0{\cdot}27\pm0{\cdot}03\times10^{-4}\,T$
1910 Etna	7	$0{\cdot}42\times10^{-4}\,T$	$0{\cdot}42\pm0{\cdot}05\times10^{-4}\,T$	$0{\cdot}39\pm0{\cdot}05\times10^{-4}\,T$
1926 Hawaii	3	$0{\cdot}37\times10^{-4}\,T$	$0{\cdot}34\pm0{\cdot}02\times10^{-4}\,T$	$0{\cdot}34\pm0{\cdot}02\times10^{-4}\,T$
1955 Hawaii	3	$0{\cdot}37\times10^{-4}\,T$	$0{\cdot}42\pm0{\cdot}02\times10^{-4}\,T$	$0{\cdot}40\pm0{\cdot}02\times10^{-4}\,T$
1973 Heimaey	4	$0{\cdot}51\times10^{-4}\,T$	No acceptable data	

points are rejected at stage 6 the internal scatter of results from several specimens from within one lava is slightly reduced.

The 'mean deduced fields' in column A are larger than those in column B. Empirically, changes in the coercive force spectrum, due to heating, usually result in an increase in the magnitude of the TRM which, according to equation (1), produces a low value for B_{anc}. The ARM test rejects all the altered regions of the coercive force spectrum except those which are so slightly altered that the difference between the ARM's is comparable to the measuring error. These slightly altered regions will be accepted for the TRM/NRM comparison, but will deviate from the straight line fit through the origin and will therefore be rejected at stage 6, with a resultant slight increase in the value of the 'mean deduced field' (column A, Table 1).

All measurements were made on a parastatic magnetometer equipped with automatic feedback and damping, and linked to a small computer. The totalmeasuring and demagnetizing time for one sample (four sets of readings) was 4 hr.

4. The results from five historic lavas

Experiments were carried out on five historic lavas (Table 1) and the palaeofield was determined for four of these.

The 1973 Heimaey lava was totally altered by laboratory heating within the observable region of the coercive force spectrum (up to $0{\cdot}13\,T$) and consequently the palaeofield was not determined.

The three Hawaiian lavas each gave internally consistent results. The maximum alteration occurred in the 1907 lava, which remained unaltered only above $0{\cdot}08\,T$ af demagnetizing field, and consequently only four or five points could be used from each specimen from this lava. The magnetic field at Hawaii is not accurately known. The value quoted in Table 1 is the magnetic field at Honolulu, which is 300 km north-west of Hawaii. It is therefore likely that the discrepancies in Table 1, between the deduced and the known fields, are in part due to the uncertainty of the known field at Hawaii.

The 1910 Etna lava has been used for palaeofield studies by Angenheister, Peterson & Schweitzer (1971), who were unable to obtain any results from it; and also by Tanguy (private communication), who has derived consistent results from it by the application of another new technique.

This lava, while producing the largest scatter of individual results, also produced a mean palaeofield which was closest to the known 1910 magnetic field, probably because of the large number of samples used. The magnetic field at Etna is accurately known.

Table 2

The table contains the results from the five archaeological samples discussed in this paper. 103–A is a recent sample and is compared with the observed magnetic field at the time of firing. Three other samples are directly compared with Weaver's results (Thellier's method).

						Comparisons		
Sample	Description	Number of specimens	Date (years AD)	Banc 10^{-4} T	Standard deviation 10^{-4} T	Banc 10^{-4} T	Standard deviation 10^{-4} T	Investigator
103–A	Pottery	3	1965	0·49	0·03	0·485		Direct observations
S2–1	Brick	3	1900	0·53	0·01	0·49	0·09	Weaver (Thellier's method)
5.PT	Tile	3	1356	0·62	0·02	0·68	0·26	Weaver (Thellier's method)
H–1	Tile	5	350	0·94	0·12	No acceptable result		Weaver (Thellier's method)
48–A1	Pottery	3	150	0·68	0·04			

5. The results from five archaeological samples

Experiments were successfully carried out on five English archaeomagnetic samples of known age. The experimental results are listed in Table 2. Thellier's method (Thellier & Thellier 1959) was applied by Weaver (Weaver 1966) and his results for three cases are listed in the comparison section of Table 2.

The 103–A pottery sample was fired in 1965. The derived value of the magnetic field is in very good agreement with the observed magnetic field at the time. The S2–1 brick came from a Sheffield glass furnace. Weaver had applied Thellier's method to part of this brick. Although the mean values agree within the errors, the new palaeofield method reduced the error by a factor of 9. The 5 PT tile came from a mediaeval tile kiln at Boston. In this case Weaver did not use the same tile but used a brick from the same kiln. The mean results are in agreement and the error from the new palaeofield method is an order of magnitude better than Weaver's error. The H1 tile is from a fourth century grain drier at Hampstead Marshall (Berkshire). In this case the new palaeofield method produced a large error (12 per cent).

The H1 tile was highly oxidized on the outside (red) and light grey on the inside. Experiments were carried out on a red only and a grey only sample. The red sample NRM was very hard (haematite) while the grey NRM was quite soft (magnetite). The red sample gave a value for B_{anc} of $1{\cdot}21 \pm 0{\cdot}10$ and the grey a value of $0{\cdot}98 \pm 0{\cdot}05 \times 10^{-4}\,T$. Both values are within the limits of the other three whole

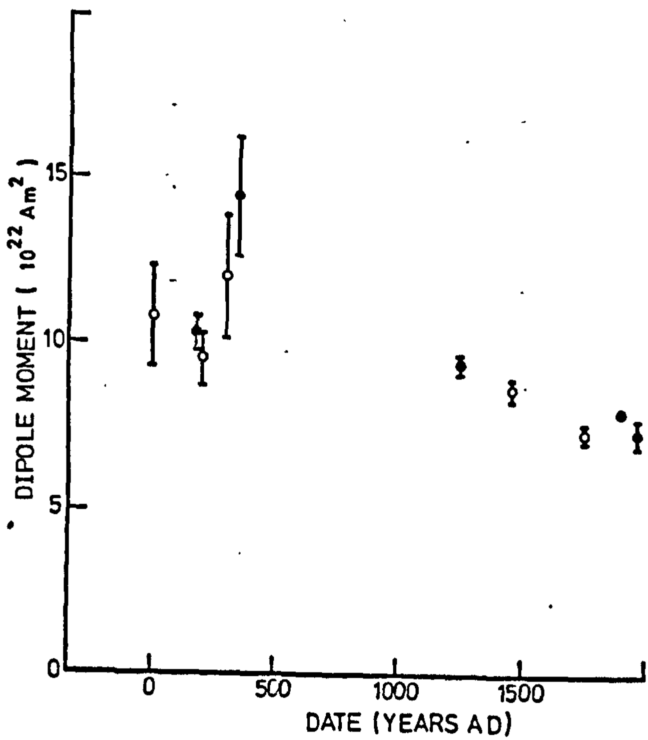

FIG. 3. A graph of virtual geomagnetic dipole moment against time. Closed circles represent English data (this paper), open circles represent European data (Thellier & Thellier 1959). The standard deviation is plotted for both sets of data.

sample values and are included among the five samples in Table 1. Weaver applied Thellier's method to this tile but failed to obtain any result from it.

The 48–A1 pottery specimen came from Stibbington (Huntingdon). The pottery was white throughout and the total NRM was considerably weaker than the other four. This specimen gave an acceptable result although the error was fairly large (6 per cent).

To ensure that the derived results are correct it is at least necessary to be sure that the NRM firing temperature exceeded the Curie temperature. X-ray diffraction patterns indicate that the clay minerals were in various stages of dehydration, from which it was possible to estimate that, in each case, the firing temperature was in excess of 700 °C, well above the Curie temperature.

The English archaeomagnetic results determined by the new palaeofield method compare very well (Fig. 3) with the nearest European results (Thellier & Thellier 1959).

Both sets of data indicate a general decrease in the magnitude of the geomagnetic field over the past 1800 years.

6. Conclusions and discussions

Thirty-seven specimens, from ten samples, were used for palaeofield studies. Thirty-three gave very acceptable results (Tables 1 and 2). The remaining four specimens, which were all from the same lava, gave no result.

Weaver carried out experiments on some of the samples (Thellier's method) but the errors produced were much larger than those from the new palaeofield method, and one sample (H–1) gave no result at all.

Empirically, only the high coercive force region of the coercive force spectrum is suitable for palaeofield studies. This region is not easily affected by viscous magnetization, and therefore it is hoped that the new method described in this paper will be successful when applied to older rocks.

The new palaeofield method has so far yielded positive results on nine out of ten lavas/archaeological samples, with errors much smaller than hitherto (on the same specimens). This 90 per cent 'success rate' greatly exceeds earlier success rates, which, for lavas, were often 5 or 10 per cent. This makes much more worthwhile the task of accumulating a basic body of reliable data on which to base wider generalizations about the nature of the geomagnetic field.

Acknowledgments

I would like to thank Professor R. L. Wilson for many useful discussions and a critical appraisal of the manuscript, Drs M. J. Aitken, R. S. Coe and J. C. Tanguy for generously giving their samples and Dr G. C. Brown for assistance in interpreting X-ray diffraction patterns. I would also like to thank Mr A. G. McCormack for help and advice in writing the computer program, the Icelandic Government for allowing me to collect and transport samples, and the Natural Environment Research Council for supporting this research.

Sub-Department of Geophysics,
Oliver Lodge Laboratory,
Oxford Street,
Liverpool L69 3BX.

References

Angenheister, G., Petersen, N. & Schweitzer, Chr, 1971. Bestimmung der Intensitat des erdmagnetischen Feldes aus Messungen der thermoremanenten Magnetisierung von rezenten Laven des Atna (Sizilien), *Cayer. Akad. Wiss., Sitz-Ber. Math. Naturwiss.*, Kl., 51–76.

IAGA, 1973. Second Scientific Assembly, Kyoto, Japan.

Nagata, T., 1943. The natural remanent magnetism of volcanic rocks and its relation to geomagnetic phenomena, *Bull. earthq. Res. Inst.*, **21**, 1–196.

Rubens, S. M., 1945. Cube-surface coil for producing a uniform magnetic field, *Rev. Sci. Instr.*, 16, 243–245.

Thellier, E. & Thellier, O., 1959. Sur l'intensite des champ magnetique terrestre dans le passe historique et geologique, *Ann. Geophys.*, **15**, 285–376.

Weaver, G. H., 1966. Measurement of the past intensity of the Earth's magnetic field, *Archaeometry*, **9**, 174–186.

IN PRESS - GEOPHYS. J. R. ASTR. SOC. (b)

Strong Geomagnetic fields during a

single Icelandic polarity transition

by

J. SHAW

Sub-department of Geophysics,
Oliver Lodge Laboratory,
Oxford Street,
P.O.Box 147,
Liverpool L69 3BX

SUMMARY

Both the magnitude and direction of the palaeomagnetic field have been determined during a field reversal. The results indicate that the geomagnetic field was large and stable when the magnetic pole was close to the equator.

Introduction

A new method of determining the magnitude of the palaeomagnetic field has been developed and tested on historic lavas and archaeomagnetic specimens (Shaw 1974). This new method which compares anhysteretic remanent magnetisations given before and after heating to detect and isolate regions of no thermal alteration, has now been applied to the well documented R_3 to N_3 transition of Western Iceland which was first discovered by Einarsson (1957) and explored in detail by Sigurguirsson (1957), Brynjolfsson (1957) and later by Wilson et al. (1972(a)). This paper describes how both the magnitude and the direction of the palaeomagnetic field changed during this transition and places certain further restrictions on any proposed dynamo theories.

The R_3 to N_3 transition

Basing the collection on previous knowledge of the R_3 to N_3 transition I sampled six lava sequences in the Hvalfjordur district just north of Rekjavik in Western Iceland. 289 oriented cores were taken from 38 lavas. Measurements of the directions of magnetisation of at least two cores from each lava revealed that 32 lavas from five sections contained the R_3 to N_3 transition. The directions of magnetisation are represented as virtual geomagnetic poles (V.G.P'S. Cox and Doell, 1960) in Fig.1(a) (results from this work) which agree very well with the results in Fig.1(b) (from Wilson et al, 1972(a)). It seems likely from the number of intermediate lavas that the assumed dipole must have remained in a fixed equatorial orientation for a considerable length of time.

The magnitude of the palaeofield

The same specimens that were used to determine the V.G.P's in Fig.1(a) were also used to determine the magnitude of the palaeofield. The specimens from 21 of the 32 lavas produced reliable results. Of the remaining 11 lavas that did not produce values of the magnitude of the palaeofield, the specimens from 2 lavas exploded on heating, the specimens from another 2 lavas were magnetically unstable when a.f. demagnetised in high fields (0.08 to 0.14 T, 1T = 10^4Oer), and the specimens from 7 lavas underwent severe thermal alteration throughout the observable region of their coercive force spectra (0 to 0.14 T). The magnitude of the palaeofield was also determined from 2 lavas sampled by Wilson et al. (1972(a)) thus making a total of 23 determinations (Table 1). Each palaeofield value was determined from at least 2 specimens. As a measure of the work done more than 2500 a.f. demagnetisations and remanence measurements were made to achieve these 23 results.

Previous determinations of the magnitude of the palaeofield for intermediate palaeomagnetic pole positions have indicated that it is much weaker than in the more usual 'normal' and 'reversed' states (Momose, 1963; Prevot and Watkins, 1969; Lawley, 1969). Wilson et al. (1972(b)) presented a statistical analysis of the dependance of virtual dipole moments (V.D.M's, Smith 1967) on colatitude of V.G.P. position (Fig.2(a)). Their results indicate the possibility of large V.D.M's at intermediate colatitudes. Unfortunately the large errors associated with these intermediate values were very large, ostensibly because of small numbers of specimens.

The results of this paper are presented in Fig.2(b) and listed in Table 1. The error shown in Fig.2(b) is the standard deviation, the error shown in Fig.2(a) is the error on the mean.

Clearly one would not expect one individual palaeofield transition to be the same as, or even necessarily similar to, the mean or average transition of Fig.2(a). However it is clear that both the individual (Fig.2(b)) and the mean (Fig.2(a)) transitions do agree in two respects:-

1. They both agree that the intermediate V.D.M's can have large values.

2. They both agree that the V.D.M's can fall to low values between the usual large 'normal' (or 'reversed') V.D.M' and the large intermediate V.D.M's. The smallest recorded V.D.M. in Fig.2(b) is $0.35 \pm 0.10 \times 10^{22} Am^2$ ($1\ Am^2 = 10^3 G\ cm^3$) which is only 4 per cent of the present value.

A sharp increase of the V.D.M. will not be easily detected in Fig.2(a) because these V.D.M's are averaged over 5^o colatitude intervals and so the large intermediate values will be combined with smaller values to provide an average value. This probably explains the large 'spread' of results associated with three of Wilson's intermediate V.D.M's (90 to 110^o).

Although only the R_3 to N_3 transition has been examined in detail, the statistical data of Fig.2(a) also support the possibility that the earth's magnetic field has a third stable state (intermediate state). This intermediate state would appear to have similar characteristics to the more usual 'normal' and 'reversed' states in that the position of the V.G.P remains fixed for large values of V.D.M., and that changes from one state to another occur when the V.D.M. is small.

When, during the R_3 to N_3 transition, the V.G.P. reached the geographic equator it remained in a fixed position and the V.D.M. increased smoothly to a maximum recorded value of $9.7 \pm 0.3 \times 10^{22}\ Am^2$, which is larger than the present dipole moment of $8.0 \times 10^{22}\ Am^2$. The V.D.M. then decreased smoothly in magnitude before the V.G.P. moved to the more usual 'normal' state.

Discussion

The evidence suggests that the geomagnetic field may have a third metastable state. This intermediate state obviously happens less frequently than the 'normal' and 'reversed' metastable states.

The existance of this intermediate metastable state and the fact that large angular changes of the V.G.P. are associated with small values of V.D.M. must impose constraints on any theories relating to the generation of the geomagnetic field.

A knowledge of this intermediate metastable state may help in interpreting unusual palaeomagnetic directions (e.g. Cox, 1957). If intermediate metastable states have been a general feature of the geomagnetic field and if they can be individually identified they will provide a means by which the geographic longitude of the collecting site can be determined relative to that intermediate V.G.P. This may tell us the relative longitude of each continent at the time of the transition and thus show more clearly how the continents have moved in the past.

Because intermediate metastable states only exist for a relatively short time it may be necessary to examine quickly deposited sediments in order to provide an estimate of the time spent in that state.

Another transition which is well documented is the N_4 to R_3 transition of Western Iceland (Wilson et al, 1972(a)). This transition also seems to spend a considerable period of time (12 lavas) when the V.G.P. is at the equator and may possibly give a similar result for an inversion in the opposite sense.

Two particularly well documented American transitions are the Steens Mountain transition (Watkins, 1965(a), (b), 1969; Goldstein, Larson and Strangway, 1969) and the Lousetown Creek transition (Heinricks, 1967). If these transitions also give similar results to the Icelandic R_3 and N_3 transition then we will know that this phenomena is not restricted to Iceland and may be a worldwide effect. Certainly local magnetic anomalies, unless possibly due to a very large magma chamber under Iceland, could not produce a magnetic field of $0{\cdot}38 \times 10^{-4}$ T at the surface.

Acknowledgements

I would like to thank Olafur Flovenz for his skilful assistance in locating and drilling the lavas. I would also like to thank Professor R.L.Wilson for suggesting the project, Dr.L.Kristjansson for his help and assistance, and the Icelandic government for allowing me to collect and transport specimens.

Particular thanks are due to Mrs.B.Bridges for carefully measuring and a.f. demagnetising many of the specimens.

This work is supported by the British Natural Invironment Research Council (grant No. GR/3/2396).

TIME

Magnetic field 10^{-4} T	Standard deviation 10^{-4} T	V.D.M. 10^{22} Am^2	Standard deviation 10^{22} Am^2	V.G.P. lattitude deg	V.G.P. longitude deg East	α_{95} deg
0.777	0.066	13.6	1.2	- 63	306	4
0.501	0.097	7.2	1.4	- 81	273	1
0.497	0.222	7.2	3.2	- 81	278	3
0.303	0.005	4.6	0.1	- 75	284	4
0.202	0.006	3.4	0.1	- 21	131	2
0.018	0.005	0.4	0.1	- 12	117	4
0.155	0.053	2.9	1.0	- 13	122	2
0.061	0.025	1.3	0.5	- 9	114	2
0.105	0.012	2.3	0.3	- 4	114	4
0.075	0.009	1.7	0.2	- 3	110	5
0.095	0.003	2.1	0.1	1	117	9
0.083	0.019	1.8	0.4	1	107	4
0.054	0.003	1.3	0.1	5	114	4
0.062	0.002	1.5	0.1	6	108	2
0.204	0.008	5.0	0.2	5	106	2
0.246	0.003	6.0	0.1	3	107	1
0.386	0.013	9.7	0.3	8	107	2
0.208	0.011	4.8	0.3	- 2	107	8
0.099	0.015	2.3	0.4	2	112	9
0.095	0.002	2.3	0.1	6	107	1
0.076	0.012	1.5	0.2	5	359	12
0.175	0.005	2.3	0.1	71	339	3
0.537	0.071	8.1	1.1	65	72	2

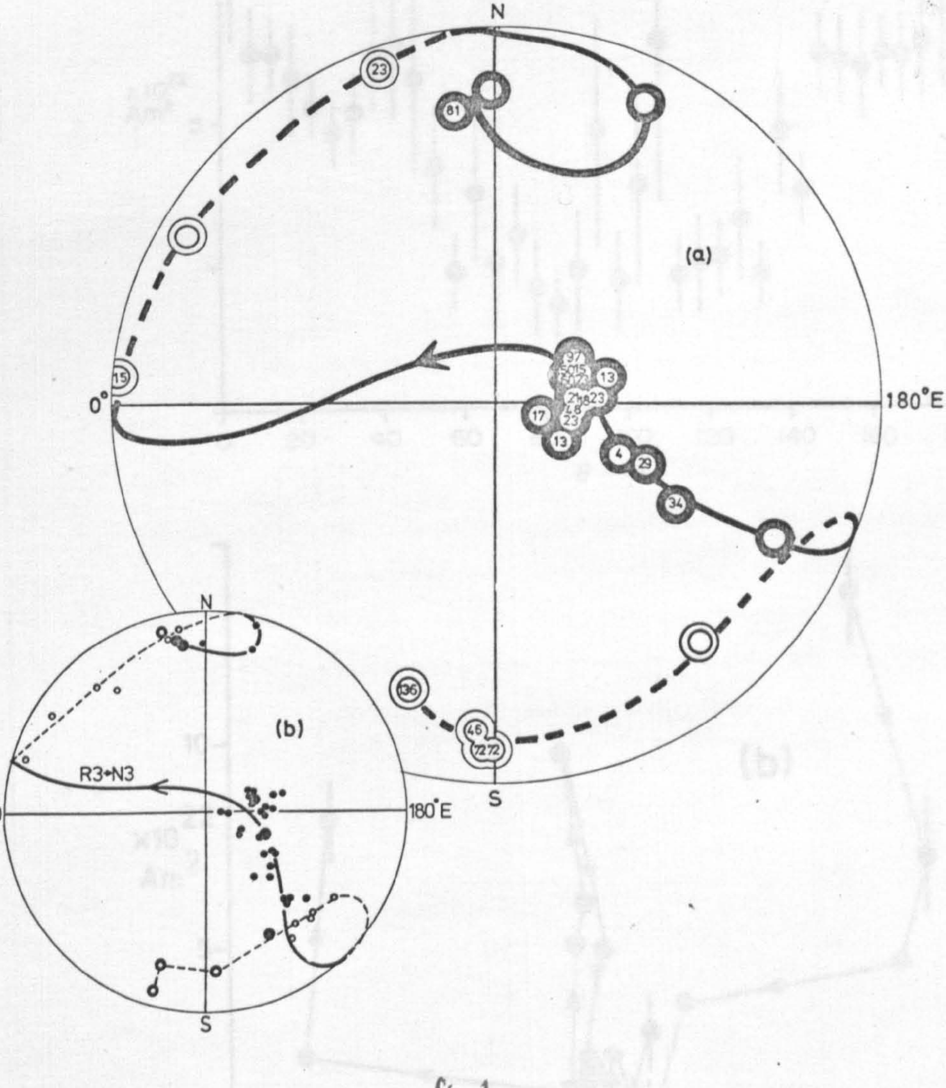

fig 1.

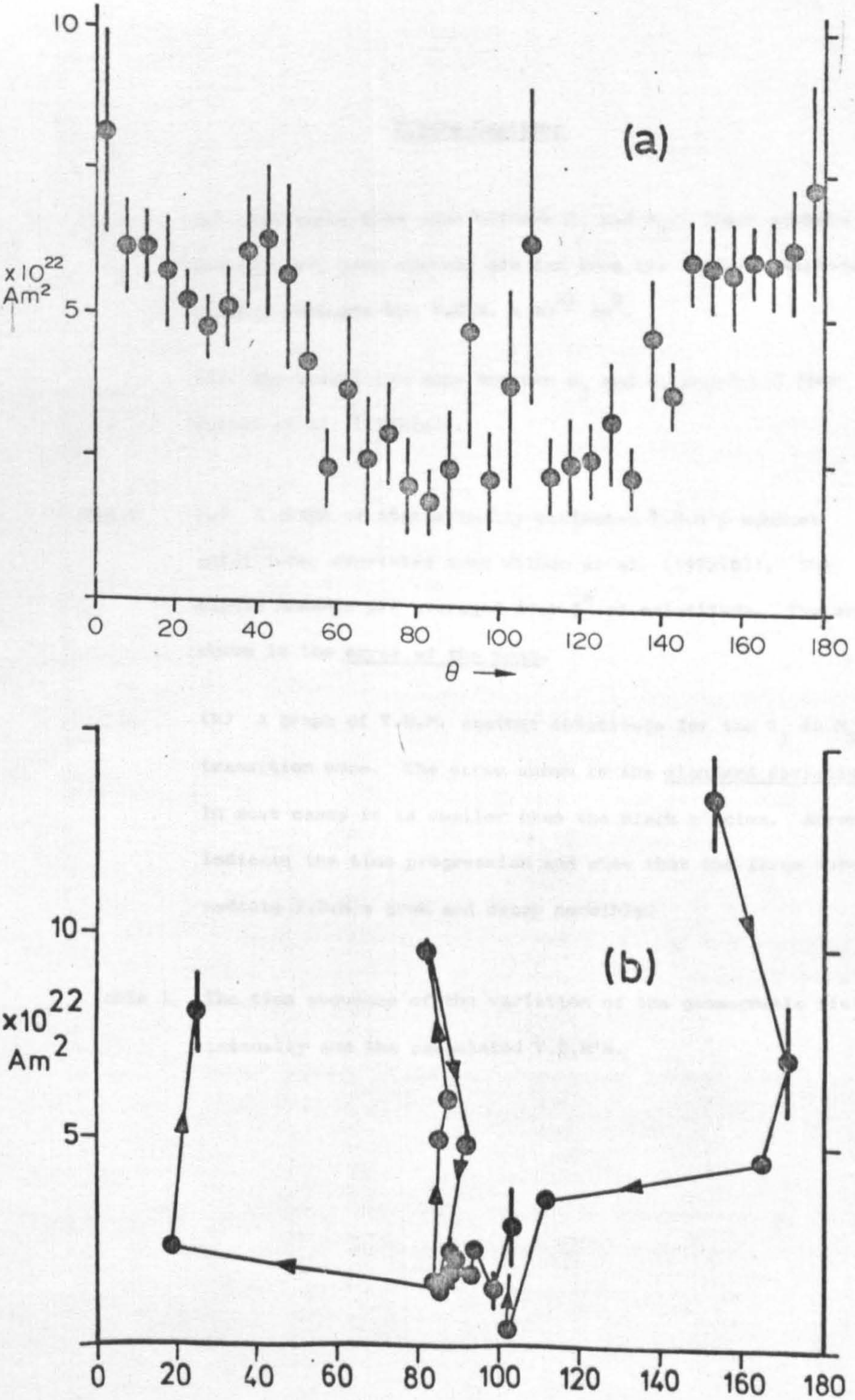

(a)
x10^22
Am²
10
5
0
20
40
60
80
100
120
140
160
180
θ →
(b)
x10^22
Am²
10
5
0
20
40
60
80
100
120
140
160
180
θ →

fig 2.

Figure Captions

Fig.1 (a) The transition zone between R_3 and N_3. Black symbols are near to, open symbols are far from the reader. Enclosed numbers indicate the V.D.M. x 10^{21} Am^2.

(b) The transition zone between R_3 and N_3 reprinted from Wilson et al. (1972(a)).

Fig.2 (a) A graph of statistically estimated V.D.M's against colatitude; reprinted from Wilson et al. (1972(b)). The dipole moments are averaged over 5° of colatitude. The error shown is the error of the mean.

(b) A graph of V.D.M. against colatitude for the R_3 to N_3 transition zone. The error shown is the standard deviation. In most cases it is smaller than the black circles. Arrows indicate the time progression and show that the large intermediate V.D.M's grow and decay smoothly.

Table 1 The time sequence of the variation of the geomagnetic field intensity and the calculated V.D.M's.

References

Brynjolfsson, A., 1957. Studies on remanent magnetism and viscous magnetism in the basalts of Iceland, Adv.Phys., Phil.Mag.Suppl., 6, 23, 248-254.

Cox, A, and Doell, R.R., 1960. Review of palaeomagnetism, Bull.Geol. Soc.Am., 71, 645.

Cox, A., 1957. Remanent magnetisation of lower to middle Eocene basalt Flows from Oregon. Nature, 179, 685-686.

Einarsson, Tr., 1957. Magneto-geological mapping in Iceland with the use of a compass, Phil.Mag.Suppl., 6, 232-239.

Goldstein, M.A., Larson, E.E. and Strangway, D.W., 1969. Palaeomagnetism of a Miocene transition zone in South East Oregon, Earth Planet. Sci.Lett., 7, 231-239.

Heinrichs, D., 1967. Palaeomagnetism of Plio-Pleistocene Lousetown Formation, Virginia City, Nevada, J.geophys.Res., 72, 3277-3294.

Lawley, E.A., 1969. Measurements of the intensity of the geomagnetic field during polarity transitions and a study of the magnetic and opaque petrological properties of a single lava. Ph.D. Thesis, University of Liverpool.

Momose, K., 1963. Studies in the variation of the Earth's magnetic field during Pliocene time, Bull. Earthq. Res.Inst., Tokyo Univ., 41, 487-534.

Prevot, M., and Watkins, N.D., 1969. Eassai de determination de l'intensite du champ magnetique terrestre au cours d'un renversement de polarite, Ann. Geophys., 25, 351-369.

Shaw, J., 1974. A new method of determining the magnitude of the palaeo- magnetic field: Application to five historic lavas and five archaeo- logical samples., Geophys.J.R.astr.Soc., in press.

Sigurgeirsson, T., 1957. Direction of magnetisation in Icelandic Basalts, Adv.Phys., 6, 240-247.

Smith, P.J., 1967. The intensity of the tertiary geomagnetic field, Geophys. J.R.astr.Soc., 12, 239-258.

Watkins, N.D., 1965(a). Frequency of extrusion of some Miocene lavas in Oregon during an apparent transition of the polarity of the geo- magnetic field, Nature, 206, 801-803.

Watkins, N.D., 1965(b). Palaeomagnetism of the Columbia Plateaus, J. Geophys. Res. 70, 1379-1406.

Watkins, N.D., 1969. Non-dipole behaviour during an Upper Miocene Geo- magnetic Polarity transition, Geophys.J.R.astr.Soc., 17, 121-149.

Wilson, R.L., Watkins, N.D., Einarsson, Tr., Sigurgeirsson, Th., Haggerty, S.E., Smith, P.J., Dagley, P., and McCormack, A.G., 1972a. Palaeo- magnetism of ten lava sequences from South-Western Iceland, Geophys. J.R.astr.Soc., 29, 459-471.

Wilson, R.L., Dagley, P., and McCormack, A.G., 1972b. Palaeomagnetic evidence about the source of the Geomagnetic Field, Geophys.J.R. astr.Soc., 28, 213-224.